ELECTRICAL pH CONTROL IN AQUEOUS SOLUTIONS

Presented By
Jordan Todorov Bourilkov

THESIS SUBMITTED FOR EXAMINATION FOR THE DEGREE OF DOCTOR OF PHILOSOPHY

Department of Engineering and Mathematical Sciences

City University, London

20 September, 2005

TABLE OF CONTENTS

LIST OF FIGURES

Chapter 3

3.1 Ion selective electrode, based on measurement of the potential difference between two reference electrodes separated by an ion-selective membrane.

3.2 Typical electrode system for measuring pH, where an ion-selective electrode for hydrogen ions concentration is used.

3.3 A combination pH electrode system, where the reference and glass electrodes are integrated in one compact body for convenience of use.

3.4 Electronic pH meter circuit diagram, showing a high-impedance FET input, gain and bias controls, and analogue meter reading.

Chapter 4

4.1 pH optical fibre probes using indirect measurement method: the optical properties of a pH sensitive indicator incorporated on the sensing tip.

4.2 Optical fibre pH sensor for physiological use, where miniature polystyrene spheres are used to augment the backscattered light response and increase sensitivity.

4.3 A comparison of optical and electrochemical pH sensor responses shows that optical sensors suffer from limited sensing range and non-linear response.

4.4 Sol-gel based sensor, involving optical fibre with a sol-gel coated sensing tip attached to a fluorometric instrument.

4.5 Absorbance of a prepared in-house sol-gel sample.

4.6 The produced sol-gel samples show good optical transmittance in the visible range, enabling chemical sensor applications.

Chapter 5

5.1 Electrochemical cell equivalent circuit, taking into account the electrodes double layer capacitance, polarization resistance and the electrolyte resistance.

5.2 Potentiostats principle of operation diagram, showing the electrochemical cell included in an operational amplifier feedback control loop.

5.3 Potentiostats circuit diagram revealing the main building blocks: WE voltage control power amplifier, RE high-impedance voltage follower, and current to voltage converting power amplifier.

5.4 The frequency response of a compensated operational amplifier follows the 6dB/octave (20 dB/decade) rule.

LIST OF TABLES

LIST OF APPENDICES

ABBREVIATIONS KEY

KH - carbonate hardness
GH - general hardness
H^+ - hydrogen ion
ORP - oxidation/reduction potential
REDOX - reduction/oxidation
HA - proton donor (acid)
B - proton acceptor (base)
A - activity
Ka - acidity constant
Kw - autoprotolysis constant of water
ATC - automatic temperature compensation
atm - atmosphere
emf - electromotive force
ISE - ion-selective electrode
PD - potential difference
PI - proportional integral
PID - proportional integral derivative
TOC - total organic carbon
COD - chemical oxygen demand
AA - atomic absorbtion
ICP - inductively coupled plasma
TEOS - tetraethyl orthosilicate
sol-gel - solution gelation
OA - operational amplifier
FET - field effect transistor
PA - power amplifier
WE - working electrode
CE - counter electrode
RE - reference electrode

OCV - open circuit voltage

NiCd - nickel cadmium

NiMH - nickel metal hydride

IC - integrated circuit

PTC - polymer temperature cutoff or positive temperature coefficient

LED - light emitting diode

ppm - part per million

CC - constant current

CV - constant voltage

II - denotes parallel connection of resistors

ACKNOWLEDGEMENTS

The Author wishes to express sincere recognition to prof. K.T.V. Grattan for his continuous support and guidance from the initiation throughout the research and the completion of this thesis.

Sincere appreciation is also extended to Dr. William Boyle and all the academic and administrative staff in the Department of Electrical, Electronic and Information Engineering for their relentless support and the friendly atmosphere that helped me to carry out this research.

The author is also very grateful to his external supervisors Dr. Fraser Walsh and Dr. Michael Pozin for their support without which it would have been impossible to complete this work.

I am sincerely thankful to my employer Duracell and my supervisor David Klein for supporting the continuation and completion of this work.

Many thanks go to my parents and my wife Emilia for their continuous understanding, encouragement and support despite all challenges and transitions over the years.

DECLARATION

The author hereby grants the powers of discretion to the City University Librarian to allow this thesis to be copied in whole or in part without further reference to the author. This permission covers only single copies made for study purposes, subject to normal conditions of acknowledgement.

ABSTRACT

In this thesis is described the development of a novel method and instrumentation for electrical pH control in aqueous solutions. The work is targeted to environmental and industrial on-line remote *in-situ* chemical and optical fibre sensors conditioning, measurement, and process control. The method is a more flexible alternative to the existing automatic pH controllers, based on correction buffer reagent addition and mixing. It operates free of chemicals and mechanical valve systems and involves only pure electrical bias and feedback control in conductive, especially aqueous solutions.

Dissolved gaseous species which produce acidic and basic waters are of great concern for the preservation of the environment. Significant research effort is aimed at the development of on-line, *in-situ* monitoring methods. The measurement of such pollutants has been previously maintained by using preconditioned water samples and ion-selective electrodes, or absorption spectrometry. A gas-permeable membrane has been successfully used in this application to separate the molecular form from the ionic form of the measured species. The solution pH has been controlled by chemical means to ensure the reversible transition of measured species from ionic to gaseous form and hence allow their permeation through the membrane.

An electrochemical pH controller based on electrolysis was developed and evaluated. Multiple feedback-control systems for biasing of the modulation electrodes were investigated, including constant voltage (potentiostatic), constant current (galvanostatic) and combined methods. The instrument's speed, settling time, accuracy, power requirements and battery runtime are discussed. Battery power sources for on-line monitoring were evaluated and improved hybrid power supply was developed. Two different feedback control options, involving electrochemical and optical sensors, are presented. Real instruments implementing the two feedback approaches were built and analyzed, and the test results discussed. Possible applications of the new method for environmental monitoring and process control are demonstrated.

CHAPTER 1: INTRODUCTION

1.1 Goals of the thesis

This thesis investigates the developments of methods for pH measurement and control using electrochemical techniques and most importantly without recourse to reagents in the control of pH.

1.2 Achievements of this thesis

This work presents the electrochemistry of industrial and natural aqueous systems, methods of battery service life improvement suitable for remote control of pH sensors and regulators and the optical spectrometry of pH indicators. Developments by the author presented in the thesis include new electrochemical methods for control of pH and thereby, the measurement of concentration of pH dependent analytes by optical spectrometry and the development of suitable hybrid battery technology for remote operation of pH control and measurement electrochemical instruments. Much of the work has been published in journals and conference proceedings as discussed in Appendix 9. Also the work on battery development is subject to patents.

1.3 The pH factor

The determination of pH is one of the oldest methods of analysis in human history. When foods and drinks are tasted, some are noticed acidic and some to be alkaline. With modern analytical instruments, these sensations can be measured in exact figures.

The concept of a pH factor was first introduced in 1909 by the Danish biochemist Peter Lauritz Sorensen, who was working on the optimization of acidity of water in the brewing process of beer. He defined the pH value as the negative logarithm (base 10) of the hydrogen ion molar concentration in a solution:

$pH = - \log [H^+]$

Hence, different substances are objectively compared with each other, where pH = 0 is extremely acidous, pH = 7 is neutral and pH = 14 is extremely alkaline. The pH factor is very important to water chemistry, because the hydrogen ions are small and very active and therefore affect most chemical reactions in water.

During the last decade, the pH factor is gaining in importance. For the regulation of chemical and biological processes, it has become indispensable to monitor and control the pH values, for example to:

- Produce a substance with defined properties
- Optimize production processes
- Develop environmentally friendly technologies
- Follow legal requirements
- Research new materials and processes

1.4 Typical areas of pH control application

1.4.1 Agriculture

The pH of soils is important, as plants tend to grow better within specified narrow pH range, which varies between different types of plants. The water pH is even more important than in the soil, since it can cause precipitation of some chemicals if out of limits. Helpful soil bacteria grow best in slightly acidous soil, and also toxic metals are found if pH is too low.

1.4.2 Fermentation

The fermentation processes are optimized by the specification of pH. Different pH with some bacteria can produce even different products, which might be unwanted or harmful. In the brewing process, pH is important at all stages, and for beer aging as well. Lower pH will reduce the solubility of the bitter parts of hops and permits the use of stronger hops without increasing harshness. The pH of bottled beer should be in the range from 3.9 to 4.1 to ensure stability during storage.

1.4.3 Corrosion

The corrosion of iron occurs below pH level of 4.3, which is common for acidous soils. A semi-protective oxide layer is formed at values above 4.3, but more resistant coating is formed above pH 10.5.

1.4.4 Dairy Production

Below pH 4.7 the milk curdles. A pH 4.9 is right for ageing cheddar cheese. Ice cream can be spoiled by the addition of fruits and juices with too low pH.

1.4.5 Dyeing

pH must be specified for processes such as bleaching and dyeing for best results without damage to the fabrics. For example, wool is neutralized to a specified pH for effective dyeing. The acid content of the dye must also be controlled.

1.4.6 Pharmaceuticals

Antibiotics are grown at precise pH control. Incorrect pH can produce a poison rather than a medicine.

1.4.7 Fertilizers

To prevent waste of acid and to standardize products, the pH of fertilizers is controlled.

1.4.8 Jams and Jelly Manufacturing

A narrow range about pH 3.3 is best for proper gelling. At 3.1 it becomes stiff and at 3.5 tender, and over 3.5 no gelling occurs. Usually the control is maintained by the addition of tartaric or citric acid.

1.4.9 Metallurgy

Sand for casting can be optimized to hold its shape better by pH control. In metal plating, the pH of baths determines the quality and speed of the process. Some alloys can be plated only at very strict pH control.

1.4.10 Water Supply

To prevent pipe and boiler corrosion, the pH of feed-water should be continuously controlled. Optimum values range between pH 7.4 and 8. If required, the pH is brought up to 9 through suitable additions. The soda lime softening process requires a pH of 9.4 for calcium removal and 10.6 for magnesium removal.

1.4.11 Laundries

The efficiency of soaps and detergents can be optimized by pH control. Generally, higher pH makes the process more effective, but it should not exceed the specified value for the material being cleaned – 11 for undyed cottons, 10 for wool, 9.6 for colored clothes and 9.2 for silks.

1.4.12 Sewage

In biological purification plants, organic substances are decomposed by bacteria in the activated sludge basin, where pH control helps for efficient coagulation of sludges. Also, to prevent contamination, the pH of the effluent water must be controlled in the range from 6.8 to 7.6. The filtration process can be controlled by pH - for example pH 3.4 is used for ferric chloride and 4.4 for aluminum.

1.4.13 Swimming Pools and Aquariums

To prevent skin irritations, pH in swimming pools should be maintained neutral to slightly alkaline. Also, high pH levels cause solid salts deposits in the heather lines, and low pH – corrosion of iron pipes. In aquariums, each species has its own best pH environment, ranging from 6 to 8 in freshwater and 8.3 fixed for saltwater.

1.4.14 Water pollution and quality

The pH of water in rivers, lakes and seas is measured to study natural conditions of wildlife and also to determine the extent of pollution and the quality of drinking water. The uptake of certain species like ammonia, carbon dioxide, sulfur dioxide and hydrogen sulfide by aqueous solutions is a function of pH (Boniface, 2000). In water monitoring, conditioning of ion-selective sensors for measurement of these species dissolved in water could be performed by controlling the pH value outside the sensor in the proximity of a gas-permeable membrane. In addition to that, internal pH control of the sensor solution could allow for reversible operation, self-cleaning and calibration.

1.4.15 Water ionizers

Called also "micro-water" or "restructured" water machines, or ionized water purifiers, in fact they are water electrolysis machines (e.g. Aqua-Tonic AT-500 from Natural Solutions). With electrolysis, the water is divided into alkaline water and acidic water. The resulting pH of the two water fractions is manually tested by the user with a color pH indicator, as it is dependent on the water composition and is predictable only when using municipal treated water and within certain limits. The alkaline ionized water is used for drinking and cooking, as it has some similarities with high-altitude mountain drinking water. The ionized acidic water is a natural astringent and is used for skin and hair treatment.

1.5 Existing methods for pH control

As shown above, the measurement and control of the pH factor is of great concern for many chemical and biological processes, including environmental monitoring, water treatment, drinking water disinfection and quality control, aqua-culture, plating industry, food processing etc. Methods for pH control are developed, based on addition of chemical reagents in the controlled media. Acids are used to decrease the pH of aqueous solutions, usually hypochloric acid (HCl) or sodium bisulfate ($NaHSO_4$). Bases like sodium hydroxide (NaOH) or sodium carbonate are used to raise pH (Chemberlin, 1995). The addition of pH correction chemicals routinely used to be done manually or with a chemical feeder. Modern instrumentation has changed this – now it is done on demand with automatic controllers, like IOTRONIC pH s2380, DUPLA pH SET 300, CHEMITROL PC6000, PULSE INSTRUMENTS 117E-PH and 170E-PH, to name a few.

A chemical controller operates through monitoring the pH of the water with direct input from an electronic sensor, consisting of a glass pH electrode and in-line static mixer. It is making adjustments with two independent dosing outputs, one for acid and another for alkaline dosage, to produce the desired pH (PULSE INSTRUMENTS, 2002). More details of existing pH control methods and instrumentation are given in the next chapter.

The control of pH is a complex problem because of the time lags in the chemical reactions that occur (Mahuli, 1992). Unless the diluent and the reactant are stable and known exactly - all the time - the control action is difficult to predict, at best. That is the main reason predictive control demands elaborate computations to be effective.

Routinely, the conditioning of chemical sensors for water monitoring is performed by the addition of chemical reagents (buffer solutions) to the aqueous environment to achieve the specified values of pH inside and outside of the sensor. This works well in laboratory conditions, but is not practical for on-line remote monitoring of the chemical composition of water in the river or in the sea, especially in depth. In the latest case, water samples are taken and eventually analyzed in the chemical laboratory.

1.6 Objectives of the research

The aim of the intended research is the development of a novel method for electrical pH control in aqueous solutions. The method should allow for chemical-free on-line pH control. A prototype pH sensor/controller is developed as a proof of the above concept. The instrument permits remote pH control, using battery power at low-maintenance (monthly or quarterly). In this way, "smart" chemical sensors could be conditioned for the monitoring of different pollutants in water.

The novel method idea is based on the modulation of pH in aqueous solutions by electrolysis. When electric current flows between two electrodes, immersed in aqueous electrolyte, at certain current density electrolysis begins - hydrogen gas bubbles evolve at the surface of the negative electrode (cathode) and oxygen gas bubbles are produced on the positive electrode (anode) interface. In the electrolysis process, water is oxidized at the anode and reduced at the cathode. If the solution is divided by ion-permeable separator, pH will gradually change over time to basic values in the cathode area and to acidic values respectively in the anode area. Due to diffusion limitations, even without a separator, dynamic pH unbalance is present in the cell. A precise electrolysis regulation is necessary to not only bias, but also accurately control pH in a desired location. A closed-

loop negative feedback electrical control system is developed to bias the cell and maintain a preset pH.

The current between the polarizing electrodes is supplied by a regulator, controlled by the feedback signal, taken from a pH-measurement sensor (electrochemical or optical), located in the controlled volume of the electrolyte.

Additional goal is to develop a prototype instrument to demonstrate the method operation and test in particular environmental monitoring applications. The desired features of the instrument are:

- Chemicals – free pH control
- On-line pH control
- Remote (battery powered) operation
- Low-maintenance
- Quick time response
- Two-way (bipolar) control
- Small area control

The presumed steps towards achieving the above objectives are listed in the next paragraph.

1.7 Structure of the thesis

The work begins with description of the existing methods and instrumentation for chemical pH control (Chapter 2). Critical analysis leads to the need of a better on-line pH controller to be developed for a number of applications. The basics of pH modulation by electrolysis in aqueous solutions and how it affects specific sensor selectivity are presented. The electrical energy and time needed to bias the pH of certain volume aqueous solution to preset limits is estimated. The idea of electrical pH controller is specified and the need for detailed development of its building blocks is identified – a pH measurement sensor and an electrolysis-based pH controller, including the measurement sensor in its closed negative feedback loop.

In Chapter 3, the pH measurement methods and sensors as part of the proposed pH controller are presented. Attention is given to the widely used electrochemical methods and instruments for pH measurement, based on a glass hydrogen ion-selective electrode

and an electronic pH-meter. Specifications of electrochemical reference electrodes and ion-selective electrodes are also discussed, focusing on their application as part of the closed feedback control loop of an electrical pH controller.

Another major topic of interest is optical fibre pH sensors, described in Chapter 4. The use of chemical buffers and colorimetric pH indicators at the sensing edge of a transducer are discussed. They may be dissolved in the controlled solution or entrapped in a soluble glass (sol-gel) layer. Also some advantages of the optical fibre sensors, applied in the electrical pH controller, such as small size, mechanical stability and especially their immunity from the electrical field of the electrolyte are addressed.

Chapter 5 is a review of the electronic feedback control instruments, applied in electrochemistry, namely potentiostats and galvanostats (used for voltage and current control, respectively). The electrochemical pH bias and control is achieved by regulation of the potential difference between the electrodes or by the electrical current flowing through them. Both systems are carefully investigated with account to their limitations, including output voltage, current, speed and bandwidth.

The power supply as a critical part of the targeted on-line controller is addressed in Chapter 6. Different primary and rechargeable battery systems are considered as power sources for an independent or remote (including wireless) monitoring. The focus is on hybrid battery systems as preferred power source, maximizing energy utilization and instant high-current drain capability. A very efficient hybrid power supply with low-maintenance is developed and tested. The instrument runtime using the developed hybrid battery power supply is estimated.

Chapter 7 contains description of the original method of electrical pH control. Examples of different possible configurations of electrical feedback control systems and alternative approaches of electrochemical and optical pH sensors incorporated in the feedback loop are demonstrated. Both the electrochemical and the optical sensors could be successfully implemented as measurement devices in the pH control system. The discussion involves specific applications and critical comparison between the two approaches.

In Chapter 8 are presented the experimental results. They confirm the feasibility of the method and show the performance of the developed prototype instrument. It contains data and graphs of the time response of the controller using either electrochemical or optical feedback methods. The spectral response of a universal pH indicator is evaluated and the accuracy and limitations of the method discussed. The experimental part begins with conditioning of ammonia optical sensor by electrical modulation. Further, applications of electrochemical pH cell control at different power supply voltages and using chemical and optical sensing are developed.

The main conclusions of the research and instrument development follow. The two basic approaches – electrochemical and optical sensing, are compared and tested against the desired specifications. Also, suggestions for future work are made.

At the end are listed the references and bibliography cited or used in this thesis in alphabetical order by the surname of the first author (the Harvard system). Also patent applications, commercial specifications and internal City University reports are also listed.

CHAPTER 2: METHODS OF PH CONTROL

Introduction

This chapter begins with a description of the pH control problem. The existing methods and instrumentation are challenged by the extremely wide range and high sensitivity required for chemical pH control. Instrumentation sensors are also subject to difficulties arising from the contact of the measurement electrode with hostile fluids. Critical analysis leads to the need of a better online pH controller to be developed for a number of applications. Here, the basis of pH modulation by electrolysis in aqueous solutions and how it affects specific sensor selectivity are presented. The idea of electrical pH controller is specified and the need for detailed development of its building blocks is identified: an electrolysis controller and a pH measurement sensor included in its feedback loop.

2.1 The pH control problem

The main difficulty in pH control is the large sensing range. The pH scale corresponds to hydrogen ion concentrations from 10^{-0} to 10^{-14} moles per liter (McMillian, 1964). Few other common measurements cover such a wide range, shown on fig. 2.1.

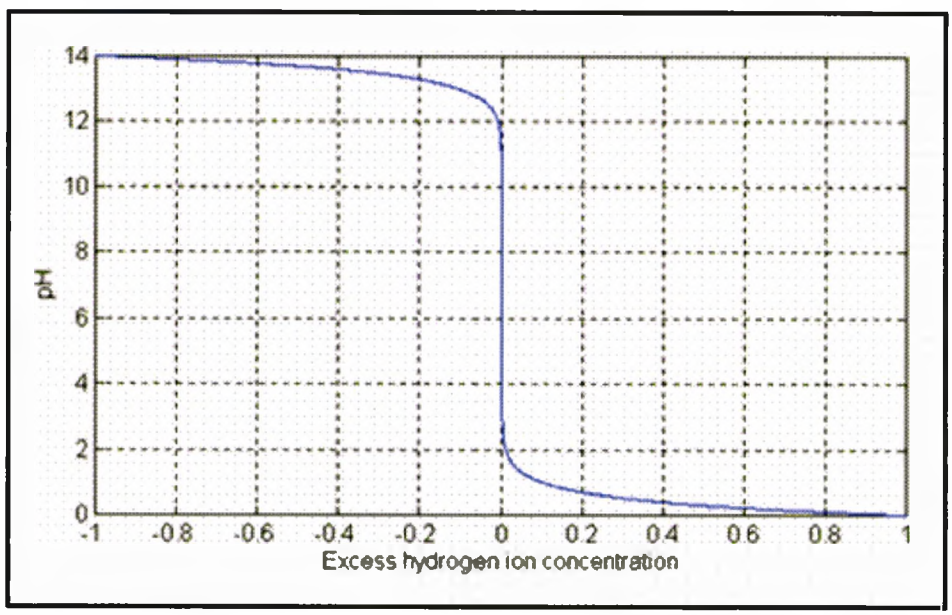

Fig. 2.1: The pH control range - minor changes in the hydrogen ion concentration lead to great pH changes and extremely high-sensitivity of the pH sensor is needed.

As the resolution of the glass pH measurement electrodes could be as low as 0.001 pH, the control instruments should be able to track hydrogen ion concentration changes of $5x10^{-10}$ moles per liter at 7 pH.

The impact of the wide measurement range and great sensitivity requirements can be illustrated by an on-line feedback control system for a strong acid and a strong base. The pH-correction reagent flow should be proportional to the difference between the hydrogen ion concentration of the process media and the set point. A reagent control valve hence should cover a range over 10,000,000:1 for a set point of 7 pH if the controlled solution is in the range of 0 to 7 pH.

Moreover, uncertainties in the control valve stroke translate directly into pH errors, such that hysteresis of only 0.00005% can cause an offset of 1 pH for a 7 pH set point (Omega Engineering, 2000). Because of the high probability to overshoot the control reagent, more sophisticated systems usually approach the set point in stages, using successively smaller control valves with high performance actuators (fig. 2.2).

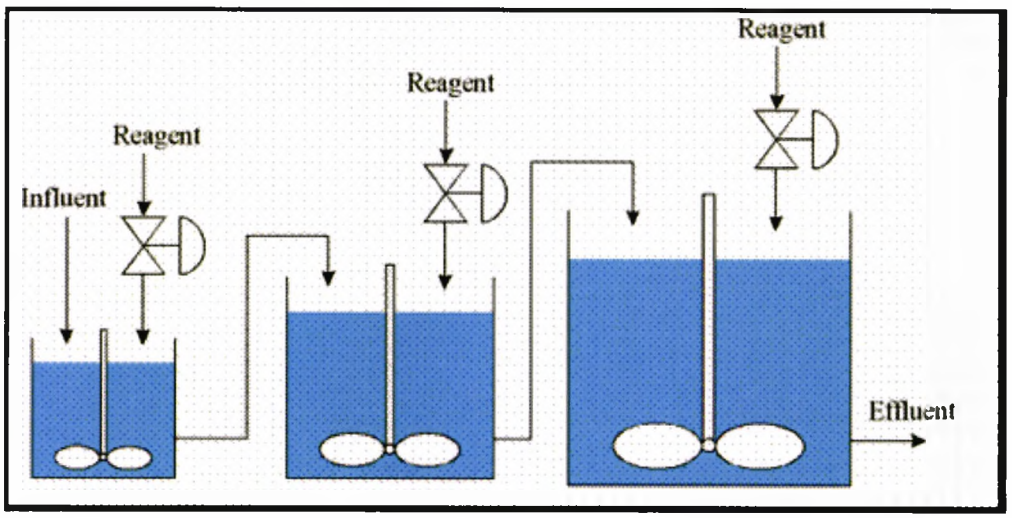

Fig. 2.2: Successive treatment pH control – precision is achieved in three stages from "coarse" to "fine" regulation to prevent the system response overshooting (Omega Engineering).

Another problem with control is the long delay, needed to mix large volumes of process material with small amounts of reagent. The reagent valves should be closely coupled to the injection point to reduce delays. PID (proportional-integral-derivative) controllers are widely used in sensors and industrial automation (Cheng, 2004). Their control algorithm is described as:

$$OUTPUT(t) = PE(t) + \frac{1}{I}\int E(t)dt + D\frac{d}{dt}E(t)$$

Equation 2.1

Where:

t = time

E = the controlled variable in the form of a tracking error, defined as the pH sensor actual measurement minus the pH set point.

P = proportional gain

I = integral gain's reciprocal

D = derivative gain

After calibration, the controller uses the output valve to force the solution pH to settle at the set point (i.e., E = 0). The first term on the right side of the equation represents the main P- action, which is the basic mode of control, but zero error could be achieved only at infinite gain. To overcome this limitation, the second term, I-mode, is introduced. This integral accounts for the sum of all previous errors in a specified time scale and slightly modifies the set point to completely eliminate errors. The third term, D-mode, is intended to speed up the control action, and also to prevent overreaction, when the process is changing rapidly (sudden disturbance away from the set point).

Analog or microprocessor pH control systems, by means of a combination of software and hardware, are used to implement PID control by driving electromagnetic reagent valves, similar to that shown on fig. 2.3 below.

Fig 2.3: Solenoid actuated valve - the reagent flow is switched "on" and "off" by electrical control signal.

A number of challenges have to be overcome in a chemical pH controller design. On-line pH control loops are likely to oscillate, if the set point is on the steep part of the titration curve. The instrumentation is frequently the source of disturbance for pH control systems, through repeatability error, measurement noise, or hysteresis of the electromagnetic valve.

There are many other problems in real applications, particularly short sensor life and glass breakage, reference electrode contamination and depletion, shelf life, maintenance requirements, power supply, noise and inconsistent readings (Electro- Chemical Devices, 2000). Concentrated chemicals, especially under pressure, are also a safety concern.

2.2 Methods of pH control

2.2.1 Chemical control

The pH of aqueous solutions traditionally is adjusted by the addition of acidic or basic chemicals into the controlled medium. Typical examples for additives to increase pH are soda ash (sodium carbonate) or caustic soda (sodium hydroxide), and to decrease pH - muratic acid (hydrochloric acid) or dry acid (sodium hydrogen sulfate). In case the

original solution contains only typical salts without acidic or basic properties, the rise or fall of pH could be very significant.

However, where there are weak acids and bases in a solution, the variation of pH with added reagents is reduced, slowing the adjustment of pH when the salt/acid concentrations are nearly equal. This is the basis of buffer action – the ability to oppose changes in pH when small amounts of acid and base are added to the solution. There are, however, many other solutions, which can receive such additions with only a slight change of pH. A weak acid becomes a buffer when alkali is added, and a weak base becomes a buffer on the addition of acid. A simple buffer may be defined as a solution containing both a weak acid and its conjugate weak base. Buffer action is explained by the mobile equilibrium of a reversible reaction:

$$A^+ + H_2O \leftrightarrow B + H_3O^+ \qquad \textbf{Equation 2.2}$$

in which the base B is formed by the loss of a proton from the corresponding acid A. The acid may be a cation such as NH_4^+, a neutral molecule such as CH_3COOH, or an anion such as $H_2PO_4^-$. When alkali is added, hydrogen ions are removed to form water; but, as long as the added alkali is not in excess of the buffer acid, many of the hydrogen ions are replaced by further ionization of A to maintain the equilibrium. When acid is added, this reaction is reversed as hydrogen ions combine with B to form A.

Buffering action has practical significance in real systems of interest. An important case is pH control in hard water, where the hardness will affect the speed of change and the stabilization of pH. There are two types of water hardness: general hardness (GH) and carbonate hardness (KH). GH is primarily the measure of calcium (Ca^{++}) and magnesium (Mg^{++}) ions in the water. Other ions can contribute to GH but their effects are usually insignificant and the other ions are difficult to measure. GH will not directly affect pH, although hard water is generally alkaline due to some interaction of GH and KH. In freshwater (of neutral pH), hydrogen carbonate ions predominate and in saltwater basins carbonate ions begin to play a role. Alkalinity is the measure of the total acid binding capacity (all the anions which can bind with free H^+) but is comprised mostly of carbonate hardness in freshwater systems. Thus, in practical freshwater usage, the terms carbonate hardness, acid binding, acid buffering capacity and alkalinity are often used interchangeably. KH acts as a chemical buffering agent, helping to stabilize pH. KH is

generally referred to in degree of hardness and is expressed in $CaCO_3$ equivalents just like GH.

If a strong acid such as nitric acid is added to water, it completely dissociates into hydrogen ions (H^+) and its "conjugate base" or "salt", NO_3^- or nitrate. The hydrogen ions freed in the reaction then increase the concentration of hydrogen ions and reduce the pH. Since nitric acid is the end product of the nitrogen cycle, this explains why water pH tends to decrease and nitrates tend to increase over time. When the water has some carbonate buffering in it, the hydrogen carbonate ions will combine with the excess hydrogen ions to form carbonic acid (H_2CO_3), which then slowly breaks down into CO_2 and water. Since the excess hydrogen ions are used in the reaction, the pH does not change very much. Over time, as the carbonate ions are used up, the buffering capacity will drop and larger pH changes will be noted. From this it is clear why water with low KH seem unstable - as acid is produced by biological action, the KH is used up; when this has happened, the pH is free to drop rapidly as H^+ ions are generated.

The GH of water could be raised by the addition of calcium sulfate or magnesium sulfate. This has the drawback of introducing sulfates (SO_4^{--}) into the water, so care should be exercised. Calcium carbonate can be used, but it will also raise the KH. Various combinations can be used to produce the desired results. KH can be increased easily by adding sodium hydrogen carbonate. Calcium carbonate will increase both KH and GH in equal parts. For example, one tea spoon (about 6 grams) of sodium hydrogen carbonate ($NaHCO_3$) per 50 liters of water will increase KH by 4 units and will not increase general hardness (Booth, 1993). Two teaspoons (about 4 grams) of calcium carbonate ($CaCO_3$) per 50 liters of water will increase both KH and GH by 4 units. Different proportions of each can be used to get the correct KH/GH balance.

In more detail, the pH of a buffered solution can be expressed by the Henderson-Hasselbach equation:

$$pH = pK + \log \frac{C_B}{C_A}$$

Equation 2.3

in which pK is the negative logarithm of the apparent ionization constant of the buffer acid and the concentrations are those of the buffer base and its conjugate acid. In the hydrogen carbonate and carbonate buffering cases, this is:

$$pH = 6.37 + \log \frac{[HCO_3^-]}{[H_2CO_3]} \quad \text{and} \quad pH = 10.25 + \log \frac{[CO_3^{--}]}{[HCO_3^-]}$$

Equation 2.4

The values of pK are affected significantly by temperature and chlorinity. If the pH versus the ratio of base to acid is plotted, the logarithmic graph on fig. 2.4 is obtained.

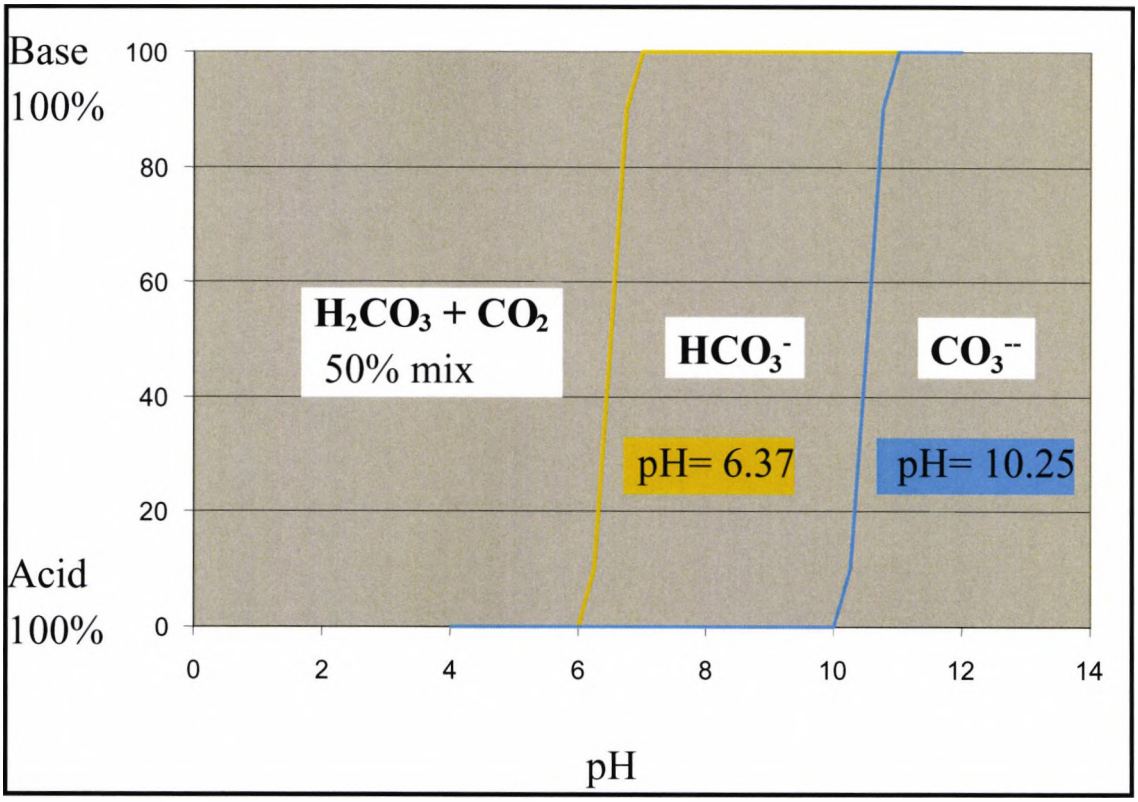

Fig. 2.4: Buffer action helps sustain narrow pH range over wide acid to base ratio in aqueous solutions.

Hydrogen carbonate buffering is effective over ratios from 1:100 up to 100:1. This gives an effective pH range of 4.37 to 8.37, which, not coincidentally, defines the pH range of most aquatic life.

2.2.2 Basic types of chemical pH control

Several options for chemical pH control are most commonly used (Novak, 2002), as discussed further.

2.2.2.1 Discontinuous batch processing (System A)

This system uses an on/off relay controller for "batch" processing, as shown on fig. 2.5 below. The process sequence is the following:

A. The process fluid is pumped into the controlled tank

B. Mixing starts and chemical is added until the desired pH is reached

C. Process fluid is pumped out of the tank

A delay between adding the chemical and sensing the resulting pH change should be considered when sizing the final control element. If the last is oversized, the system will have unacceptable overshoot. With faster mixing, the delay and overshoot can be reduced. This simple system cannot easily handle a continuously flowing process.

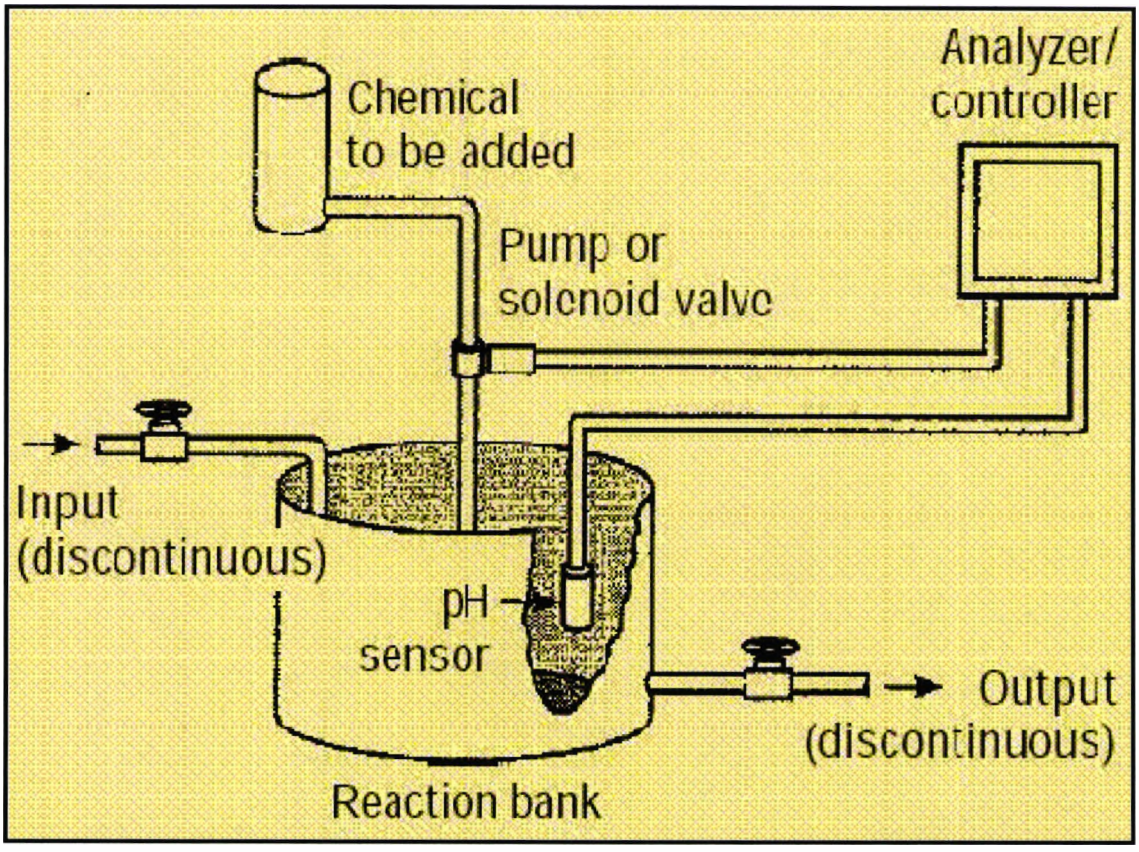

Fig. 2.5: Discontinuous batch processing where the input, chemical control and output of the controlled media are carried out in sequence (Novak, 2002).

2.2.2.2 Continuous batch processing (System B)

In this system the process fluid input is continuous, and an on/off relay controller with hysteresis is required. The "deadband" will hold the final control element "on" longer than System A. The result is smoother operation without rapid cycling.

The final control element can be a pump or an on/off valve as the one shown previously on fig. 2.6. Its sizing is complicated and depends on many factors. In this case, a titration curve is valuable. It may be necessary to use two final control elements, each delivering different amount of chemical and having different set point. For example, one valve may deliver stronger sodium hydroxide below pH 3 and another weaker sodium hydroxide below pH 4. Good mixing is very important to this system. In general this system can be fairly accurate, but pH will tend to cycle between levels.

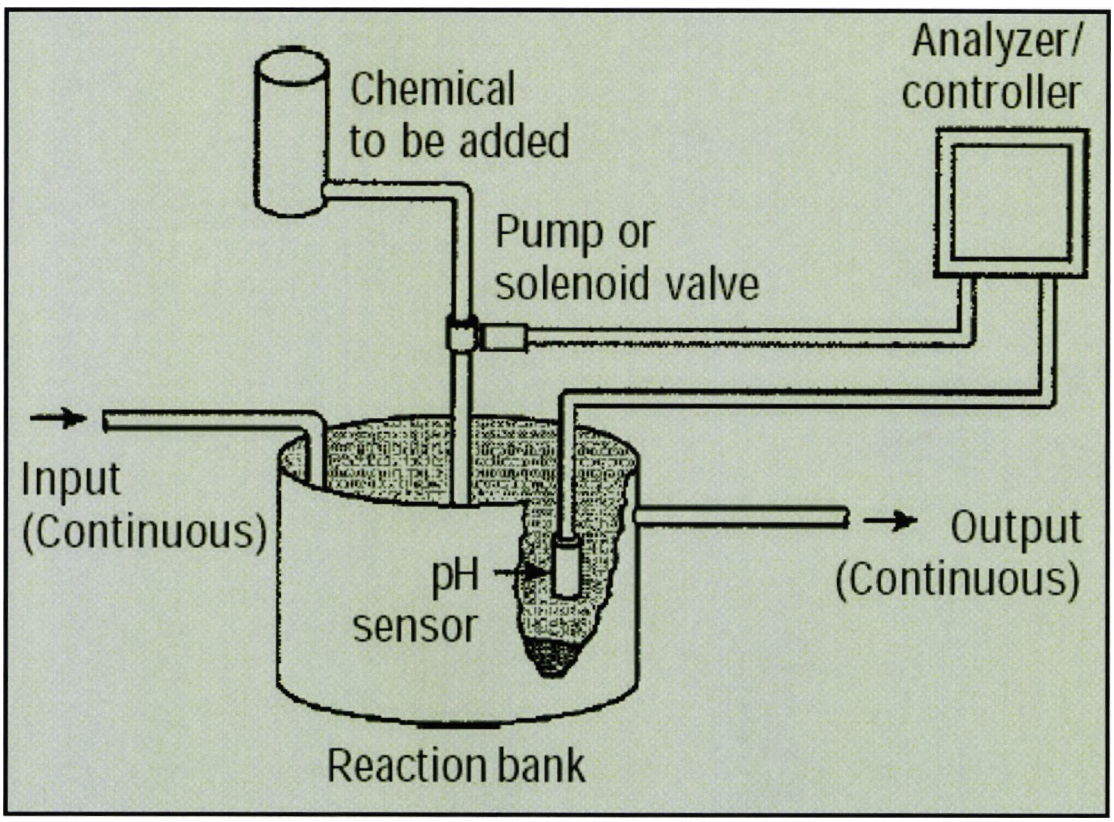

Fig. 2.6: Continuous batch processing where the input, chemical control and output of the controlled media are carried out simultaneously (Novak, 2002).

2.2.2.3 Continuous batch processing with time delay (System C)

This type of system uses a proportional gain controller with time variation (duty cycle) output for application like System B, but with significant delay between the chemical addition and the pH sensing. This is the case when the controlled solution flows through a long tank or a series of tanks, as previously shown on fig. 2.7.

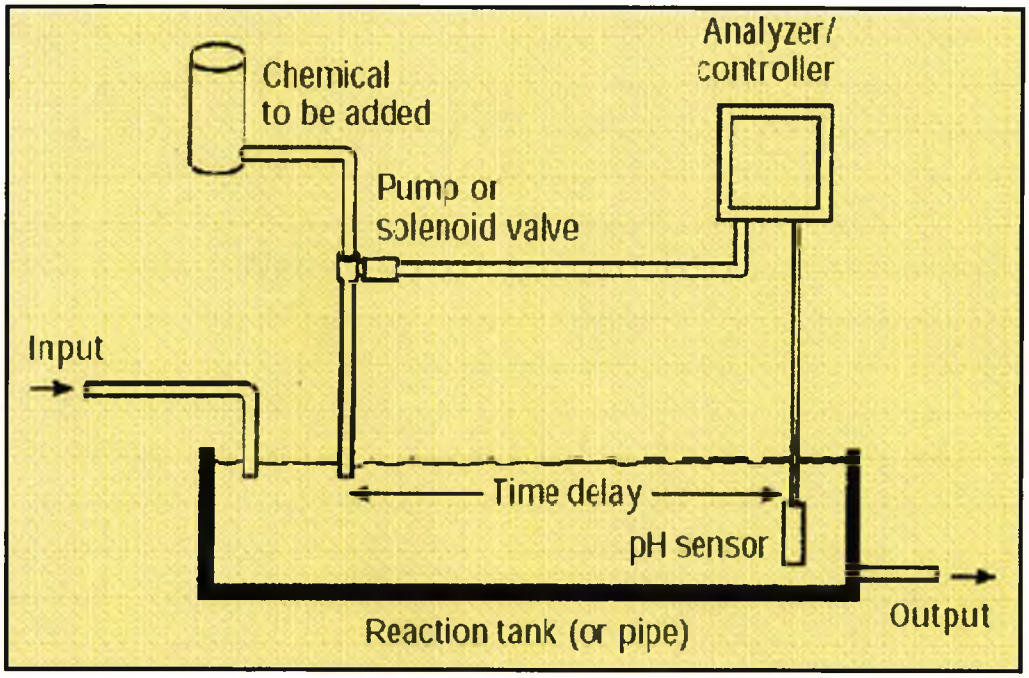

Fig. 2.7: Continuous proportional batch processing with time delay to prevent premature sensor reaction to the added chemicals (Novak, 2002).

The time proportioning output is a switch closure that activates a solenoid valve or pump. The analog output of the controller is fed to an electronic "precedent of cycle timer" to electrically adjust the "on" time from 0 to 100%. The time base of the cycle timer is electrically adjustable from a few seconds to a few minutes. The chemical delivery to the system is in a series of "shots" of chemical. If the added chemical is not sufficient, the controller output will affect the timer and shorten the "off" time. The cycle time should usually be less than the delay time of the system, so that a series of shots are in the tank and gradually mixing. By the time the chemical reaches the sensor, it should be mixed enough, so that the sensor does not measure large variations of pH. The final control element should be sized so that it cannot deliver more than five times the amount of chemical required at the maximum system load.

2.2.2.4 Continuous on-line control (System D)

This system uses a proportional gain controller with an analog output for two general types of pH control:

A. pH is only to be adjusted slightly

B. PH is to be adjusted to a value over 10 or fewer than 4 (away from neutral)

The controller (fig. 2.8) consists of the following components:

- pH sensor
- Controller with analog output
- Proportional valve or pump (electrically controlled)
- Mixing device, placed between the reagent delivery and the pH sensor

Critical to the proper operation of this system are the mixing and the delay between adding chemicals and sensing the resultant pH. The mixing must be thorough and the delay time should be not more than few seconds. A long delay time will result in the process pH cycling back and forth about the desired set-point. An inherent characteristic of this system is that the actual controller pH set point will be slightly different from the desired process pH value.

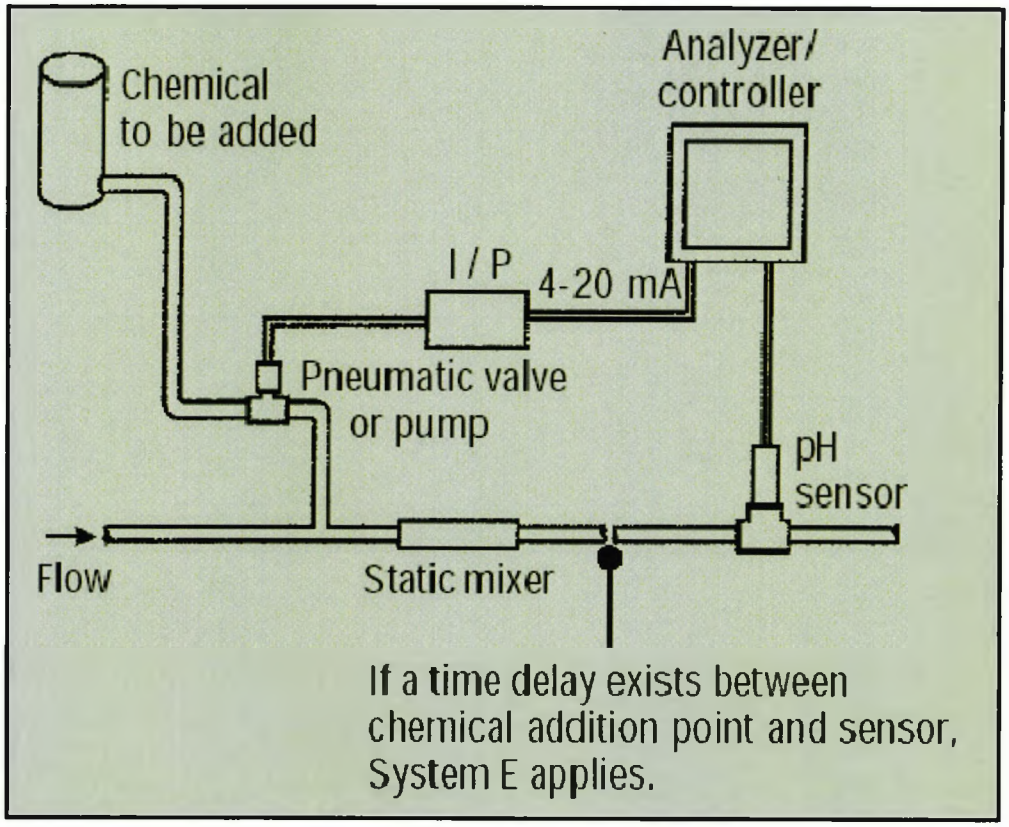

Fig. 2.8: Continuous on-line pH control using a proportional reagent valve with analog control signal (Novak, 2002).

2.2.2.5 Continuous on-line two-mode control (System E)

The two-mode controller is much more complex than the proportional, one-way controller, and is used where the last under-performs.

An integral (reset) function of this controller will try to adjust the process to the desired set point if it is physically possible. The two-mode controller also has a sample/hold feature that allows to a delay between the chemical addition and the pH sensing.

2.2.2.6 Two-mode control with on/off switch (System F)

This system is a hybrid between Systems E and C and is used when the chemical to be added is abrasive or tends to clog small openings (lime slurry, for example). For this reason, an on/off valve is preferred over the proportional valve, to avoid erosion of its internal parts and to provide more reliable reagent addition.

2.2.3 Examples of automatic pH controllers (based on chemical control)

Automatic pH controllers based on chemical control are available from many manufacturers. An example of a remote pH controller is shown on fig.2.9 below.

Fig. 2.9: Remote pH controller that is safely located away from the chemical reactor area (Omega Engineering).

2.2.3.1 Irrigation water pH control

The pH of irrigation water is controlled by acidic additive. This is generally either sulfuric acid, or pHAIRWAY (A Unocal pH adjusting fertilizer, Werecon, 2000). These systems are used where water is alkaline, high in salts, or high in Total Dissolved Solids (TDS). Almost all systems are proportional, injecting varying amount of chemical, corresponding to the water flow from the system. This is important in order to ensure constant chemical to water ratio and hence the same amount of nutrients at high flow rates as at low flow rates.

2.2.3.2 Water hardness control

If hydrogen carbonate ions are added to the control fluid (for example sodium hydrogen carbonate or calcium carbonate), the base to acid ratio will increase and the pH will increase. From fig. 2.1, the rate of increase will be determined by the starting pH: at pH = 6.37, a lot of hydrogen carbonate ions are needed to change the pH; at pH=7.5, a lot less are needed.

The rise in pH that occurs when KH is added will be balanced to a degree by the dissolved CO_2 in the water. The CO_2 will form small amounts of carbonic acid and hydrogen carbonate that will tend to reduce the pH. This mechanism gives a way to regulate pH. If the pH of a solution is determined primarily by the carbonate buffering system, then the relation of pH and KH and dissolved CO_2 is fixed. A change of either KH or CO_2 will set the pH. An automatic CO_2 injection system will measure pH and inject CO_2 to lower it if it exceeds a set point. In this case KH is fixed. As the CO_2 is used by plants and diffuses into the atmosphere, the pH will rise. The controller cycles the CO_2 on and off to keep the pH around a fixed value. A chart showing dissolved CO_2 levels in ppm for a range of KH and pH values is enclosed in Appendix 1.

2.2.3.3 Non-linear controller

A nonlinear model-based control technique is developed and laboratory demonstrated for in-line acid neutralization using a multiple base injection approach (Desai, 1994). The controller chooses one of two simple, steady-state, three-parameter, nonlinear phenomenological models which together mimic a wide range of titration curves from strong acid to highly buffered systems. The models are parameterized from on-line process data whenever nearly steady-state conditions are statistically identified. Control performance was achieved in the presence of both ramp and step changes in acid type, acid concentration and flow rate upsets. Both industrial wastewater and mixtures prepared with acetic, phosphoric and sulfuric acids with and without common ion buffering and sodium carbonate were neutralized with sodium hydroxide.

2.2.4 Electrical pH modulation

2.2.4.1 Principle of operation

The method of electrical or electrochemical pH modulation is based on the electrical decomposition of water to its components, hydrogen and oxygen. Electrical decomposition of water is known for the last two centuries. When direct current is submitted through an aqueous solution of inorganic acid or base, hydrogen and oxygen develop at the cathode and the anode, respectively, in gaseous form and in quantities conforming to Faraday's law (Atkins, 1990). Two electrolysis reactions take place:

Anode: $\mathbf{2H_2O = 4H^+ + O_2 + 4e^-}$	**Equation 2.5**
Cathode: $\mathbf{2H_2O + 2e^- = H_2 + 2OH^-}$	**Equation 2.6**

The electrical current is applied through a pair of non-reactive (to prevent any adverse side-reactions) electrodes. Regardless of the basic or acidic nature of the electrolyte, the water is dissociated into ions, which will be the carriers of the electrolytic current. Their presence in the aqueous medium improves its conductivity without affecting the overall electrolysis process. The released hydrogen gas will cause hydrolysis of more water molecules to maintain the balance in the electrolyte and hence cause an increase in OH^- concentration. Thus the pH around the cathode will increase, while in the anode area the oxygen liberation leads to increased concentration of H^+ or H_3O^+ (hydronium ions) and hence an associated decrease of the pH (Bourilkov, 1996).

2.2.4.2 Potential – pH equilibrium diagrams

It is desired to describe the electrochemical reactions that occur in aqueous solution considering the water, H_2O, the dissolved hydrogen ions, H^+, and the free electrons, e-, which take eventually part in the reaction. The equilibrium conditions of all reactions are a linear function of pH and the electrode potential as well as the gas partial pressure and the activities of the dissolved species other than the H^+ ions. The range of equilibrium conditions is expressed graphically by a straight line, called a Potential /pH diagram. This relation for 1 atmosphere partial pressure of the hydrogen or oxygen is shown on fig. 2.10 (Hampel, 1964).

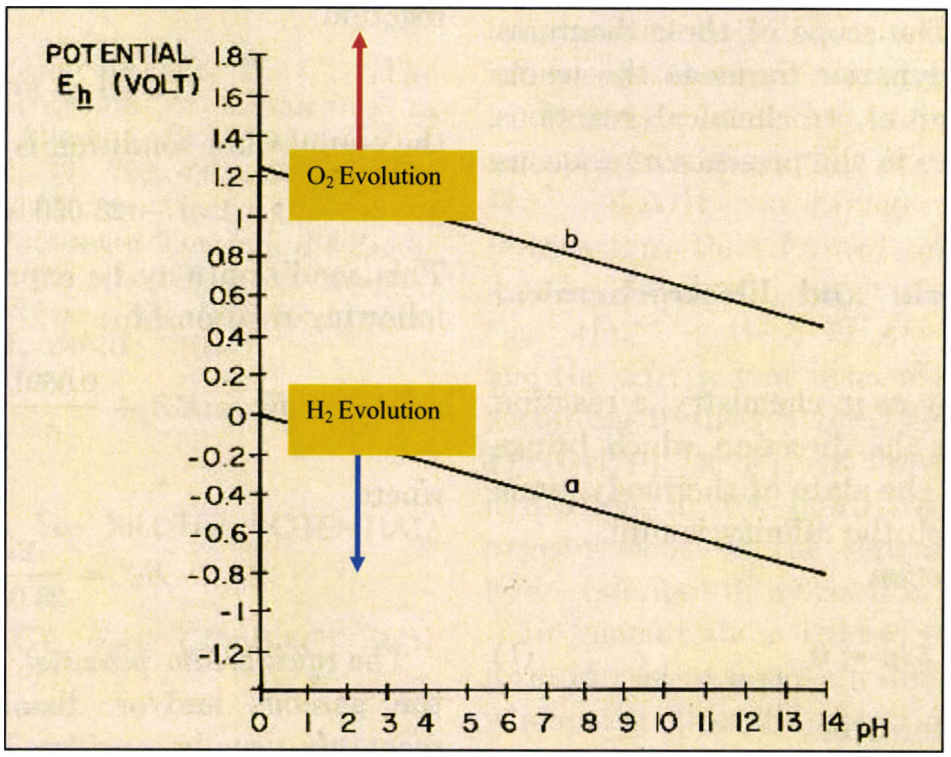

Fig. 2.10: Potential/pH diagram showing linear relation between electrode potential and pH, the basis of electrochemical pH sensing (Hampel, 1964).

The area between the two lines is the area of thermodynamic stability of water at 1 atm. Under line "a" the evolution of hydrogen will cause water reduction and increase of pH. Above line "b" the evolution of oxygen will cause water oxidation and decrease of pH. This graph shows a constant minimum potential difference (PD) needed between the two electrodes to cause water dissociation regardless of the solution pH.

The simple electrolysis cell shown on fig. 2.11 is used to demonstrate the basics of electrochemical pH modulation in water. The configuration of the electrochemical cell, separated between the two electrodes as in batteries, illustrates that reduction/oxidation (REDOX) reactions can be separated into an oxidation half reaction, and a reduction half reaction. Half reactions are also referred to as half-cell reactions because they occur in physically separate cells. Anode is the electrode where the oxidation occurs. It will be charged positive. Cathode is the electrode where reduction is occurring. It will be charged

negative. Electronic conductor provides for electron movement between electrodes exterior to the solution.

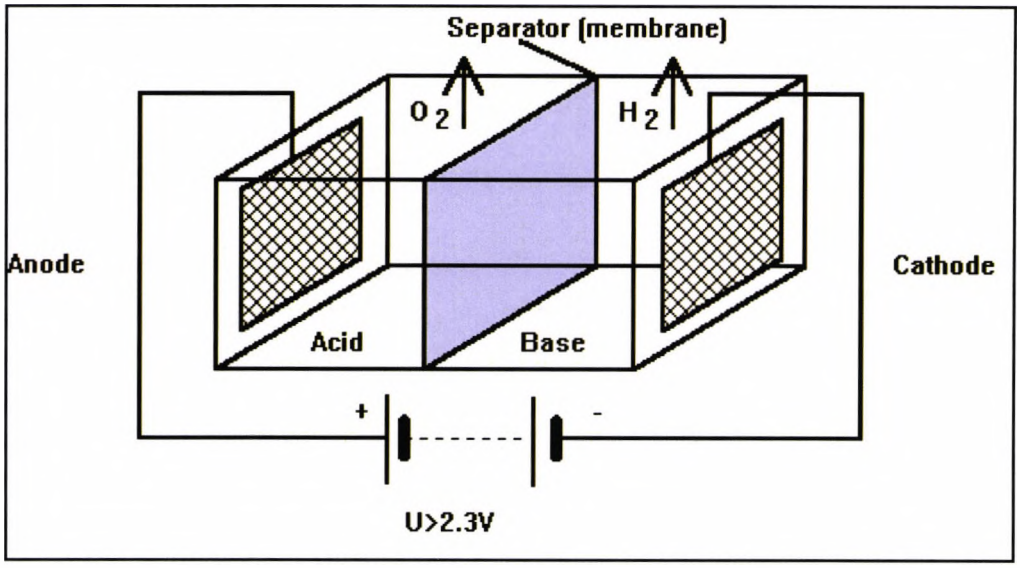

Fig. 2.11: The electrical pH modulation principle, where by electrolysis in a separated electrochemical cell, the pH of the cathode and anode parts can be varied.

Ionic conduction provides for charge movement between the electrodes in the interior of the solution. Permeable membrane allows ion transfer between the half- cells. The time for neutralization is long due to the different diffusion rate of the hydronium and hydroxyl ions through the membrane. This permits for dynamic pH unbalance between the two half-cells.

The release of hydrogen will increase the OH^- concentration and thus the pH around the cathode, while in the anode area the oxygen liberation leads to increased concentration of H^+ and hence an associated pH decrease. Either the cathodic or the anodic reaction could be used for pH modulation, by separating the complementary reaction using a membrane or distance from the controlled area. In some cases, if the complementary reaction is undesired (for example the evolution of hydrogen gas), it can be substituted by more suitable reaction (Spinu, 1997):

$$Cu^{2+} + 2e^- = Cu^0 \text{ or } Fe^{3+} + e^- = Fe^{2+}$$ **Equation 2.7**

Water pH electrochemical modulation can be achieved over a wide range (Rogov, 1989). Values of pH up to 10 in the cathode region and down to 4 in the anode region may be achieved in a reasonably short time, depending on the power supply voltage and the chemical composition of the aqueous solution.

One Farad (F) of electricity through the pair of electrodes will cause 1 mol of hydronium (H_3O^+) ions to be generated at the anode (acid) and 1 mol of hydroxyl OH^- (base) ions at the cathode. According to Faraday's law,

1F = 96 467 C (Coulombs)

where C = As (Amperes x seconds) **Equation 2.8**

One Farad or 26.8 Ah of electricity will be necessary to change pH of 1 litre neutral water from 7 to 0 or from 7 to 14 by generating correspondingly 1 mol of hydronium or 1 mol of hydroxyl ions. Thanks to the logarithmic pH scale, for practical purposes, e. g. ion-selective sensor conditioning, where pH is regulated from 7 up to 10 or down to 4, 10^4 times less electricity, or only 2.68 mAh are required. This can be achieved for example by applying between the two electrodes electrical current from a battery with a magnitude approximately 200 mA for 48 seconds.

The minimal cell voltage, under thermodynamic equilibrium conditions at 25°C, atmospheric pressure and in pure water, is equal to 1.229V. In practice, the required cell voltage is higher due to dissolved salts, the hydrogen and oxygen over-voltage, the IR voltage drop through the electrolyte and the polarization due to the concentration gradient around the electrodes. Noticeable evolution of O_2 and H_2 gases begins around 1.7V (Regner, 1957) and becomes more visible above 2.3V. As described in detail further in Chapter 6, Li-ion batteries with an operating voltage range from 4.2V (charged) down to 3V (discharged) are preferred as a power source for autonomous operation of the pH controller.

The required battery energy can be calculated from:

$$E_{batt.}\,[Wh] = V_{batt.\,av.} \times I_{cell}[A] \times t[h] \qquad \textbf{Equation 2.9}$$

For the above example of 2.68 mAh supplied for sensor conditioning from a Li-ion battery with a 3.7V average discharge voltage, about 10 mWh energy will be used. In most practical cases the aqueous solution contains dissolved salts and much larger quantities of ions are required to achieve the set pH point. The buffering action of the electrolyte slows down the pH modulation. Also, if the electrolytic cell is not divided to a cathode and an anode areas by an ion permeable membrane (fig. 2.11) there will be a neutralization process simultaneously with the pH modulation, slowing down pH control. The hydroxyl ions in water solutions are known to diffuse at a rate of 5.2×10^{-5} cm/s, hence intermittent local control is possible without mixing the solution. A dynamic equilibrium can be maintained for continuous control.

The number of generated hydroxyl ions at the cathode equals the number of hydrogen atoms released as gas (eq. 2.6). The volume of hydrogen gas released by the cathode in the above example can be calculated by the ideal gas equation:

$$V = nRT/P \qquad \textbf{Equation 2.10}$$

If case of room temperature and atmospheric pressure (STP):

$n = 10^{-4}$ mol

R = 0.0821 atm/mol-K

T = 273 K

P = 1 atm.

V = 2.24 ml

The volume of the oxygen gas generated at the anode will be half of this amount (eq. 2.5). The pH controller cell design needs to allow for safe release of the generated gases in the atmosphere.

2.2.4.3 Selectivity and pH modulation

Proton movement across membranes is part of many important processes. The net proton flux to or from membranes can be determined by measuring the proton electrochemical potential gradient in the adjacent solution. For a given concentration of a buffer, which has a single pK, the flux ratio rises with pH when the solution pH is lower than the buffer pK. The slope is about 2 on a log10 scale. As the pH increases above the pK, the flux ratio levels off to approach its maximum. With mixed buffers, or one having two or more pK values, the flux ratios are additive: each buffer acts independently based on its concentration and its pK value. Solutions always have buffering effects of water itself and also of carbonates due to carbon dioxide dissolved from the atmosphere. If a solution is at pH 6, the flux carried by water and carbonate is only about 1% of the measured proton flux.

The measurement of gaseous species [for example those containing sulfur dioxide (SO_2), carbon dioxide (CO_2) and ammonia (NH_3)] producing acidic or basic waters is of great importance for environmental monitoring applications. Routine measurements of such species are maintained in laboratory environment, using preconditioned water samples and ion-selective electrodes, or absorption spectrometry. In case of ammonia ion-selective electrode, additional chemical reagents (such as pH ion-selective adjusting solution containing 5 mol NaOH) are added to the sample, to ensure that the ammonia is in the molecular form and can permeate the membrane, i.e. travel from the external sample to the internal sensor solution (Bourilkov, 1996). In the second case of absorption spectrometry, a reagent mixture containing sodium dichlorisocyanurate and sodium nitroferricyanide is added and the sample is thermally treated, before concentration measurements of the species of interest are performed.

An optical analogue of a commercial electrochemical ammonia sensor has been reported, which uses a gas permeable membrane and a pH-sensitive dye (Fneer, 1995). Some important pollutants in water such as nitrous oxide (N_2O, SO_2, CO_2 and NH_3) are soluble in the molecular form and partially ionize in water, in a way that is independent of the sample pH. For the purpose of ion-selective measurement, a gas-permeable membrane can be used to allow only the transport of the molecular form of the pollutant. The

solution pH is modulated to ensure the transition of the species of interest from ionic to molecular form (NO, NH_3, SO_2, CO_2) and to allow their permeation through the membrane. This is usually carried out by the addition of reagents to allow such a pH change, e.g. in work reported by Mouaziz et al. (1993). In the case of ammonia measurement, NaOH is used to ensure a high pH (10) where ammonia exists as NH_3. The ammonia gas then can be transported through the membrane, while other soluble species that require acidic environment to transform to molecular form will be in the ionic state e.g. (NO_3^-, SO_3^-, CO_3^- etc.).

Following the goals set in the beginning, the pH control system will be developed further with the implementation of electrochemical techniques for pH modulation, applicable to both gas-permeable and ion-selective membrane sensors. Electrochemical modulation of pH is used to replace the addition of chemicals and allow the reversible operation of the sensors. It is anticipated that composite transducers based on the described method will find field applications, such as on-line monitoring of waste water chemical composition.

2.2.4.4 Example 1: Electrochemically Regenerated Ion Suppression (ERIS)

A new suppression technique called ERIS with application in Ion-chromatography had been developed, patent pending (Alltech, 2000). A solid-phase chemical suppressor is regenerated via an electrochemical pH modulation technique for continuous, reagent free operation.

Suppressor-based conductivity detection is one of the most popular detection methods for low-level ion analysis. The suppressor improves the detection sensitivity by reducing the background conductivity of the eluant, while enhancing the analyte signal.

In the Alltech ERIS 1000 Autosuppressor, two electrochemical cells are packed with either cation (for anion analysis) or anion (for cation analysis) exchange resins, and a constant current power supply. The eluant from the analytical column flows through one cell at a time. While one cell is being used to suppress the column effluent, the detector effluent is recycled back through the second cell where electrochemical regeneration takes place.

The suppressor cells are equipped with two electrodes. The cation and anion exchange resins are sandwiched between these two electrodes. The detector effluent (typically water or carbonic acid) that is passed through the cell will undergo electrolysis when current is applied across the cell. The products of electrolysis regenerate the anion and cation suppressor cells. For anion analysis, the anode is connected to the inlet side of the detector effluent. Hydrogen ion and oxygen gas are generated at the anode. Since the detector effluent is flowing from the anode to the cathode side of the cell, the released hydrogen ion is carried by this flow across the sodium form resin, converting it back to the hydrogen form by ion exchange. The released oxygen gas, hydrogen gas, and sodium hydroxide are delivered to waste.

If the polarity of the cell is reversed and the anion exchange material is replaced with cation exchange material, the same configuration may be used as a cation suppressor. For fast visual verification of the suppressor operation, the resin is coated with an inert dye, as shown on fig. 2.12:

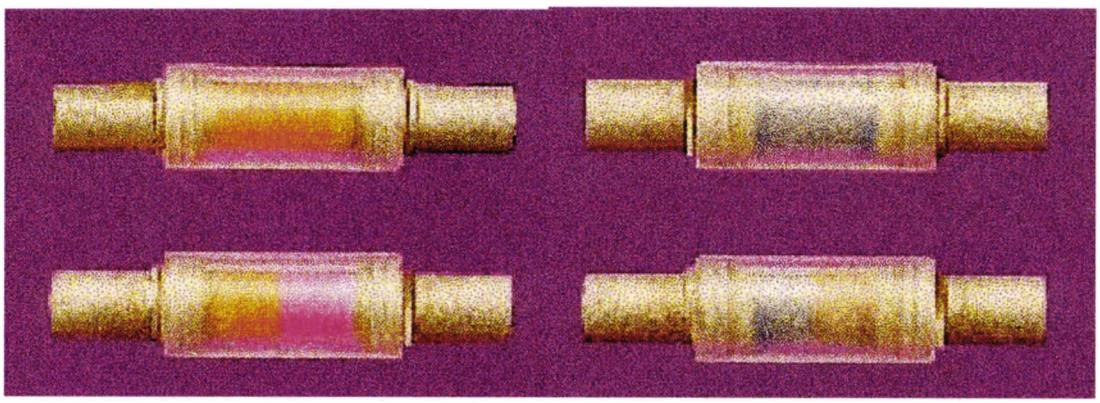

Fig. 2.12: Dye (pH indicator) color changes in the process electrochemical cells allow fast visual verification of electrochemical regeneration.

For anion analysis, the color changes from gold to magenta, as the hydrogen ions are being replaced by the sodium ions from the effluent. The color change may be monitored easily through the transparent suppressor cell housing. For cation analysis, the color changes from blue to beige as the hydroxide ions are being replaced by chloride (or methane sulfonate) ions from the effluent.

2.2.4.5 Example 2: Integrating an electrochemical pH control unit into a hydroponics system

Hydroponic plants growth is mostly an acid consuming process. The quantity of nutrients transferred by electrical migration through the membrane will be proportional to the

quantity of H^+ ions required to maintain the desired pH level in the root-zone environment (Spinu, 1999). The diagram on fig. 2.13 illustrates the approach of integrating an electrolytical pH apparatus in the supply water line of a hidroponic system.

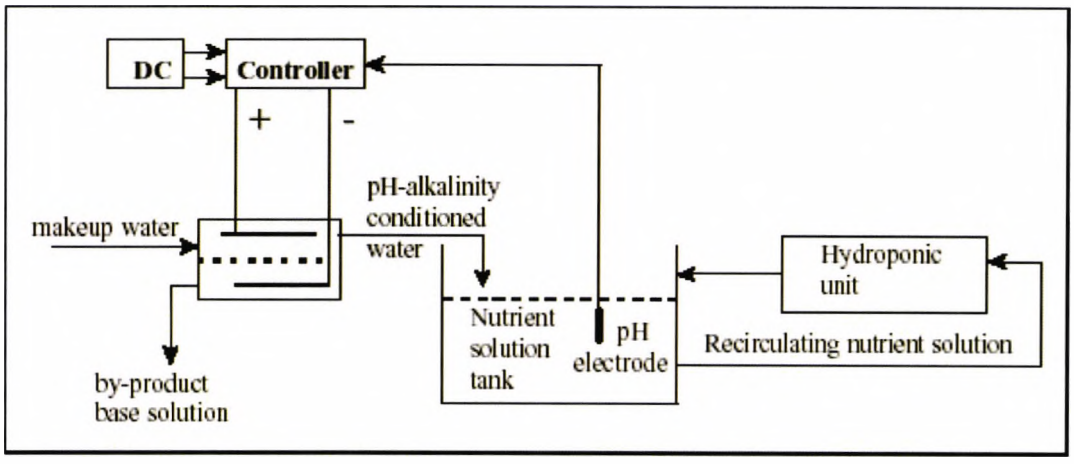

Fig 2.13: Hydroponic system using electrochemical control to condition the plants root water to the desired pH value.

Summary

In this chapter, the basics of the pH control problem were discussed. The numerous difficulties in the implementation of chemical control were shown – the need to add chemicals in the controlled fluid using mechanical devices, the delayed and unstable operation, the system complexity, the need of maintenance, the safety concerns etc. The basic types of chemical pH control were explained and examples of existing pH control systems - demonstrated. The method of electrical pH modulation was presented as an alternative of the chemical control method. Several implementations of pH biasing for conditioning of sensors were offered. Our goal is to develop a method to regulate and maintain a set pH using a closed loop feedback electrical control system. This is the next logical step in the development of the open-loop systems described above.

An important part of the control system, the pH measurement sensor will be addressed in the next chapter. Also the components of this subsystem - Reference electrodes, Ion-selective electrodes and the electronic measurement interface - will be discussed in more detail.

CHAPTER 3: ELECTROCHEMICAL PH SENSORS

Introduction

The electrochemical method of pH measurement in aqueous solutions is based on the relation between the hydrogen ion concentration and the electrochemical potential of a hydrogen ion- selective electrode. This potential is measured differentially, versus the potential of a reference electrode, immersed in the same solution. The high internal resistance of the electrochemical electrodes requires the use of high impedance electronic measurement interface. In this chapter, we start with basic pH definitions, followed by a review of the ion-selective and reference electrodes, as components of the pH sensor. Later, the entire measurement instrument, including the electronic circuit, is presented, and the problems related to the pH control application are discussed.

3.1 Definitions related to pH measurement

3.1.1 Auto-ionization of water

The self-ionization of water may formally be treated as a dissociation of the water molecule:

$$H_2O = H^+ + OH^-$$ **Equation 3.1**

although it should better be considered as a proton transfer from one water molecule to another:

$$H_2O + H_2O = H_3O^+ + OH^-$$ **Equation 3.2**

For either representation, thermodynamic reasoning leads to a constant ionic product for water:

$$a_{H+}a_{OH-} = \text{constant} \times a_{H2O} = K_w$$ **Equation 3.3**

where **a** is the activity and K_w is the autoprotolysis constant of water.

Water is amphiprotic - it can act as both an acid and a base:

$$\underset{\text{Acid}}{HCl} + \underset{\text{Base}}{H_2O} \text{ ---- } H_3O^+ + Cl^-$$ **Equation 3.4**

$$\underset{\text{Acid}}{H_2O} + \underset{\text{Base}}{NH_3} \text{ ---- } NH_4^+ + OH^-$$

Equation 3.5

One molecule may act as an acid by donating a proton to another water molecule acting as a base. This is an example of auto-protolysis equilibrium, a proton transfer equilibrium involving a single substance:

$$\underset{\text{Acid}}{H_2O} + \underset{\text{Base}}{H_2O} = H_3O^+ + OH^-$$

Equation 3.6

The autoprotolysis constant is:

$$K_w = a(H_3O^+)a(OH^-)$$

Equation 3.7

$$pK_w = -\log K_w$$

Equation 3.8

3.1.2. pH

The pH factor represents the acidity or basicity of water on a logarithmic scale that is the negative logarithm of the molar concentration of hydrogen ions H^+ in the water:

$$pH = -\log (H^+)$$

Equation 3.9

The range of pH values is from 0 to 14, with 7 being neutral. The pH scale is logarithmic. Small changes in pH therefore have large effects and this is why close pH control is critical to aqueous solutions.

$$K_w = 1.008 \times 10^{-14} \ (pK_w = 14.00) \text{ at } 25^\circ C$$

Equation 3.10

Equation 3.10 shows that only a few of the water molecules are ionized. The concentrations of H_3O^+ and OH^- are equal and so are their activities:

$$a(H_3O^+) = a(OH^-)$$ **Equation 3.11**

Therefore

$$a(H_3O) = K_w^{1/2} = 1.004 \times 10^{-7} \text{ at } 298^\circ \text{ K}$$ **Equation 3.12**

The wide span of values is compressed if we use the pH scale, where

$$pH = - \lg a(H_3O^+)$$ **Equation 3.13**

It is also convenient to use pOH, which is defined as:

$$pOH = - \lg a(OH^-)$$ **Equation 3.14**

By taking logarithms of Equation 3.7:

$$pK_w = pH + pOH$$ **Equation 3.15**

In pure water pH = pOH, because the activities of the two ions are equal:

$$pH = 1/2\ pK_w = 7.00$$ **Equation 3.16**

In acidic aqueous solutions, $\mathbf{a(H_3O^+)}$ is greater than in pure water, and so **pH<7**; in basic solutions, **pH>7**. At higher temperatures, pK_w decreases and so does the pH at neutrality.

3.2 Electrochemical reference electrodes

In Potentiometry, a field of Electroanalytical Chemistry, a potential is measured under the conditions of no current flow. The measured potential may then be used to determine the analytical quantity of interest, generally the concentration of some component of the analyte solution. The potential that develops in the electrochemical cell is the result of the free energy change that would occur if the chemical phenomena were to proceed until the equilibrium condition has been satisfied.

This concept is typically introduced in quantitative analysis in relation to electrochemical cells that contain an anode and a cathode. For these electrochemical cells, the potential difference between the cathode electrode potential and the anode electrode potential is the potential of the electrochemical cell. If the reaction is conducted under standard state conditions, this equation allows the calculation of the standard cell potential. When the reaction conditions are not standard state, however, one must utilize the Nernst Equation (3.19) to determine the cell potential.

Three electrodes which meet most adequately the requirements for reference electrodes will be considered in more detail: these are the hydrogen, silver-silver halide, and mercury- mercurous chloride (calomel) electrodes. An assessment, in tabular form, of additional electrode systems and their potentials at different temperatures, is presented in Appendix 2 (Hampel, 1964).

An electrode consists essentially of two conductors in contact - one electronic and the other electrolytic. The difference of electrical potential that exists at the interface is termed the electrode potential. Two electrodes form a galvanic cell, if combined in a way that an electrical current flows, if electrical conductor is connected across. Individual electrode potentials can than be assigned by choosing a standard reference electrode potential as virtual zero. For convenience this is chosen to be the potential of the standard hydrogen electrode, described below.

Reversibility is a main feature of the reference electrodes. At each electrode during operation a chemical reaction occurs, that provides the electrical energy of the cell. An electrode may be said to be reversible if:

- No reaction occurs when the potential is balanced with external source.
- When the external source potential is increased with infinitely small amount, electrical current should flow and chemical reaction should occur, and if decreased with the same amount, the current and reaction direction should reverse with the same amount.

A reversible cell is made with two reversible electrodes. Three main types are known:

- A metal or nonmetal in contact with a solution of its own ions (hydrogen in an acidic solution).

- A metal and a correspondingly soluble salt of the same in contact with a solution of a soluble salt of the same anion, like Ag/AgCl(s)/HCl, where:

$$Ag(s) + Cl^- = AgCl(s) + e$$

Equation 3.17

- An inert metal is immersed in a solution containing both oxidized and reduced states of an oxidation-reduction system, for example gold immersed in a solution containing Fe^{3+} and Fe^{2+} ions.

These oxidized and reduced states need not necessarily be ionic. All of the three types are used as reference electrodes.

Each reference electrode should meet the standards for reversibility, reproducibility, and stability.

3.2.1 Standard hydrogen electrode

The standard hydrogen electrode consists of platinum metal in contact with a solution of hydrogen ions (of unit activity) and dissolved molecular hydrogen, which is specified to be in equilibrium with hydrogen at 1 atmosphere (atm) in the gas phase. The hydrogen electrode is chosen as the primary standard reference electrode for many reasons. The construction of this electrode is relatively easy. It is also the most reproducible by far, because the hydrogen ion discharge at the platinum surface allows a high exchange current density – a very important experimental factor. This could be best proven in micro-polarization reversibility experiments.

The electrons in the metal, the hydrogen ions in the solution and the dissolved hydrogen all participate in the equilibrium. The difference with other oxidation-reduction electrodes is that the exchange equilibrium is catalyzed by the absorption of hydrogen atoms on the metal:

Equation 3.18:

$$H_2 \text{ (aqueous solution)} = 2H \text{ (absorbed on metal)} = 2H^+ \text{ (aqueous solution)} + 2e$$

This equilibrium does not solely rely on electron transfer. The surface properties of the metal substrate are of prime importance, since the equilibrium is established at the metal-solution interface. It should not dissolve or otherwise react with the solution, nor absorb

hydrogen atoms out of certain limits. Platinum metal, electrodeposited with finely divided platinum, is most suitable in this respect. The application of this coating enhances the catalytic activity of the metal, and at the same time increases the number of catalysis-active centers.

3.2.2 Silver-silver chloride electrode

The silver-silver halide system is the most popular of the secondary reference electrodes for the reasons restricting the application of the primary hydrogen standard: compactness, indifference to orientation and lack of liquid junction requirements.

The silver-silver chloride system is represented by: $Ag/AgCl/Cl^-$. This is a solid silver chloride in contact with metal silver and a soluble chloride solution. Formally, it is equivalent to a silver-silver ion electrode where the silver ion activity is controlled by the product of the silver and the chloride ions activity/ solubility. The standard electrode potential is defined as the emf (electro-motive force) of the cell: H_2(1 atm)/HX(m=1)/AgX/Ag, all the components being in their standard states. The standard potential E_o has been derived from experimental emf values for the cell $H_2/HX(m_1)$, $MX(m_2)/AgX/Ag$.

3.2.3 Mercury-mercurous salt electrode (calomel electrode)

The two most-common types of mercury-mercurous salt electrodes are:

$Hg/Hg_2Cl_2/Cl^-$ (calomel electrode) and **$Hg/Hg_2SO_4/SO_4^{--}$**

The calomel electrode, like the silver-silver halide system, is an electrode of the second kind, but has one great advantage – the metallic component is liquid and irrespective of its history remains in a standard state. Calomel electrodes with potassium chloride, used with a salt bridge, are calomel electrodes of fixed potential. Variable potential calomel electrodes are obtained with hydrochloric acid. Three forms, containing respectively saturated, 1M and 0.1M KCl are most commonly used.

3.3 Ion-Selective Electrodes (ISE)

ISE is one analytical technique that gives direct measurement of both cations and anions - common ones like sodium, chloride, potassium, nitrate, calcium, sulfide and many others. ISEs also measure dissolved gases such as ammonia, nitrogen dioxide, and carbon dioxide. Indirect electrode methods increase the number of species that can be measured. For example, aluminum, magnesium, manganese, nickel, and zinc can be determined by titration. Physical phenomena which do not involve explicit redox reactions, but whose initial conditions have a non-zero free energy, will generate a potential. An example of this would be ion concentration gradients across a semi-permeable membrane. This can also be a potentiometric phenomena, and is the basis of measurements that use ISE. An ISE produces a potential that is proportional to the concentration of an analyte. Making measurements with an ISE is therefore a form of potentiometry. The most common ISE is the pH electrode, which contains a thin glass membrane that responds to the H^+ concentration in a solution. The potential difference across an ion-sensitive membrane is defined by the Nernst equation:

$$E = K - (2.303RT/NF)\log(a)$$ **Equation 3.19**

where **K** is a constant to account for all other potentials, **R** is the gas constant, **T** is temperature, **N** is the number of electrons transferred, **F** is Faraday's constant, and **a** is the activity of the analyte ion. A plot of measured potential versus log (a) will therefore give a straight line.

ISEs are susceptible to several interferences. Samples and standards are therefore diluted 1:1 with total ionic strength adjuster and buffer (TISAB). The TISAB consists of 1M NaCl to adjust the ionic strength, acetic acid/acetate buffer to control pH, and a metal complexing agent.

ISEs consist of two reference electrodes and an ion selective membrane (LaF_3), which separates the internal reference electrode solution from the analyte solution, where the external reference electrode is immersed (Fig. 3.1):

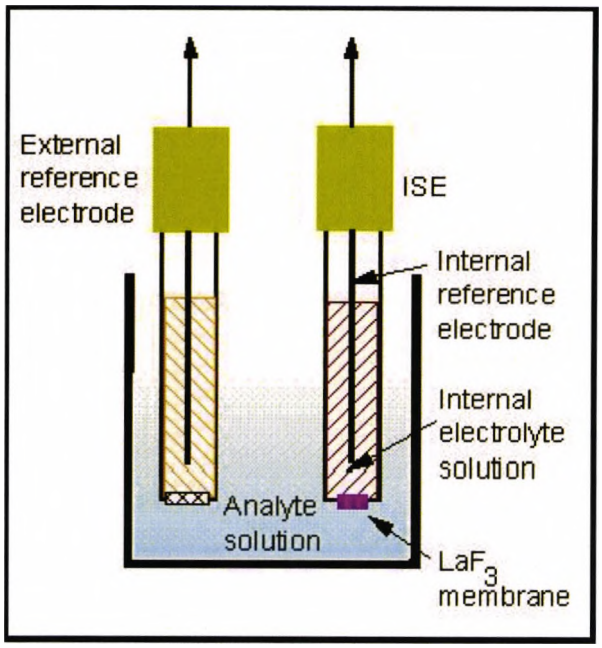

Fig. 3.1: Ion selective electrode, based on measurement of the potential difference between two reference electrodes separated by an ion-selective membrane (Omega Engineering).

The concentration can be read directly on a Specific Ion Meter, or a pH meter can be used to detect the potential difference between the two electrodes. If a digital pH/mV meter or a high input resistance potentiometer, for example the pH-meter circuit shown later (fig. 3.4) is used, the concentration is read from an easily drawn straight calibration line.

3.4 Instrumentation for pH measurement

3.4.1 Glass electrode

The glass pH electrode predates all other membrane electrodes by several decades. Since the early 1930s, the most convenient way for determining pH has been by measuring the potential difference across a glass membrane separating the analyte solution from a reference solution of fixed acidity. General use of the glass electrode for pH

measurements, however, was delayed for two decades, until the invention of the vacuum tube allowed for accurate measurements of potentials across glass membranes having resistance of 100 MOhm and more.

A typical cell for measuring pH (Fig. 3.2) consists of a glass indicator electrode and a silver/silver chloride or a saturated calomel reference electrode immersed in the solution whose pH is to be determined:

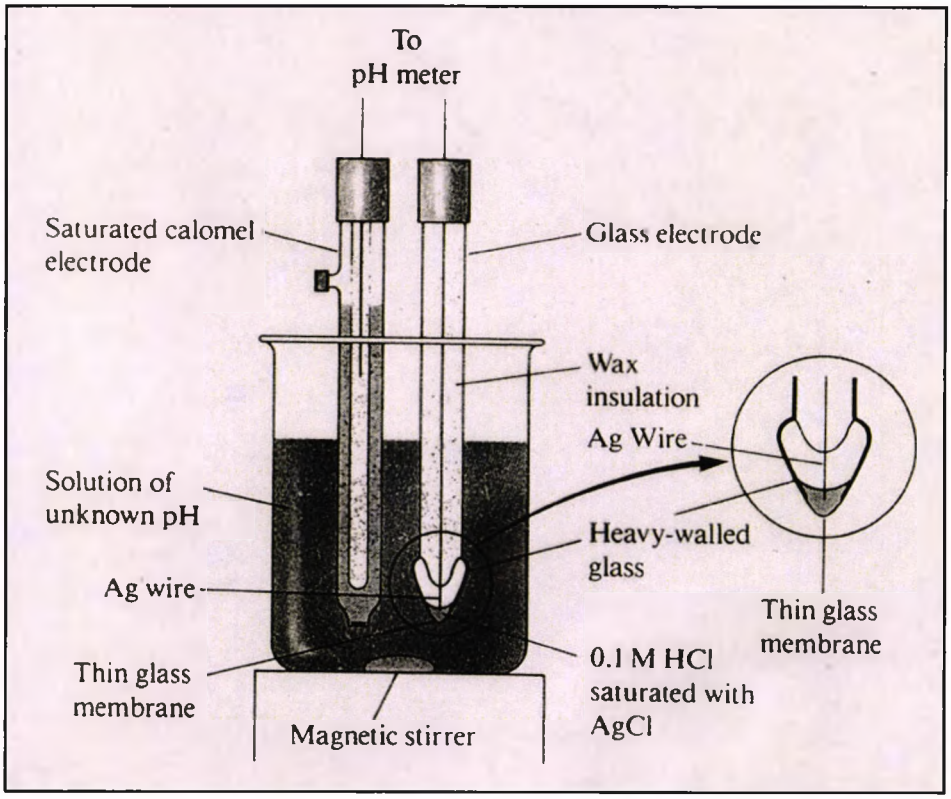

Fig. 3.2: Typical electrode system for measuring pH, where an ion-selective electrode for hydrogen ions concentration is used (Corning).

The indicator electrode consists of a thin, pH-sensitive glass membrane, sealed onto one end of a heavy-walled glass or plastic tube. A small volume of dilute hydrochloric acid saturated with silver chloride is contained in the tube. A silver wire in this solution forms a silver/silver chloride reference electrode, which is connected to one of the terminals of a potential- measuring device. The reference electrode is connected to the other terminal. While the internal reference electrode is part of the glass electrode, it is not the pH-sensing element. Instead, it is the thin glass membrane at the tip of the electrode that responds to pH.

To serve as an indicator for cations, a glass membrane must conduct electricity. Conduction within the hydrated gel layer involves the movement of hydrogen atoms. Sodium ions are the charge carriers in the dry interior of the membrane. Conduction across the solution/gel interfaces occurs by the reactions:

$$H^+_{(sol1)} + GL^-_{(glass1)} = H^+GL^-_{(glass1)} \qquad \textbf{Equation 3.20}$$

$$H^+GL^-_{(glass2)} = H^+_{(sol2)} + GL^-_{(glass2)} \qquad \textbf{Equation 3.21}$$

where subscript 1 refers to the interface between the glass and the analyte solution and subscript 2 refers to the interface between the internal solution and the glass. The positions of these two equilibria are determined by the hydrogen ion activities in the solutions on the two sides of the membrane. The surface at which the greater dissociation occurs becomes negative with respect to the other surface where less dissociation has taken place. A boundary potential thus develops across the membrane, with magnitude depending on the ratio of the hydrogen ion activities of the two solutions. It is this potential difference that serves as the analytical parameter in potentiometric pH measurements with a membrane electrode.

The potential of the glass indicator electrode (E_{ind}) has three components - the boundary potential (E_b), the reference electrode potential (E_{ref2}) and a small asymmetry potential (E_{assy}):

$$E_{ind} = E_b + E_{ref2} + E_{assy} = I_{(const)} - 59.16\ mV.pH \qquad \textbf{Equation 3.22}$$

A combination pH electrode system with a free diffusion junction is shown on fig. 3.3.

The electrode response is characterized by a zero offset point and slope. A two-point calibration may be used for greater precision. The response of a pH electrode is defined by the Nernst Equation (3.19).

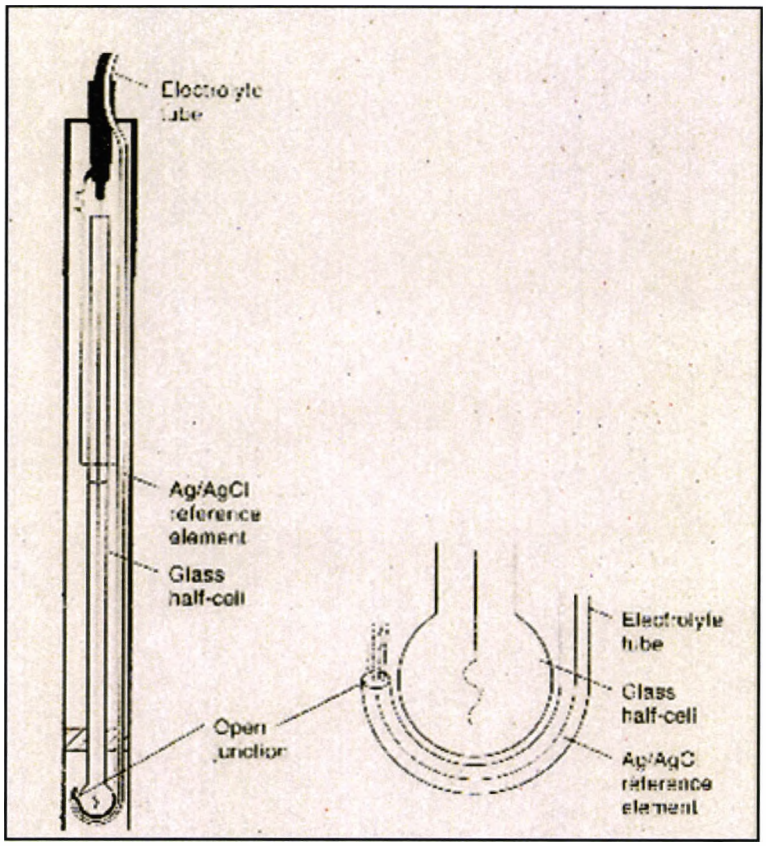

Fig. 3.3: A combination pH electrode system, where the reference and glass electrodes are integrated in one compact body for convenience of use (Corning).

If measuring hydrogen ions (i.e. N = 1), the slope factor at 25°C (298 K) has a value of 59.16 mV. When using glass pH electrodes, large errors are often observed due to the existence of cations, similar to the proton in solution. In particular, Li, Na, and K can give rise to proton measurement errors in concentrated solutions. These cations can exchange with the protons in the glass membrane of the pH electrode, resulting in erroneous potentials across the glass membrane and thus erroneous pH measurement. Another source of error is the change in proton activity due to the ionic strength of the solution. Also, temperature can affect several equilibria giving rise to complicated measurement errors. Temperature will affect the equilibria of the solution phase species, as well as chemical species used in the reference electrode. Every measuring solution has a characteristic temperature and pH behavior (temperature coefficient), shown in table 3.1.

PH value at:	20°C	30°C
0.001 mol/l HCl	3.00	3.00
0.001 mol/l NaOH	11.17	10.83
Phosphate buffer	7.43	7.40

Table 3.1: Dissociation is temperature dependent and hence the real pH changes with buffer temperature.

It is the temperature dependent dissociation, which causes a change in the H^+ concentration. The pH change is real, not a measuring error, and cannot be compensated for by use of automatic temperature compensation (ATC). This has to be taken into consideration if pH values obtained at different temperatures are to be compared. Experimentally, samples should be measured at the same temperature. When the temperature change of the medium is rapid, a conventional pH electrode will drift until the temperature of the electrode and the medium become equal. In order for a combination electrode to react rapidly to the temperature changes of the medium, the temperature of the inner lead-off element and the outer reference element must always be identical. Optimal electrodes are distinguished by the symmetrical warming up or cooling down of their lead-off elements. They also have the same temperature coefficient and isothermal intersection at pH7 and 0 mV (Corning, 1993).

The slope of the measurement line has also a temperature dependent component, as it can be seen from the Nernst equation (3.19). When making pH measurements, the temperature effect can be compensated in a number of ways. The majority of pH meters have the facility for manual or ATC. ATC is achieved by the use of a separate temperature probe or a thermistor fitted into the pH electrode. Each measures the solution temperature and the meters electronically adjust the pH reading according to the Nernst equation factor. On table 3.2 are shown the potential differences for a unit pH changes at different temperatures.

Temperature [^{0}C]	E_N value [mV]
0	54.2
25	59.2
50	64.1

Table 3.2: Nernst potential temperature dependence – this is a predictable measurement error and can be compensated using a built-in temperature probe.

3.4.2 Electronic pH meter

The pH meter measures the pH of a solution using an ion-selective electrode (ISE) that responds to the H^+ concentration of the solution. The pH electrode produces a voltage that is proportional to the concentration of the H^+. Making measurements with a pH meter is therefore a form of potentiometry. The pH electrode is attached to an electronic circuit interface, which converts the voltage to a pH reading and displays it on a meter. A pH meter consists of H^+ selective membrane, an internal reference electrode, an external reference electrode, and a meter with electronic interface and display (Fig. 3.4).

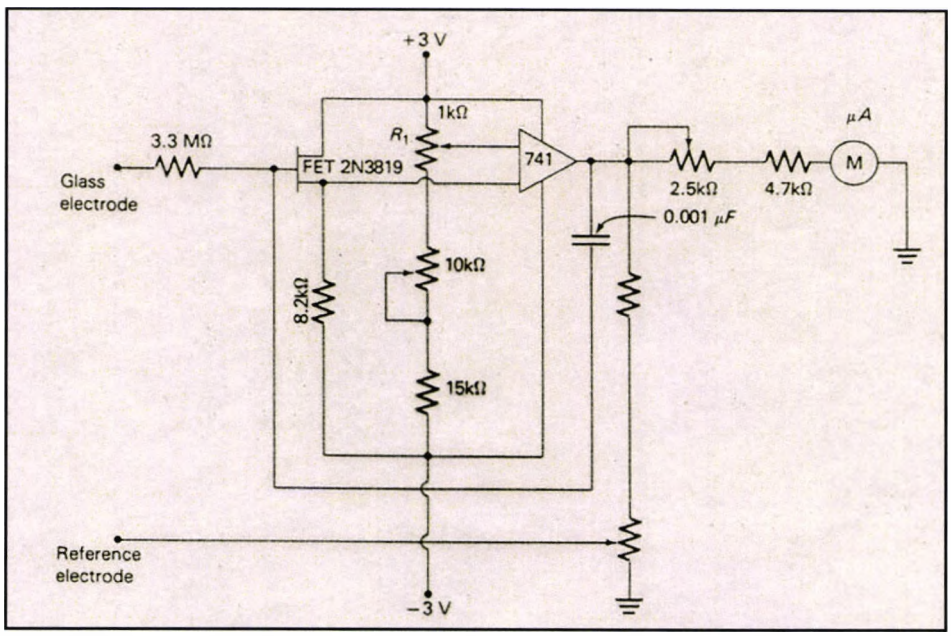

Fig.3.4: Electronic pH meter circuit diagram, showing a high-impedance FET input, gain and bias controls, and analogue meter reading (Corning).

Commercial pH electrodes usually combine all electrodes into one unit that are then attached to the pH meter. A prime consideration in the design of an instrument for measuring cell potentials is that its input resistance must be very large with respect to the cell, otherwise significant errors result as a consequence of the IR drop in the cell. The real potential of a commercially used glass/calomel electrode system in a buffer solution is about 0.8V and its internal resistance is about 20 MOhms. This is the reason that potentiometric devices with input resistance of 10^{12} or greater are used for high accuracy measurements. Usually field effect transistor (FET) input operational amplifiers with corrections for offset voltage and gain are connected to the electrochemical cell and supply the signal to a digital millivoltmeter.

Also, temperature correction is essential, as explained above. The instrument is calibrated with a particular electrode at two or sometimes three points, using standard buffer solutions of different pH (most common values are 4, 7 and 10). With membrane electrodes, recalibration may be necessary over several hours, because of the slowly changing asymmetry potential.

3.5 Electrochemical sensors and pH control

Many of the features discussed above make the electrochemical electrodes useful sensors for pH control - their availability, good accuracy, relatively short settling time, selectivity for different species in aqueous solution and reasonable cost. Although this is true in the case of chemical pH control, for electrical pH control we have to consider the influence of the electrical field across the solution to the electrochemical sensor, in particular the pH electrode. Significant voltage (V>2V) has to be applied to the electrochemical cell electrodes to produce electrolysis and eventually a pH change within a reasonable time. The pH sensor will be subjected to a PD proportional to the distance between the reference and the glass electrodes and the electrical current flowing through the electrolyte. This problem will be discussed in more detail in Chapter 7 & 8 and means of error elimination will be developed.

There are a number of additional problems associated with pH electrodes. All are composed of glass and are therefore fragile and subject to breakage. The pH electrode, due to the nature of its construction, needs to be kept moist at all times. In order to operate properly, glass needs to be hydrated. Hydration is required for the ion exchange process to occur.

The time delay is significant for high accuracy pH measurements. While stirring the sample may initially speed up response, it can interfere with the pH measurement by adversely affecting the junction potential. Reference junctions made of porous materials can also produce significant error by absorbing the sample and eventually clogging (Presley, 1999). Another challenge for pH electrodes is the run down with time and use. The resistance of the electrode glass changes with ageing. This resistance change alters the electrode potential. For this reason, electrodes need to be calibrated on a regular basis. Calibration of any pH equipment always begins with buffer 7.0, as this is the "zero point". The pH scale has an equivalent mV scale. The mV scale ranges from +420 mV to -420 mV. At a pH of 7.0 the voltage value is zero. Each pH change corresponds to a change of approximately ±60 mV. As pH values become more acidic the voltage increases. For example, a pH of 4.0 corresponds to a value of 180 mV. As pH values become more basic the voltage decreases, for example pH of 9 corresponds to -120 mV. Dual calibration using buffers 4.0 or 10.0 could improve system accuracy.

pH electrodes have junctions which may allow the internal fill solution of the measuring electrode to leak out into the solution being measured. This junction can become clogged by particulates in the solution and can also facilitate poisoning by metal ions present in the solution. Also, the lifespan of glass pH electrodes is finite due to their inherent properties. How long a pH electrode lasts depends on how it is cared for and the solutions it is used to measure. Typically, a gel-filled combination pH electrode lasts six months to a year. Even if not used, an electrode still ages. On the shelf, the electrode should last approximately a year, if kept in a moistened condition. Electrode demise can usually be characterized by a sluggish response, erratic or not changing readings. When this occurs, an electrode can no longer be calibrated. How long a pH electrode will last is mainly determined by the application – in harsher systems, the lifespan is much shorter.

Summary

In this chapter, the fundamentals of pH measurement were reviewed. The principle of operation of the electrochemical pH sensor was demonstrated and its building blocks described in more detail – electrochemical reference and ion-selective electrodes, and the electronic measurement interface.

Critical analysis indicates number of problems for using this type of sensor for the intended application of electrical pH control. Another approach, using optical colorimetric pH sensors, as described in the next chapter, offers measurement and control immunity of the electrical field through the solution.

CHAPTER 4: OPTICAL PH SENSORS

Introduction

As an alternative to the electrochemical sensors, the optical sensors for chemical measurements, especially the optical fibre sensors, are gaining popularity during the last decade. They are based on indirect measurements, using some optical variable related to a chemical parameter, i.e. color, absorption, reflection, fluorescence etc. The advantages of the optical approach, most important of which is the immunity of the measurement from the electrical field across the solution, makes it a good candidate for implementation in the electrical pH control system. Also, multiple modes of sensor selectivity are achievable by combining the optical and electrochemical approaches.

In the following chapter, the pH color indicators are discussed first, as a medium between the hydrogen ion concentration and the analyte color, an optically measurable parameter. Colourimetry is the base of operation for most optical pH sensors. The optical approach is explained further and relevant examples of the existing optical fibre chemical sensors are described in detail. Attention is given also to the sol-gel method for optical sensing, as an attractive novel approach promising suitability for on-line monitoring and control.

4.1 Colourimetric pH indicators

Acid – base indicators are dyes, which undergo slight changes in molecular structure and colour, when the pH of the solution changes. Many common coloured substances may act as indicators. Normally they are some large, water soluble, organic molecules, which can exist as weak acid (H_{in}) or conjugate base (In^-), forms that differ in colour. The indicators establish equilibrium between the molecular (colourless) and ionic (coloured) forms in solution:

$$H_{in} + H_2O = In^- + H_3O^+ \qquad \textbf{Equation 4.1}$$

$$K_{in} = \frac{a(In^-)a(H_3O^+)}{a(H_2O)a(H_{in})} \qquad \textbf{Equation 4.2}$$

The indicator equilibrium changes so as to accommodate the change of pH, with H_{in} the dominant species on the acid side of the equivalence point and In^- dominant on the basic side. The colour changes only over a limited pH range. The choice of the appropriate

indicator for every particular application (see Appendix 3) depends on the pH range of measurement or control. To cover wider pH measurement range, composite indicators (as developed in Chapter 8) with adjacent ranges and spectrally matching colours are used.

4.2 Optical fibre pH sensors

The optical methods are some of the oldest and well-established techniques for sensing chemical analytes. The colorimetric analysis was extensively used in the 1930's to the late 1950's, when the Atomic Absorption (AA) and then Inductively Coupled Plasma (ICP) largely superceded the classical methods (Mooney, 1992). Neither the AA nor the ICP techniques are convenient for continuous on-line analysis or control. The need to obtain real- time data and almost immediate action to be taken boosted the development of on-line colourimetry. The development of inexpensive, high quality optical fibres for the communications industry has provided the main component for the optical fibre chemical sensors (Appendix 4). In the last decade, there has been continuously growing effort developing optical fibre chemical sensors, with many different methods having been proposed. The glass pH electrode, as the most common electrochemical sensor, has been successfully replaced with miniaturized optical fibre sensors with competitive sensitivity, precision, selectivity, sensor lifetime and unit cost.

4.2.1 Principle of operation

Chemical sensing by optical techniques involves probing of matter by photons. The photon may either be scattered or absorbed, the later if its energy equals that between the initially occupied and the exited state of the matter. A range of different parameters are associated with the photon flux, and changes in any one could give useful analytical information for the matter tested. For example, with the absorption and reflectance spectrometry, the parameter in the photon flux that varies is intensity. The luminescence uses the wavelength change, the luminescence lifetime – the time decay, the polarized absorbance – the phase characteristics. For the vast majority of absorbing (non-scattering) matter the initial light intensity I_o will be attenuated to an intensity I given by the Beer – Lambert law:

$$\text{Log } 10 \frac{I_o}{I} = \varepsilon l C$$

Equation 4.3

where **ε** is the molar absorptivity, which is constant for particular species at a particular wavelength, **l** is the path-length [cm] and **C** is the species concentration [M]. This means that by measuring the light attenuation we can measure the absorption of a medium, in particular an aqueous solution. If a color indicator is dissolved in the solution and there is not other interfering absorbing species at the wavelength of transmission chosen, the attenuation of the optical signal will depend on the color change, respectively the pH. Usually in the optical analyzers the calibration is performed by the use of standard solutions.

Optical sensors are constructed by coupling a reagent to a transparent porous surface (the sensor head) at the tip of an optical fibre (Frishman, 1994). The sensor head, including the immobilized reagent, is either a part of the optical fibre or a particle attached to it physically by means of a membrane or optical glue (Appendix 5). Glass pH sensors with good linearity can also be produced using thick-film technology (Parr, 1986), this method is a step towards microelectronic pH sensors (optrodes).

4.2.2 Classification of optical fibre chemical sensors

The optical fibre chemical sensors could be divided into two main types, in the same manner as those for physical sensors:

- Extrinsic sensors, where the optical fibre merely acts as a light-guide between the test point and the electronics interface.
- Intrinsic sensors, where the fibre, possibly modified, is the sensing transducer of the chemical composition itself.

Another classification of the optical fibre chemical sensors and consecutively the chemical analysis techniques is:

- Species-specific sensors, comprising remote spectrometry, where the optical and hence chemical properties of the analyte are measured directly, and

immobilized reagents sensors, where the analyte chemistry affects the optical properties of an added reagent.

- Non species-specific sensors, where direct measurement of some optical property is involved, which may be influenced by any one of a number of analytes.
- Indirect techniques, where the optical fibre sensor is used to measure some non-optical parameter, and relating the measurement to the analyte of interest.

The last two types of sensors predominantly involve the intrinsic type of sensor.

4.2.3 Summary of existing optic fibre pH sensors

There is no convenient direct spectroscopic analytical technique for the measurement of the hydrogen ion concentration, H^+. This may arise because of the lack of convenient electronic transitions, or due to insufficient sensitivity, as the available absorption bands are too weak to be measured for typical analyte concentrations. In this case, a better approach is to use an added reagent, which has more appropriate pH-dependent optical characteristics. The added reagent may be dissolved in the measured solution, absorbed or chemically bonded to a substrate at the sensing end, or to the optical fibre itself (Seitz, 1988). A typical example of this type of sensor is shown on fig. 4.1 (Kirkbright, 1984):

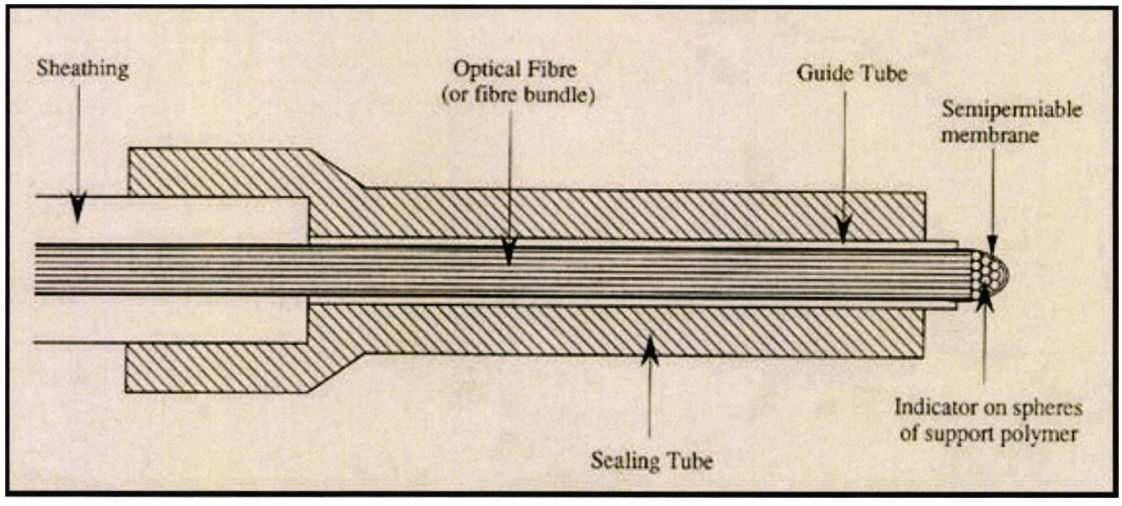

Fig. 4.1: pH optical fibre probe using indirect measurement method: the optical properties of a pH sensitive indicator incorporated on the sensing tip.

This sensor was made of a bundle of plastic optical fibres, of nominal diameter of 1 mm, with a sensitive tip consisting of styrene-divinyl benzene copolymer, onto which was absorbed the pH indicator bromthymol blue, retained at the end of the probe by a PTFE membrane. The complete sensor head had a diameter about 2 mm. pH changes in the area of the sensing tip caused absorption spectra response changes as the bromthymol changed from its acidic yellow form to a blue base form. The measured response was the reflected light attenuation, back up the fibres, at a wavelength of 593 nm relative to 800 nm, a convenient reference wavelength. The useful measured pH range by using bromthymol blue was 7 to 9. At unit pH change this sensor had a 1/e response in 65 seconds and stable reading after 5 minutes. This significant delay is believed to be due to the rate of the solvent ions diffusion across the PTFE membrane and through the sensing matrix of the polymer reagent.

Distributed sensor for pH determination in water using optical fibres and swellable polymeric systems have been demonstrated (Michie, 1995). The technique combines optical time- domain reflectometry with chemically sensitive water-swellable polymers (hydrogels). Gels have been developed that enable this sensor to be readily adapted to distributed pH measurements.

A quasi-distributed pH sensing system has been previously developed, utilising information, derived from evanescently excited fluorescence signals originating from sensor sites fabricated on an optical fibre (Wallace, 2001). The sensor sites comprise a section of fibre core exposed by polishing upon which is laid down a sensing film. The film comprises a fluorescent indicator dye immobilized covalently within a hydrogel matrix, which is then photo-polymerized and attached covalently to the exposed fibre core. Position information is determined from the propagation delay of the returning signals. A system comprising eight sensors at 10 m intervals along an optical fibre has been constructed and characterized. The sensors operate in the region pH6-pH8 with a response time of 500 s. The properties of the immobilized indicator dye are found to be similar to those of the dye in aqueous solution. Furthermore, the sensing films so created are found to be resistant to dye leaching.

Other pH sensors with 2-3 orders of magnitude shorter response time have been fabricated (Jones, 1988). A 3 μm porous cellulose acetate film, formed by spin coating, has been used as the support for an immobilized pH indicator. Optical fibre pH sensor with a response time of a few seconds was developed by Attridge, 1987. The sensing material is a sulphophthalein dye, bound in an ion exchange membrane. A coaxial directional coupler senses the changes in the refractive index of the polymer. Measurements of the combination of the two are used to discriminate against interfering index variations.

A miniature pH probe for biomedical applications has been demonstrated by Peterson, 1980 (fig.4.2):

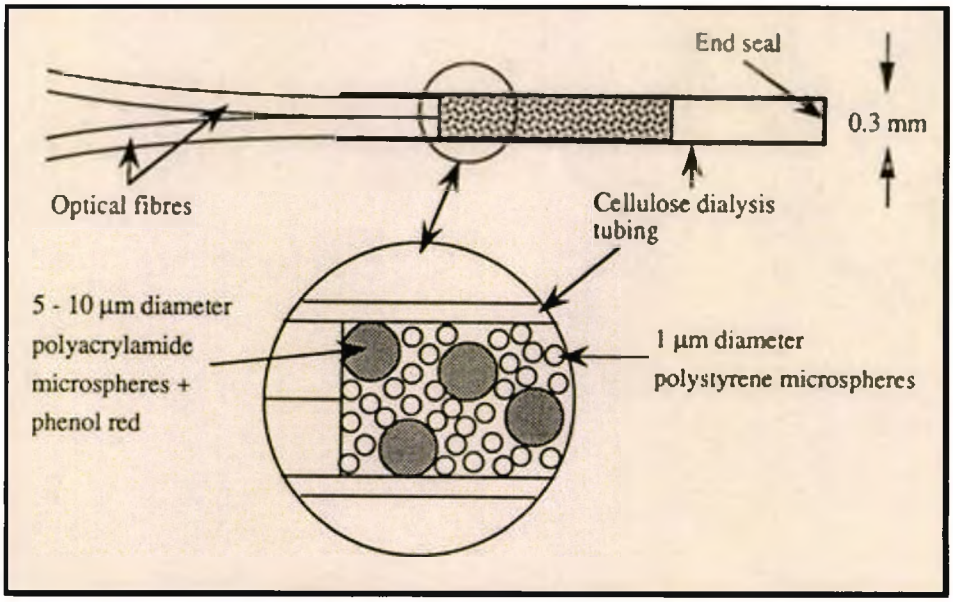

Fig. 4.2: Optical fibre pH sensor for physiological use, where miniature polystyrene spheres are used to augment the backscattered light response and increase sensitivity.

This probe is designed for in-vivo use and so it is configured to be sensitive over the physiological pH range (7- 7.4). The quoted sensitivity is 0.01 units of pH. This sensor has a lot of similarities to the probe of Kirkbright described above. However, a major difference is the use of 1 μm diameter polystyrene micro-spheres, which increase the amount of light backscattered to the fibre. Optical fibre pH sensors based on this principle are available for medical use.

Also, extrinsic species-specific sensors that use luminescence of some immobilized reagent to obtain information about a chemical's concentration have been reported. The immobilized reagent undergoes a chemical reaction to form second species whose luminescence characteristics differ from those of the original species. Fluorescein changes luminescence by approximately 90% at pH change from 3 to 9. This allows the pH of an unknown aqueous solution to be found by measuring of the luminescence intensity of a previously calibrated fluorescence probe (Wolfbeis, 1986).

A luminescent fibre optic sensor for the measurement of pH has been reported by Milo, 1992. The sensor described is based on a colorimetric pH indicator and a pH insensitive luminescent compound co-immobilized in a hydrophilic polymer. The absorption spectra of the pH-indicator and the luminescent compound overlap. Consequently, the competitive absorption between the pH indicator and the luminescent compound results in modulation of the sensor emission intensity as a function of pH in the measurement media. The feasibility of this pH measurement technique is demonstrated with on-line testing of optical fibre sensors.

Further developments of this basic concept have been published. For example, the chemical linking of fluorescein isothiocyanate to silanised, controlled porosity, glass beads has been described (Fuh, 1987). Glass beads with an average pore diameter of 50 nm and an average bead diameter of 150 μm have been used. A single bead has been stuck to the end of a 105/125 μm all silica fibre using an ultraviolet curable epoxy resin. This miniature pH probe has given a change in fluorescence intensity at 525 nm over the pH range from 2.5 to 7.5, with a response time about 20 s. The expected resolution has been around 0.25 pH units at pH = 4 and 0.1 pH units at pH = 7. The fluorescence intensity has also been found sensitive to temperature, changing by 0.8 pH units between 8°C and 33°C, and also dependent on other ions present in the solution. The covalently attached dye has improved significantly the long-term stability relative to devices where indicators are simply adsorbed onto a substrate. An exception is the application for high pH measurement, where hydrolysis of the covalent linkage occurs.

The use of porous glass as a support for the analyte-sensitive reagent in optical fibre chemical sensors has been investigated (Badini, 1994; Butler, 1995). The fluorophore fluorescein isothiocyanate has been discussed and its fluorescence properties assessed. Its suitability as a pH sensitive reagent has been confirmed using opto-electronic configurations. The presented model, with some modifications, can explain most of the observations concerning the two step immobilization reaction involving 3-aminopropyltriethoxysilane. The sol-gel process (described in more detail below) is introduced and its potential applicability to preparing glass-like structures which can be used in optical fibre chemical sensors is reviewed and further explored (Appendix 6).

An improved fibre-optic sensor with extended lifetime has been developed by Ding, 1991. The sensor is based on the absorbance change of organic indicators immobilized in a silica matrix coated as a thin film onto a porous glass optical fibre by the sol-gel technique. This approach has allowed the development of a highly stable, chemically durable and ruggedized fibre optic pH sensor, with potential applications in aqueous solutions at high temperatures and in those containing organic solvents.

A pH sensor using multiple sol-gel coating (Lee, 2001) is based on evanescent wave absorption. The unclad portion of a multi-mode optical fibre is coated with a pH sensitive dye (bromcresol purple or bromcresol green), which is immobilized in sol-gel. By using multiple sol-gel coatings in the sensing region, the sensitivity of the device was increased.

A wireless optical multisensor comprising temperature, conductivity, pH and dissolved oxygen sensors, a control chip and transmitter is described by Tang, 2003. This "Lab-in-a-Pill" sensor prototype measures only 16x55 mm and consumes 6.3 mW of battery power. Example applications include wastewater analysis and in-situ studies of the gastro-intestinal tract.

A sensor based on spectro-electrochemical techniques, possessing three modes of selectivity has been described (Heineman, 2003). The selectivity of this type of sensor comes from the ability of the analyte to (1) partition into an ion-exchange film coating an

optically transparent electrode, (2) undergo oxidation or reduction at a given potential, and (3) absorb light at either its oxidized or reduced form at the analytical wavelength. Suggestions are made of how this sensor can be employed as a small, portable unit appropriate for field work. One such application is for detection of ferrocyanide in a nuclear waste tank. This example illustrates the effectiveness of combined electrochemical/optical sensors in harsh, real world conditions.

4.2.4 Comparison with other methods

Several potential advantages arise from the use of optical fibre chemical sensors:

- Feasibility for on-line measurements: the high transmission efficiency, chemical stability, flexibility and small size make these sensors very suitable for in-situ measurements and control.
- No need for an electrochemical reference electrode: as opposed to the electrochemical pH sensor, where a reference and a hydrogen ion-selective electrode are needed, here only one sensor may be used.
- No electrical noise interference and electrical isolation: the optical fibres are, by their nature, isolated electrically from the electronic interface. The associated immunity to electromagnetic interference (EMI) makes them a convenient choice in electrically noisy environments.
- No interference caused by the electrical current flowing through the measured solution (e.g. during electrolysis), a major problem with electrical pH control using a glass pH electrode.
- The sensor could be irreversible disposable miniature inexpensive element mechanically connected to the fibre: many sensor heads, as described further, could be fabricated from cost-effective disposable materials, e.g. sol-gel with immobilized colour indicator.
- Simple one-point calibration: some optical fibre sensors have linear response to the measured parameter. After compensation of the background signal bias, only one point taken in reference solution may be sufficient for calibration with reasonable accuracy.

- Multi-analyte measurement with one sensor, incorporating several reagents and using multiple wavelengths: the sensing head of the sensor could incorporate different indicators, reacting at different analytes and responding in different wavelength regions. Specific case of this is the use of complementary pH indicators for expanded pH range (Appendix 3).
- Optical control of the baseline stability: if a systematic error is interfering with the measurement, for example due to the turbidity of the aqueous solution, by implementing a dual or multi-wavelength approach this can be compensated for.
- Potential for distributed sensing exists: optical fibre chemical sensors, where the whole length of the fibre is sensitized to the analyte of interest. This allows for a large area to be monitored simultaneously. Alternatively, the sensor can be interrogated with a time domain resolution reflectometer and measure the analyte concentration as a function of position over the extended area.

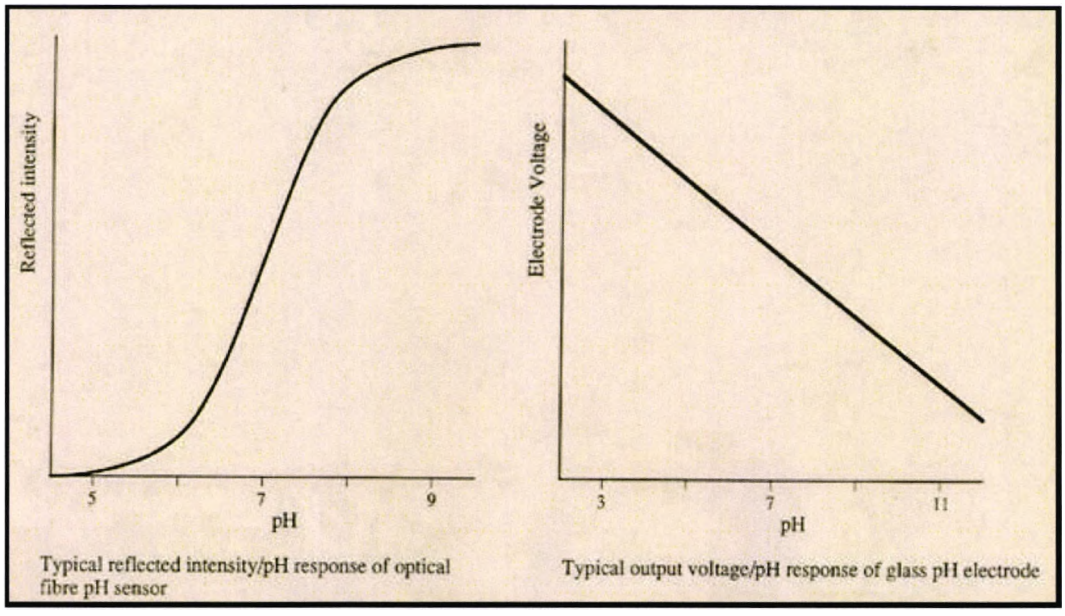

Fig. 4.3: A comparison of optical and electrochemical pH sensor responses shows that optical sensors suffer from limited sensing range and non-linear response (Mouaziz).

Some disadvantages of the optical fibre sensors are:

- Limited dynamic range: the optical pH sensors utilize acid-base indicators, which obey the law of chemical equilibrium. A plot of an optical pH sensor response follows a sigmoid shape, with a useful range of one to three pH units, compared to the wide range linear response of the electrochemical sensor (fig. 4.3). Whilst the limited dynamic range is in principle a drawback for measurement and control, it may be appropriate for many limited range applications like physiological monitoring, where the optical sensor exhibits increased sensitivity over the limited range.
- The signal depends on the amount of reagent in the optical pathway.
- Photo-bleaching and photo-degradation of the reagent: the long-term stability will degrade with the change in optical characteristics of the sensing transducer, e.g. due to fouling. For chemical sensors utilizing immobilized reagents, deterioration due to physical desorption or chemical degradation of the reagent may also limit the useful lifetime of the sensor.
- Ambient light interference: if the sensor operates in the visible range, precautions should be taken to avoid interference.

4.3 Sol-gel methods

4.3.1 History

The colourful effects produced by dropping crystals of various chemicals into a solution of sodium silicate were described by Glanber in year 1648. Small pieces of iron, copper, manganese and uranium salts have been placed in a solution of sodium silicate (water glass) and from them long filaments of gelatinous silica, coloured by the metal hydroxides, have grown. The growing action was produced by the formation around each crystal of semi- permeable film, which bursts when water enters due to osmotic pressure. This process is repeated until a stable state is reached (Information from the Science Museum of Birmingham).

4.3.2 Principle

Although applied for decoration, the above observations in principle are not far from the task of producing porous glass, which incorporates in its network chemically sensitive dyes, mixed at the liquid stage with a sol-gel material. The so-formed gel could be given any shape or applied as a thin film layer according to the sensor design.

A block diagram of measurement instrumentation using the sol-gel method is shown below:

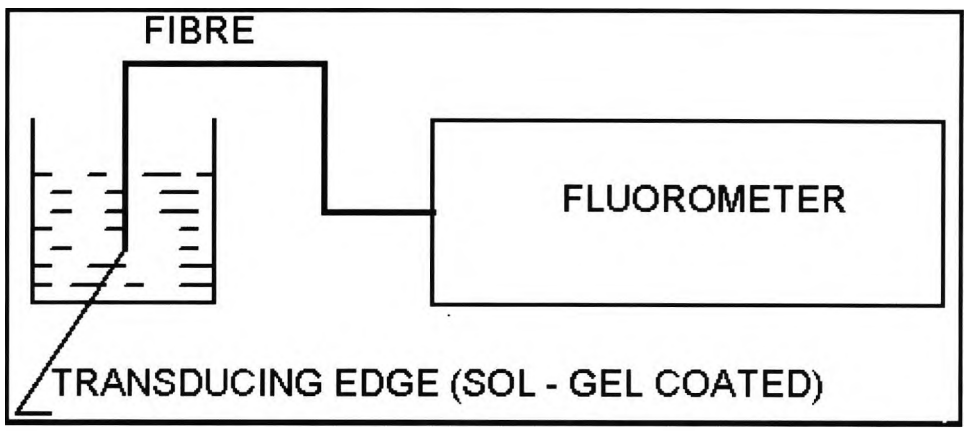

Fig. 4.4: Sol-gel based sensor, involving optical fibre with a sol-gel coated sensing tip attached to a fluorometric instrument.

The development of sol-gel technology in recent years created new opportunities of fabricating optical materials from gels, such as bulk optics, wave guides, doped oxides for laser and nonlinear optics, gradient refractive index optics, chemical and environmental sensors and smart windows. For various applications the diverse synthesis methods allow to produce microporous, amorphous, crystalline and composite materials, shaped as bulk optics, thick or thin films.

The main difference between glass and sol-gel is in the preparation process. While for glass three dimensional network is derived through high temperature melting and supercooling to preserve crystallization, the sol-gel process is maintained at room or slightly elevated temperature (below 100^{o}C) in a chemical laboratory - i.e. growing a three dimensional glass- like network in a liquid medium. From here the advantage of sol-gel technology for chemical sensors preparation - composite organic/inorganic materials,

incorporating fluorescent and chemically sensitive dyes could be derived, while glass remains inorganic.

4.3.3 Definitions

- Sol is not a solution but a suspension of very fine particles of one phase in another. It is usually liquid and as stable as solution, due to negligible gravitational forces of the very small particles.
- Gel is a sol where continuous network is formed. It loses its mobility and is usually a solid, soft material with low elastic modulus. Two basic types of gel are alkoxide, where metal alkoxides maintain hydrolysis and polymerization, and particulate, where dispersion of particles in a liquid occurs.

Here we shall concentrate on alkoxide sol-gel preparation because of its versatility and low- temperature synthesis, basic conditions for organics impregnation and chemical sensors preparation. The basic material used is tetraethyl orthosilicate (TEOS) and the reactions are described by equations (4.4) and (4.5):

$Si(OC_2H_5)_4 + 4H_2O \text{ -- } Si(OH)_4 + 4C_2H_5OH$	**Equation 4.4**
$Si(OH)_4 \text{ -- } SiO_2 + 2H_2O$	**Equation 4.5**

4.3.4 Problems

Water and TEOS are immiscible and alcohol is added to form a solution. Alternatively ultrasound could be used to accelerate the reaction (4.4). In this case the alcohol produced by the reaction helps with the mutual solubility.

4.3.5 Influence of pH

The rate of the reaction is very much pH dependent. For values of pH < 7 the reaction (4.5) is retarded by the lack of OH groups in the solution. The three dimensional network

grows slowly, accommodating the water-alcohol solution in nearby spaces. After drying, these spaces become pores and the surface area of such gels could be as high as 900 m^2/g. For pH > 7 rapid termination of the network is observed and powder precipitates - useful feature for particulate gels formation.

4.3.6 Influence of Water/TEOS ratio

When the Water/TEOS molar ratio is between 2 and 4, both reactions proceed concurrently, because there is not enough water for reaction (4.4) to be completed until enough water is released in the course of reaction (4.5). With a ratio <2 hydrolysis cannot be completed, but gel still can be formed by inclusion of non-hydrolyzed organic radicals in the structure.

4.3.7 Experimental preparation of sol- gel

Following the procedure described above we produced sol-gel samples as an attempt to develop optical pH sensor to be potentially utilized in the electrical pH control system. At room temperature (20°C), 1 part of distilled water (50 g), one part of ethyl alcohol and two parts of TEOS were mixed thoroughly. The mixture was stirred for two hours onto a magnetic stirrer until it polymerized and formed solid glass. The glass was visibly transparent and had large cracks in it. We tested the optical properties of samples of the so-formed glass particles, about 1 cm thick. The optical absorbtion and transmission response of the samples, scanned with a standard bench-top Hewlett-Packard spectrophotometer, are shown on Fig. 4.5 and Fig. 4.6. The results show good transmission in the visible range, indicating that the produced sol-gel could be used for chemical sensing applications, particularly as sensor head coating with entrapped sensitive dye for optical pH measurement.

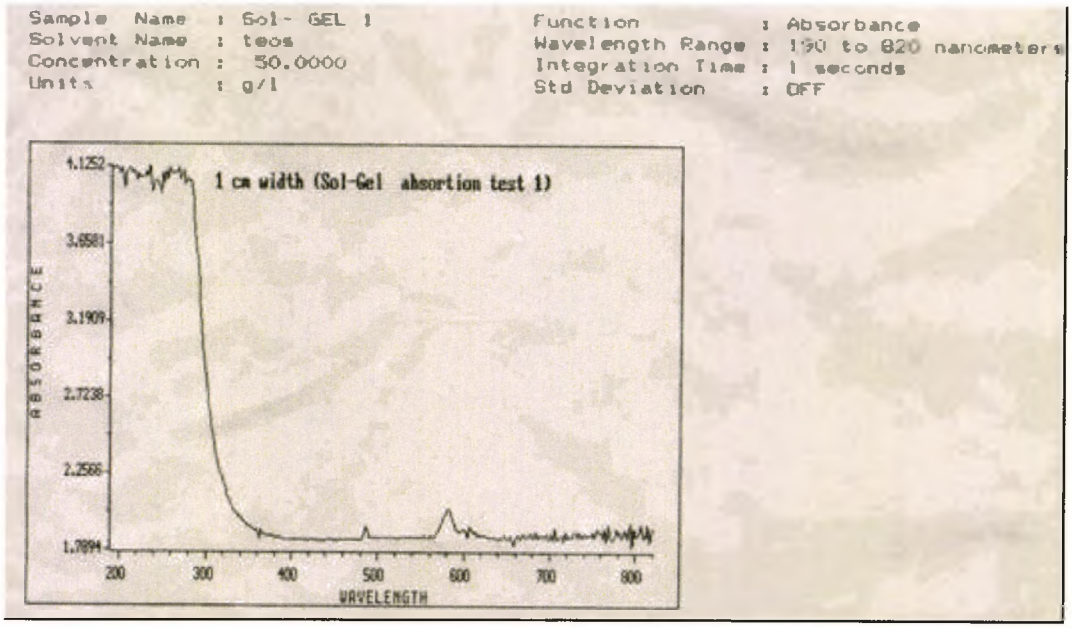

Fig. 4.5: Absorbance of a prepared in-house sol-gel sample.

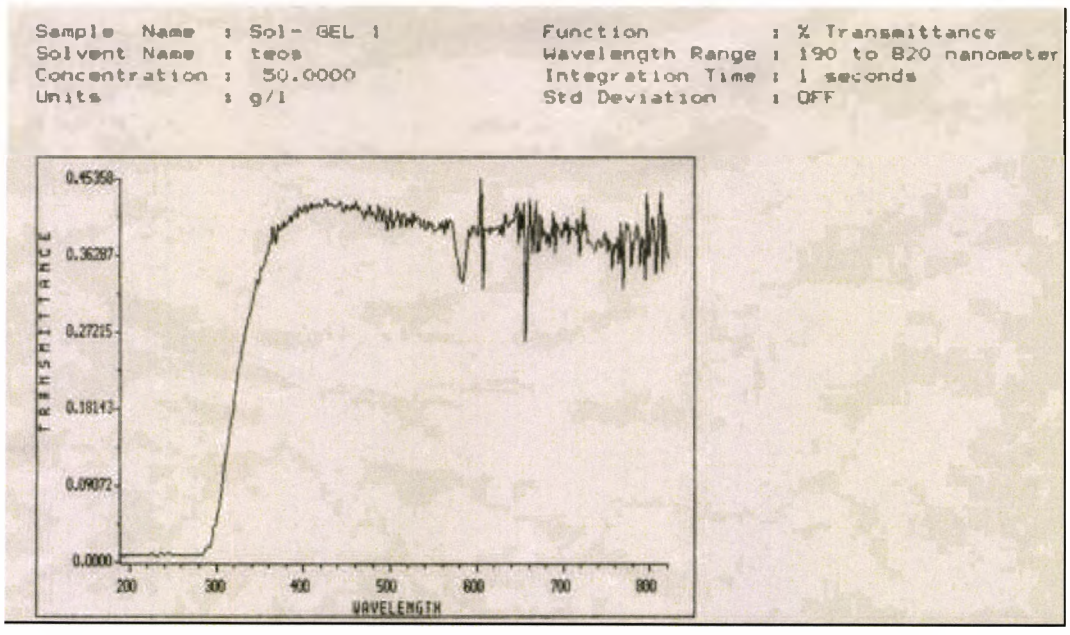

Fig. 4.6: The produced sol-gel samples show good optical transmittance in the visible range, enabling chemical sensor applications.

4.3.8 Advantages and drawbacks

Promising properties of porous silica for chemical sensing:

- Rigidity and negligible swelling in liquids
- Chemical inertness
- High stability - thermal, photochemical and bio-degradational
- Excellent optical transparency for visible and near UV regions
- Control of pore size by simple modification of the polymerization protocol
- Control of the surface area
- Control of the geometry
- Choice of supporting metal oxides
- Control of the polarity of the glass.

Significant disadvantages of the sol-gel technology are:

- Lack of large scale production know-how
- Hydrolysis of the SiO_2 network in strong base
- Fraction of monolithic glasses during gelation and drying or upon immersion in water
- Ion exchange capacity of surface silanol groups

Reported sol-gel based chemical sensing studies include:

- Fe(II) (O-phenanthroline)
- Ni(II) (dimethyl glyoxime)
- Cu(II) (α - benzoin oxime)
- SO_4^{2-} (sodium rhodizonate + barium fluoride)
- Several pH indicators
- Anions, cations, heavy metals
- Airborne ammonia and acids
- Medical diagnostics (enzymes)

Summary

Following the main topic of continuous automatic analysis in the field of on-line process control and environmental monitoring, optical chemical sensors applicable in integrated analytical systems were the main focus of this chapter. Color pH indicators were discussed as a medium between the hydrogen ion concentration in aqueous solutions and their color, which is the base of operation for most optical pH sensors. Representative examples of optical fibre chemical sensors were reviewed. Attention was also given to the sol-gel method for optical sensing as an attractive novel approach applicable for on-line monitoring and control.

The optical pH sensor is a critical part of the feedback loop of the developed electrical pH control system. The operation of the electrical regulator (in essence a power operational amplifier), which is the main building block of other electrochemical instruments, e.g. voltage regulators (potentiostats) and current regulators (galvanostats) is explained in the next chapter.

CHAPTER 5: ELECTRONIC INSTRUMENTATION FOR PH CONTROL

Introduction

In this chapter, we shall review different types of electrochemical instruments, and assess their suitability for pH control applications. By replacing the voltage signal from an electrochemical reference electrode with the calibrated voltage output of a pH sensor, the voltage feedback loop of a potentiostat is converted into a pH feedback loop. Either controlled electrochemical PD between two electrodes or current control can be used to regulate the electrolysis rate and hence the necessary pH modulation in the area of control. The specific use of potentiostatic and galvanostatic-based electrochemical instrumentation for pH regulation and their limitations in this application are addressed.

5.1 Basics

The instrumentation for pH control differs from that for pH modulation because a feedback system is implied, including a pH measurement device (sensor) and a pH modulation device (regulated power supply) in a closed feedback control loop. This approach allows for setting up a desired value of pH (by setting corresponding voltage) at the input of the control system, so that electrical bias will be applied as needed to equalize the controlled solution pH to the set pH value.

Negative feedback electronic systems that behave in the way described above exist (Bourilkov, 1992a, 1992b). Depending on the parameter that produces the feedback signal (voltage or current) they are usually a constant voltage or constant current negative feedback systems. In electrochemistry, both systems are largely applied and are called potentiostats and galvanostats (Andreev, 1985; Andreev, 1990; Atkins, 1990). The work in this chapter is focused at the above systems and reports on an investigation of their suitability for the purpose of pH control.

5.2 Potentiostats

5.2.1 Principle of operation

The potentiostat is a device for control of the electrical voltage difference between two electrochemical electrodes. Usually one of the electrodes is a reference (see Chapter 3) and the potentiostat actually controls the voltage of another, called the *working* electrode, with respect to the *reference* electrode, by applying electrical current between a third, called *counter* electrode, and the working electrode.

As the reference electrodes have very high internal resistance, they do not allow significant electrical current flow. This is the common reason to use the third, *counter* electrode. The potentiostat controls the voltage difference between the working and the reference electrodes by applying a larger biasing voltage causing current flow between the working and counter electrodes.

We shall use the potentiostat in a new way, as a controlled power source of the pH modulation electrodes and the electrolysis rate, hence the value of pH in the controlled solution. To generate electrolysis with significant rate and bias pH of an aqueous solution, the potentiostat should be capable of producing output voltage above 2.3V between the working and counter electrodes. While higher voltage accelerates the rate of electrolysis and hence speeds up pH control, the preferred output voltage is determined by the solution composition and is limited to avoid side electrochemical reactions. The output current range in the same loop may vary from tens to hundreds of mA/cm^2, dependent on the solution conductivity, the electrodes surface area and the controlled volume. The output characteristics of the potentiostat have critical impact on the speed and accuracy of pH response.

5.2.1.1 Electrochemical cell equivalent circuit

The simplified equivalent circuit of a typical three-electrode electrochemical cell is shown on fig. 5.1, where:

WE is the working electrode
CE is the counter electrode
RE is the reference electrode
C_{dl} is the double layer capacitance

R_w, R_c and R_{rc} are respectively the WE, CE and RE ohmic resistances and Rel is the ohmic resistance of the electrolyte.

From the above circuit, it follows that the negative feedback control system should supply an output bias between the WE and the CE (with corresponding polarity) and take the feedback control signal between WE and RE.

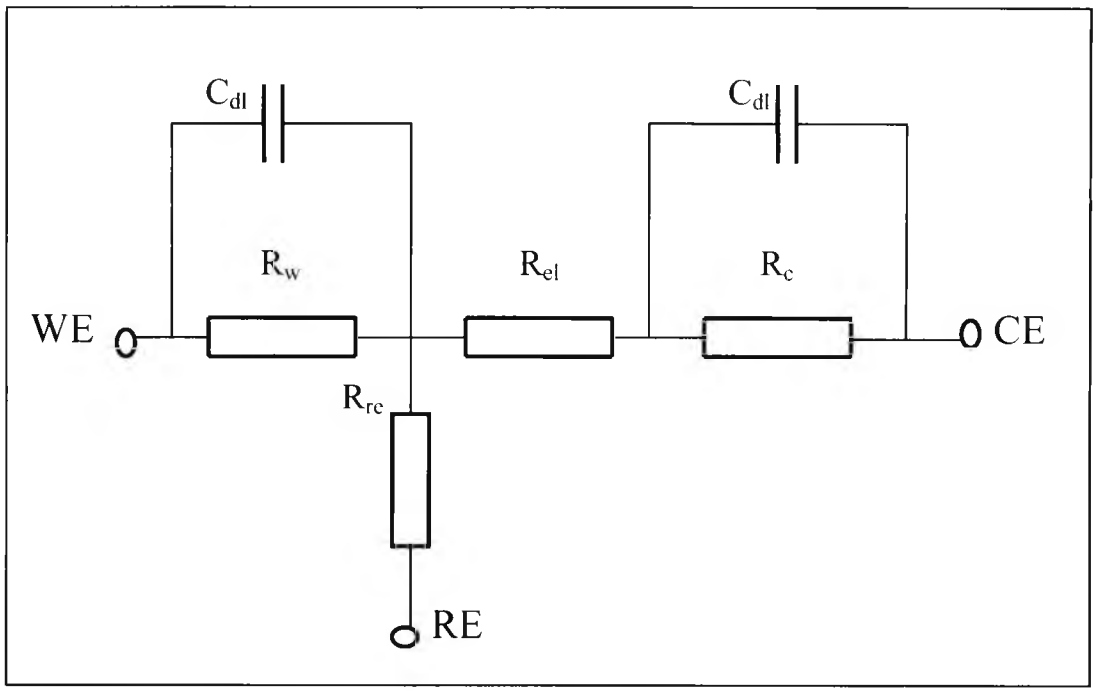

Fig. 5.1: Electrochemical cell equivalent circuit, taking into account the electrodes double layer capacitance, polarization resistance and the electrolyte resistance.

5.2.1.2 Potentiostatic control instrumentation

The potentiostat is a voltage feedback controlled power supply, designed to maintain a desired electrochemical potential of an electrode in a solution. The main circuit of the instrument is a power operational amplifier (PA), on the positive input of which is applied the desired voltage. The output of the PA is connected to the CE of the electrochemical cell. The WE is grounded and the PA output current flows through the CE/WE loop.
A simplified potentiostat circuit diagram involves one operational amplifier as shown on fig. 5.2.

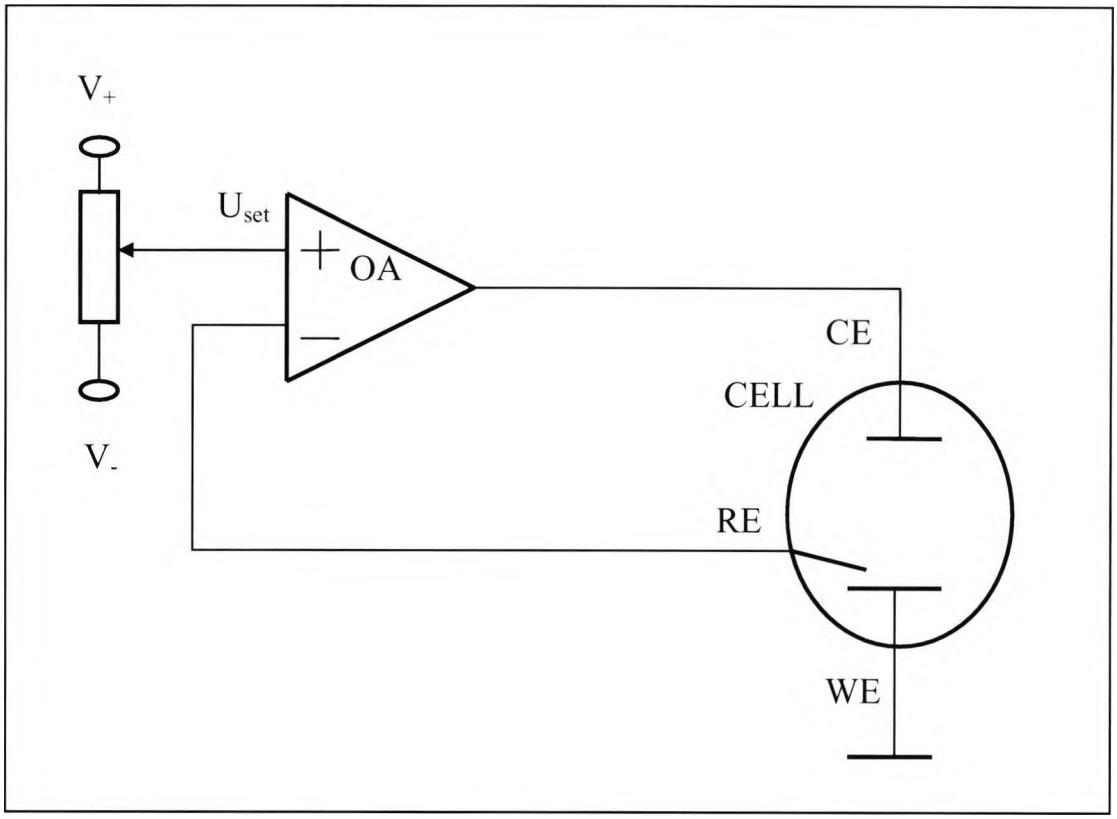

Fig. 5.2: Potentiostat principle of operation diagram, showing the electrochemical cell included in an operational amplifier feedback control loop.

The operation of this device is the following: the input control voltage is applied to the positive input of the OA (which could be a PA) and the electrochemical cell is connected as a load to its output. RE versus ground carries the voltage difference between the WE and RE, and supplies the negative feedback signal to the negative input of the OA. The OA "makes everything possible" to minimize the voltage difference between its inputs by biasing CE in a way that the voltage difference between WE and RE will be equal to the input control voltage U_{set}.

5.2.2 Limitations of potentiostatic systems

To control the set WE potential, the potentiostat needs to provide a higher output compliance voltage to the CE. Depending on the ratio R_{el}/R_w, effectively acting as a

voltage divider, the output voltage can exceed multiple times the controlled potential. This is particularly true for low-conductivity electrolytes, for example pure water. Also, the output current rate capability of the OA needs to be sufficient to drive the WE to the desired potential. Larger surface area WE and CE in a conductive solution require larger current, similar to charging a battery. For example, a lead acid battery will generate substantial amount of hydrogen and oxygen gases on the cathode and anode, respectively, when the voltage between the two electrode plates is over 2.3V, corresponding to overcharged state of the battery. To accelerate this process to practical speeds of tens of seconds up to a few minutes, larger than the nominal charging current may be needed.

The frequency response of the OA and the associated stability issues of the potentiostat, including the frequency response of the feedback control loop, also need attention to prevent self oscillation of the system.

Although difficult, the above limitations can be overcome by designing for the worst case of the specific application, including the power supply and the stability at different loads.

5.2.2.1 Output voltage

As shown above, the electrochemical cell is a voltage divider connected to the potentiostat output. To control the voltage on the WE, the PA output should be able to supply high enough voltage to fulfill the equation:

$$V_{out} = \frac{R_w + R_{el} + R_c}{R_w} V_{set}$$

Equation 5.1

so that the system will operate in its linear region.

5.2.2.2 Output current

The output of the OA should be able to supply the electrical current necessary to create the voltage drop across the electrochemical cell:

$$I_{out} = \frac{U_{out}}{R_w + R_{el} + R_c}$$

Equation 5.2

It should be also able to supply larger pulse output current to charge C_{dl} during voltage transitions.

5.2.2.3 Input resistance

The internal resistance of the negative input of the OA should not load significantly the reference electrode. For example, if the acceptable error margin is 0.1% and the internal resistance of the reference electrode R_{re} = 10 kOhm, the OA input resistance should be more than 10 MOhm. This problem is solved by the inclusion of a voltage-follower to buffer the negative input of the control amplifier. Unfortunately this adds one more pole in the potentiostat transfer function and creates possible stability problems, e.g. self-oscillation.

5.2.2.4. Current sensing

To measure the current through the working electrode and eventually to compensate for the voltage drop across the electrolyte between the WE and the RE, it is necessary to introduce a current sensing resistor in the path from the working electrode to ground. The voltage drop across this shunt resistor U=IR will allow to measure the equivalent of the current value, in voltage units, and to use it as a feedback signal, but it causes an error in the voltage control loop. This error could be eliminated by the inclusion of the current sensing shunt resistor in the negative feedback loop of another power OA. The last behaves as a virtual zero input resistance OA and needs equal to the main amplifier output capabilities to compensate for the cell current (fig. 5.3).

5.2.2.5 Frequency response

The transfer function of the system (F_t) will depend on the OA frequency response specifications and the feedback coefficient (B):

$$F_t = \frac{A}{1 + B}$$

Equation 5.3

where A is the open loop gain of the OA ($10^5 - 10^6$), B is the feedback coefficient and X_c is the double layer impedance.

$$B = \frac{R_w \text{ II } X_{cw}}{R_w \text{ II } X_{cw} + R_{el} + R_c \text{ II } X_{cc}}$$

Equation 5.4

The "II" sign denotes parallel connection. As shown on fig. 5.4 further, the closed loop gain of the PA is many times smaller than the open-loop gain and is typically in the range of 1 to 10 for highly conductive electrolyte, e.g. aqueous solutions.

5.2.3 Potentiostat design

To properly design potentiostatic instrumentation for a specific application, one should know the specifications of the electrochemical cell, or they should be evaluated experimentally. The system does not have to be limited by voltage, current or speed and be able to maintain the desired DC or AC voltage at the controlled point. To enhance the capabilities of the potentiostat for practical applications, several blocks, as shown above, could be added to the circuit, including a voltage follower with high input impedance, output power booster, current sensing amplifier and IR_{el} compensation (fig.5.3). In addition to the operational amplifier of the previous circuit, in the control loop are included the circuits described in the following paragraphs.

5.2.3.1 Power booster

This is a power operational amplifier with larger output voltage and current capabilities. Larger output voltage allows for biasing of the WE to the desired potential even when the resistance of the electrolyte is very high, and also improves pulse response rise time. The high output current capability is necessary when electrodes with large surface area are used or the electrolyte is highly conductive, and also for pulsing capacitive type of loads.

5.2.3.2 Voltage buffer

Very high input impedance is required in the reference electrode sensing line. Usually a FET-input precision operational amplifier with input resistance of more than 10^{12} Ohms is used. If the potentiostat is designed to work at high frequency or with fast pulses, a compromise between precision and frequency response should be made (Bourilkov, 1992b).

5.2.3.3 Current sensing amplifier

This PA keeps the WE at virtual ground, as its feedback acts through R_{sh} to minimize the input voltage. At the PA output the current flowing through the WE and R_{sh} is converted to conveniently measurable voltage value, referred to ground. A range of shunt resistors could be switched for wider current range specification.

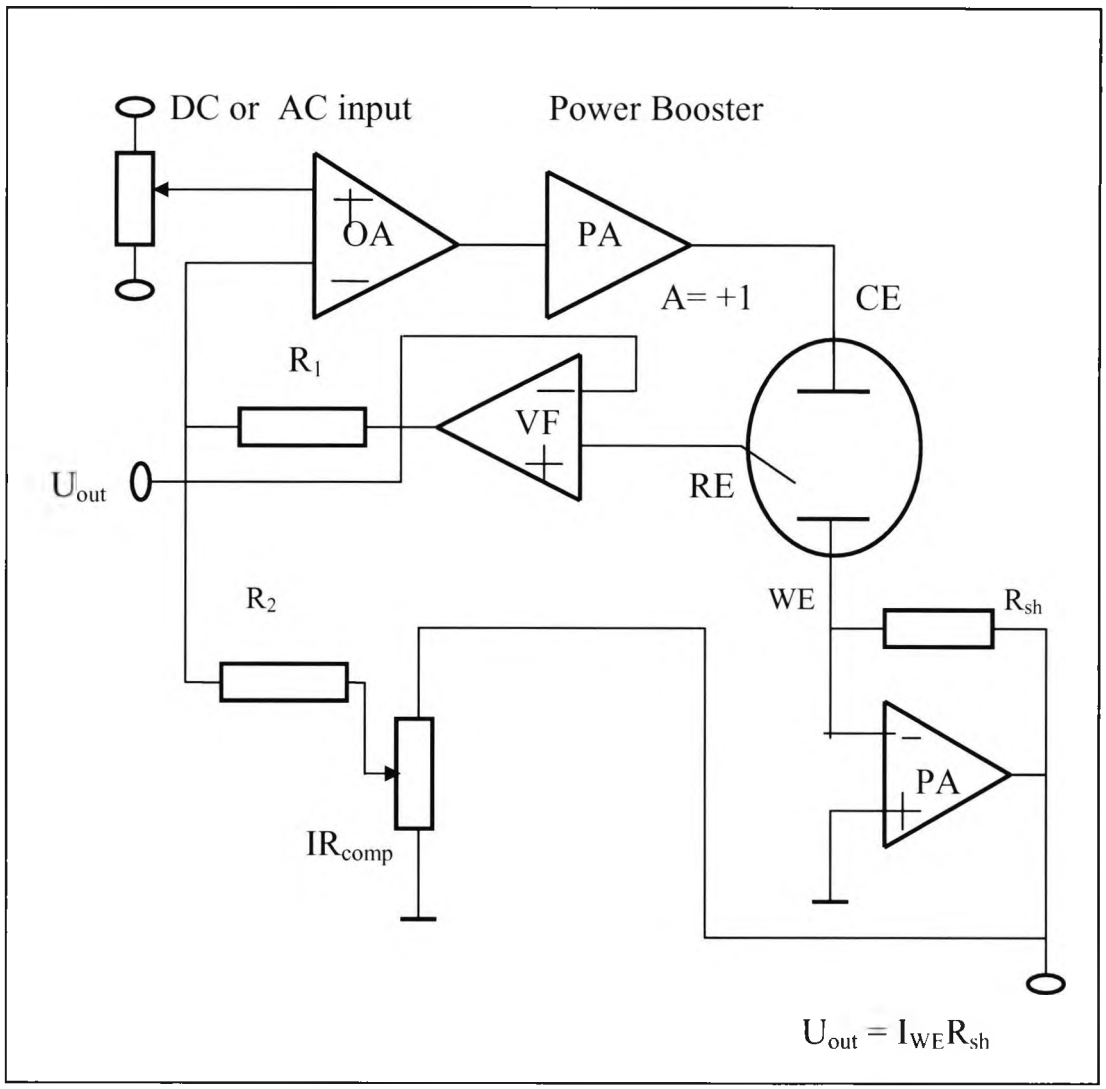

Fig. 5.3: Potentiostat circuit diagram revealing the main building blocks: WE voltage control power amplifier, RE high-impedance voltage follower, and current to voltage converting power amplifier.

5.2.3.4 Positive feedback loop for IR compensation

The output signal of the current sensing amplifier could be also used for compensation of the voltage drop in the electrolyte path between the WE and the RE. As the RE is always located at some distance from the WE because of its physical dimensions, the current flowing from the CE to the WE causes an IR drop, which represents an error in the control system. This error is proportional to the current and could be compensated by using an adjustable positive feedback from the current sensing amplifier output through potentiometer to the summing point of the control amplifier. As a positive feedback, it tends to reduce the system stability and should be used with care so as not to cause oscillations.

5.2.4 Potentiostat stability

The frequency response of a classical compensated operational amplifier is well known as shown on the Bode plot below, where A is the operational amplifier voltage gain, A_{ol} is the open loop gain, F is the frequency and f_t is the frequency at which $A_{ol} = 1$.

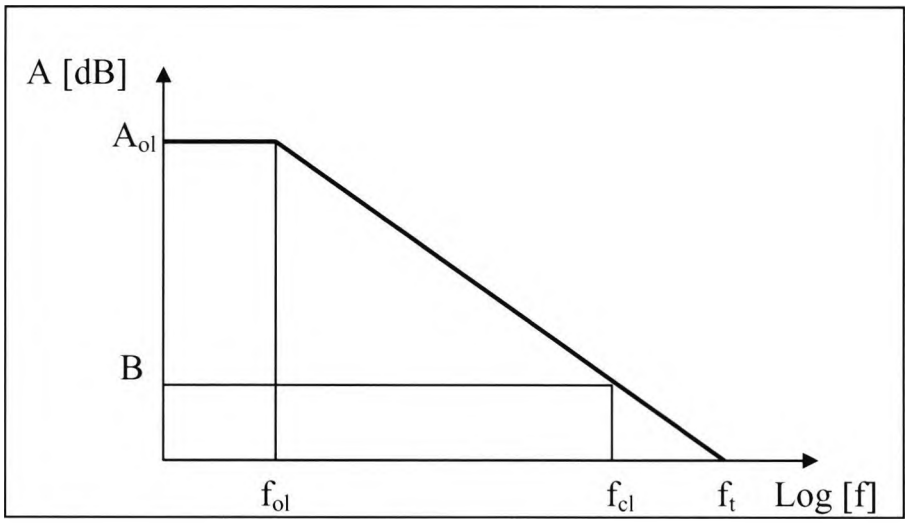

Fig. 5.4: The frequency response of a compensated operational amplifier follows the 6dB/octave (20 dB/decade) rule.

The slope after the brake point f_{ol} is 6 dB/octave and stability is guaranteed. The deeper the negative feedback, the gain is smaller and the frequency response better. If a simple potentiostat circuit with just one operational amplifier is considered, it can be seen that the electrochemical cell is included in the negative feedback loop and this will cause an additional phase shift depending on the equivalent R and C values. In the worst of cases,

when the electrochemical cell impedance has a prevalent capacitive component, as with monocrystal single wall silver electrode, the system is already on the verge of instability. The addition of a voltage buffer, power amplifier and current sensing amplifier with their transfer functions only surpasses the phase shift reserve and causes oscillation, if no frequency response compensation is used. As the voltage buffer works at a gain equal to one, its breakpoint appears at much higher frequencies and does not affect the usually slower main amplifier. Nevertheless, if a slow low-noise high-precision voltage buffer is used, the potential for instability and oscillations exists.

5.3 Galvanostats

5.3.1 Principle of operation

The galvanostat is another example of an electrochemical feedback system. The parameter under control here is the electrical current, i.e. this is a voltage controlled constant current source. It is used to supply a predetermined electrical current through an electrochemical cell, e.g. an electrolysis cell, which is proportional to the input voltage setting and is not dependent upon the changes in electrode potential and impedance.

5.3.1.1 Circuit diagram

The simplest electronic galvanostat with the use of one OA is shown in the following figure:

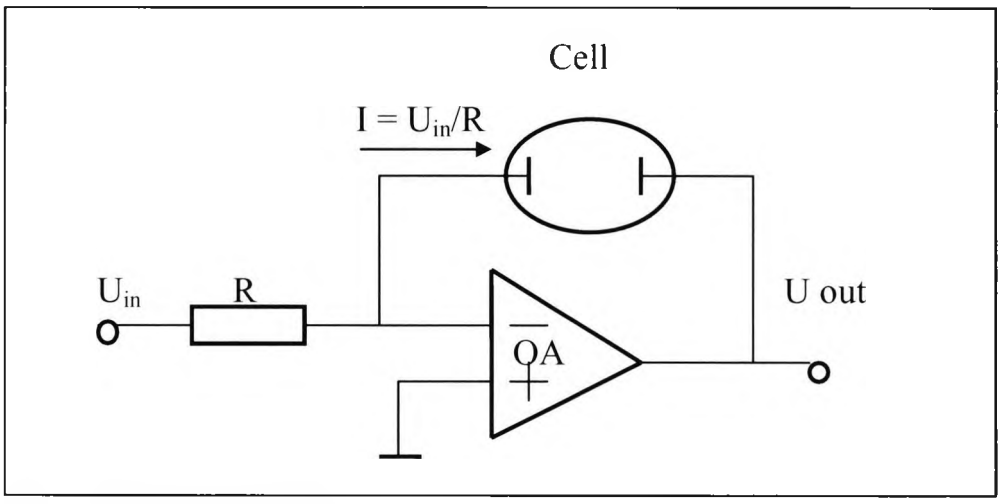

Fig. 5.5: Galvanostat principle of operation diagram, showing how set voltage is converted to set current independent on the electrochemical cell parameters.

As the input resistance of the operational amplifier is close to infinity and the voltage between the two inputs close to zero, referring to the circuit on fig. 5.5, one and the same current flows from input to output ($I = U_{in}/R$). For the same reason the output voltage of the operational amplifier is equal to the electrochemical cell voltage. This circuit allows for easy and precise galvanostatic control and monitoring of low-power electrochemical cells. Disadvantages of such a system are that the cell is floating (not grounded) and that the control voltage source should be able to carry the working electrode current without drop.

5.3.1.2 Improved circuit

Another circuit, which eliminates the drawbacks of the circuit shown on the previous figure and is suitable for more powerful applications, is the following:

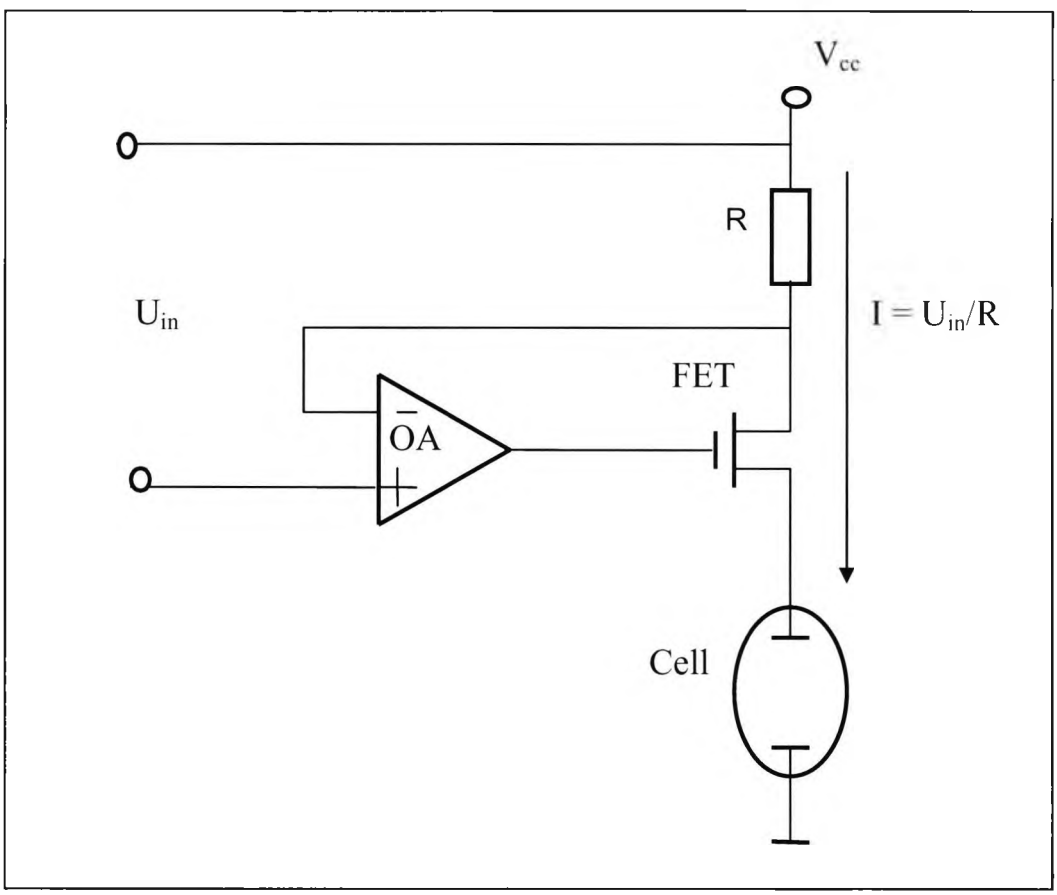

Fig. 5.6: Single polarity galvanostat, where the electrochemical cell is grounded, but the voltage control signal is floating.

Here, as mentioned before, because the OA keeps the voltage between its inputs close to zero, the output current is $I = U_{in}/R$. The cell is grounded, more immune from electrical noise and convenient for voltage monitoring.

A major disadvantage is that the input voltage is referred to the power supply rail and not to ground. This could be eliminated by the use of one more voltage to current converter as a current mirror, shown in the next paragraph.

5.3.1.3 Control voltage-shifting circuit

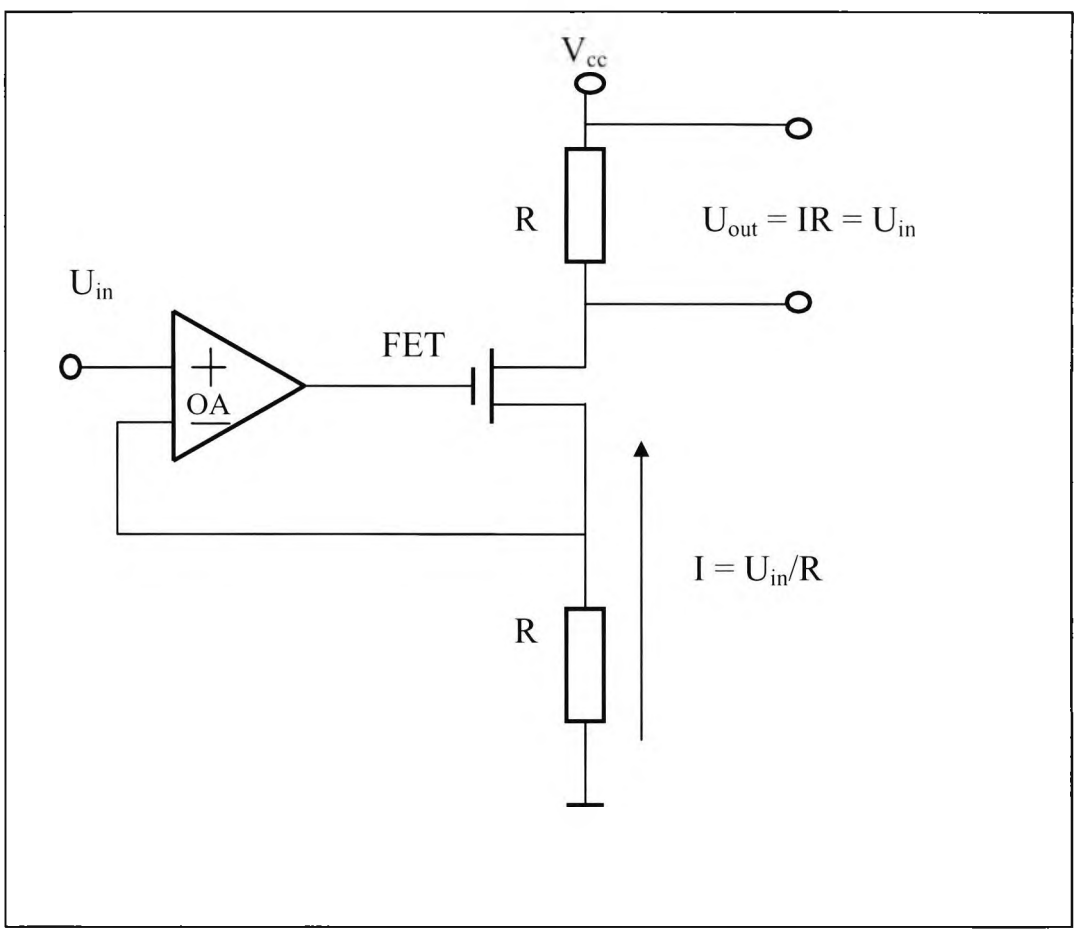

Fig. 5.7: Voltage-shifting circuit, enabling control of the potentiostat from fig. 5.6 using a grounded voltage source.

Here the output voltage is equal to the input voltage, but referred to the power supply rail, permitting to control the galvanostat of fig. 5.6 with a voltage source referred to ground. The compliance voltage of this circuit is the power supply voltage. The two resistors should be equal.

5.3.2 Limitations

5.3.2.1 Output current

The output current is limited by the field effect transistor (FET) characteristics and maximal power dissipation, the shunt resistor power, and the V_{cc} power supply specifications. All of the above should meet the worst case specification of the electrochemical cell under control.

5.3.2.2 Compliance voltage

The value of V_{cc}, called also compliance voltage, will limit the maximum output current, depending on the electrochemical cell resistance:

$$I_{max} = \frac{V_{cc} - I(R_{sh} + R_{ds})}{R_{cell}} \qquad \textbf{Equation 5.5}$$

where R_{sh} is the shunt resistor and R_{DS} is the Drain/Source resistance of the FET.

5.3.2.3 Frequency response

The frequency response of the circuit is limited by the OA and the FET frequency response characteristics and depends on the closed loop transfer coefficient B. Higher values of R_{sh} could reduce the gain and hence extend the frequency response, but the lost power dissipated across the resistor increases the thermal losses and also affects the accuracy because of the thermal coefficient of R_{sh}.

5.4 Combined potentiostat/galvanostat

From the above description of the fundamentals of potentiostats and galvanostats, it appears that there are many similarities in the negative feedback control system of both. The main difference between them is the controlled parameter – voltage or current. It is possible to implement both control modes on one and the same power circuit by switching the feedback signal from voltage to current. The switching could be realized by automatic crossover at predetermined values or maximum values of the controlled parameters, i.e. the dominating parameter will determine the type of feedback control – voltage or current. This is similar to charging a battery at constant current up to a

maximum charge voltage, where the circuit turns automatically in constant voltage mode and the current exponentially drops.

Summary

In this chapter, we presented the basic types of electrochemical instruments and investigated the relevance of these devices for pH control applications. Both controlled potential and controlled current can be used to generate the necessary electrolysis and pH modulation in the controlled volume. A pH sensor with voltage type of output signal should be used in the feedback control loop. Some limitations of the potentiostatic and galvanostatic systems arising from a pH-control point of view were also addressed here.
The power supply with its compliance voltage and current rate capabilities is a vital part of the control instrument and imposes its own limitations. The power source choice is critical for battery powered, remote on-line sensors, where minimum maintenance over extended period of time is desired. In the next chapter we shall evaluate the performance of different primary and rechargeable battery power sources in pH control applications.

CHAPTER 6: BATTERY POWER FOR ON-LINE PH SENSORS/CONTROLLERS

Introduction

The power supply is a critical part of the pH controller. Adequate time response requires significant current drain capability and compliance voltage level. In particular, remote on-line sensors are battery-powered, and the choice of the power source is critical for the device specifications and low maintenance. In this chapter, we shall review the most common types of primary and secondary (rechargeable) batteries and assess their performance in a remote electrical pH controller. Primary batteries are known for their high energy density at low rate of discharge, and rechargeable batteries – for their high power output. Hybrid systems, involving a primary battery charging a rechargeable battery, can combine the best of both worlds and provide highly efficient power solution for intermittent loads. In one hybrid system configuration, a high capacity primary battery is used as an energy source for a rechargeable battery, which serves as the principle power source for an electronic device. The primary battery indirectly powers the device through the rechargeable source. Such a hybrid system allows a low power energy source to operate a high drain device and in doing so, more efficiently utilizes the available energy powering said device. Hybrid solutions may involve alkaline, zinc-air or lithium batteries on the primary side, and lithium-ion, nickel- cadmium or nickel-metal hydride batteries on the secondary side, which powers the device. We discuss the specifics of different chemistries and select the alkaline primary/lithium-ion rechargeable battery combination as the best choice to design a simple and highly efficient hybrid power system for a remote pH controller. A patented electronic circuit (Bourilkov, 2003) was developed and optimized for energy transfer efficiency, complexity and cost. The principles of operation and how to combine a boost DC/DC converter, charger and controller into one simple circuit are discussed. The circuit was tested and the results confirmed the feasibility of the developed hybrid power system.

6.1 Battery selection

The battery selection process begins in the early stages of equipment design. In this way the most effective marriage between battery capabilities and equipment features can be made. This is especially true when considering the design-in of a new battery-powered product. Early consideration gives the designer the opportunity to increase the number and types of features offered while reducing size and weight of the new product. The fundamental requirements, which should be considered early in the battery selection process, are:

- **Voltage:** maximum permissible voltage; minimum operating voltage; start-up time (maximum permissible voltage delay). Nominal voltage and typical discharge voltage ranges for the most common primary and rechargeable battery chemistries are given in table 6.1 below:

BATTERY SYSTEM	NOMINAL VOLTAGE	TYPICAL OPERATING VOLTAGE
Nickel Cadmium and Nickel Metal Hydride	1.20	1.15 – 1.35
Mercuric Oxide	1.35	1.15 – 1.3
Alkaline-Manganese Dioxide	1.50	0.8 – 1.6
Silver Oxide	1.50	1.1 – 1.5
Lithium-Manganese Dioxide	3.00	1.8 – 3.3
Lithium ion	3.6	2.4 – 4.2

Table 6.1: Typical battery voltage ranges for the most common chemistry systems.

- **Capacity:** the output capability of a cell over a period of time is referred to as cell capacity. Cell capacity is the amount of current withdrawn from the cell multiplied by the number of hours that the cell delivers current to a specific end-point voltage. *Rated capacity* is the capacity a cell typically delivers under specific conditions of load and temperature. A cell will usually deliver less than rated capacity when discharged at loads heavier than the rated load, and/or temperatures lower than the rated temperature. Conversely, capacity greater than the rated value is usually obtained at lighter loads and higher temperatures.
- **Energy density:** the ratio of the energy available from a cell to its volume or weight. A comparison of the performance of various battery systems is normally made on practical, delivered energy density per-unit-weight or

volume using production-based cells and performance as opposed to theoretical energy density. To determine the practical energy density of a cell under specific conditions of load and temperature, we multiply the capacity in ampere-hours that the cell delivers under those conditions by the average discharge voltage, and divide by cell volume or weight.

Gravimetric Energy Density (Equation 6.1):

$$\frac{\text{(Drain in Amps x Service hours) x Average Discharge Voltage}}{\text{Weight of cell}} = \text{Wh/ Kg}$$

Volumetric Energy Density (Equation 6.2):

$$\frac{\text{(Drain in Amps x Service hours) x Average Discharge Voltage}}{\text{Volume of cell}} = \text{Wh/l}$$

Designers of battery-powered devices place minimal emphasis on the theoretical energy density of electrochemical systems. Theoretical energy density comparisons have limited practical significance: they are calculated from the weight or volume of active anode and cathode materials with no consideration given to the weight or volume of inactive materials required for cell construction. Additionally, losses due to cell polarization on discharge are not factored into theoretical values. Consequently, comparative testing may show that the battery system with the higher theoretical value does not deliver higher actual energy output.

In figure 6.1 below, the energy densities of the most common primary and rechargeable batteries are compared.

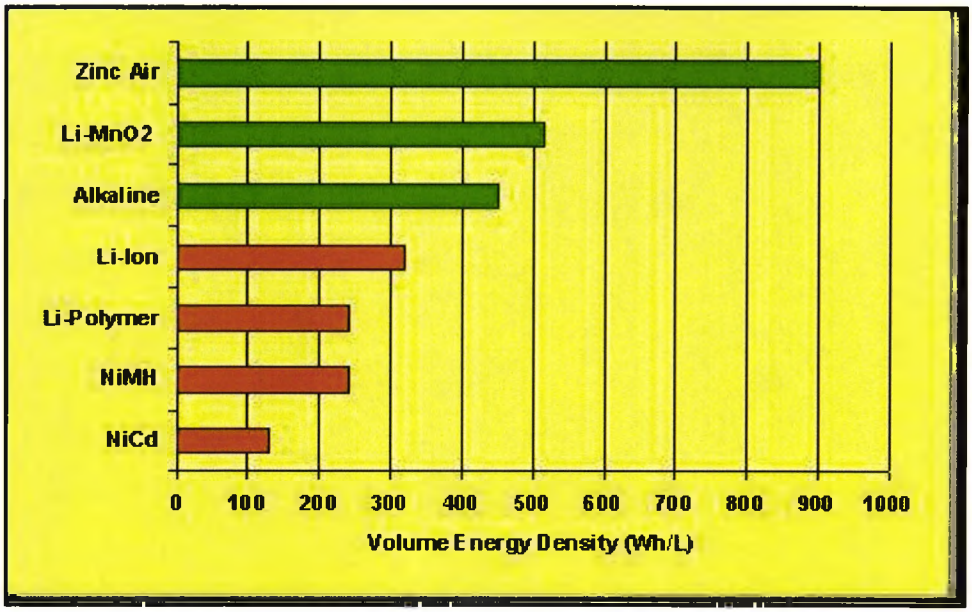

Fig. 6.1: Practical volumetric energy densities of primary and rechargeable batteries of different chemistries (primaries in green, rechargeables in red) - Duracell.

- **Load or current drain:** the battery efficiency depends of the load type: constant resistance, constant current or constant power. The most favorable discharge regime for the battery is resistive load, where the discharge current drops simultaneously with the battery discharge voltage, following Ohm's low. Opposite, constant power mode increases the current at lower voltage and loads the battery more at the end of discharge, causing an avalanche cutoff before fully utilizing the available energy. Typically, all power systems using DC/DC switching converters represent a constant power mode, as the converter output voltage and hence output power are constant, and the primary load on the battery side is of the same type, increased with the efficiency losses (5-20%). This is a problem especially for low-voltage battery powered systems using voltage boost converters, where high-current battery loads result in poor battery efficiency. The decrease of the useful battery energy as a function of the load for different chemistries is shown on fig. 6.2. From the graph is evident, that rechargeable batteries have better efficiency at high loads, and the energy advantage of primary batteries is only available at low drain, and is lost at high load.

Also variable loads, pulse loads, and peak currents need to be taken into consideration to avoid premature battery shutdown. The peak current capability of the battery is a function of the internal resistance or impedance for AC loads. Holding voltage over longer load pulses is related not only to internal impedance, but also to diffusion limitations and electrolyte conductivity, surface area of the electrodes, and temperature.

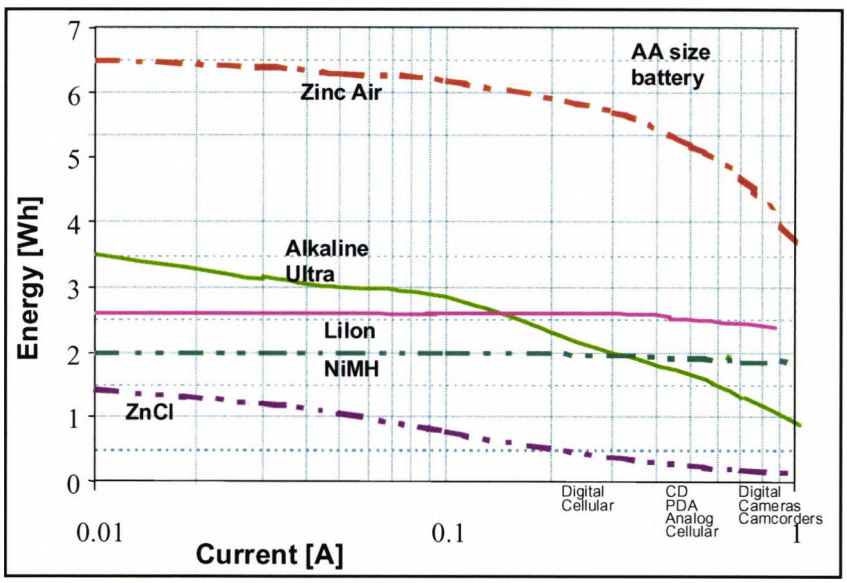

Fig. 6.2: Deliverable energy versus current drain: at high rate of discharge, primary batteries lose efficiency and rechargeable batteries provide better energy utilization (Duracell).

- **Duty cycle:** continuous or intermittent usage pattern.
- **Service life:** length of time operation is required.
- **Physical requirements:** battery size, shape and weight, terminals.
- **Temperature requirements:** operating temperature range and storage temperature range.
- **Environmental conditions:** shock; vibration; atmospheric conditions, such as humidity and pressure.

- **Shelf life:** capacity retention requirements, storage time and temperature.
- **Reliability:** permissible performance variability and failure rates, potential for gassing or leakage.
- **Safety:** consumer, industrial or military applications, usage of hazardous materials, withstanding of abusive conditions that are likely to occur.
- **Contacts:** equipment contact materials should be compatible with battery terminal materials to prevent galvanic corrosion due to use of dissimilar metals.
- **Cost:** operating or life cycle cost, as well as initial cost.
- **Replacement:** if battery replacement is required, who will replace the battery and where will a replacement be obtained?

When we have identified the important fundamental requirements, the decision as to what battery system best fits the needs of our application can be made. With so many types of batteries and battery systems available today, choosing the most suitable battery for our specific application can be a difficult task.

6.2 Primary battery chemistries

Primary batteries are replaceable electrochemical power sources. The most common types are alkaline, zinc-air and lithium batteries. We shall review these chemistries and their limitations regarding our specific application.

6.2.1 Alkaline

The zinc/potassium hydroxide/manganese dioxide cells, commonly called alkaline, have higher energy output than zinc- carbon (Leclanche) cells. Other significant advantages include longer shelf life, better leakage resistance and low- temperature performance, and worldwide availability at retail. Due to a longer service life, the alkaline cell is more cost-effective per utilized energy.

6.2.1.1 Composition and chemistry

The chemically active components are:

- **Anode**: high purity zinc powder

- **Cathode**: electrolytically produced manganese dioxide
- **Electrolyte**: concentrated potassium hydroxide solution

During discharge, the oxygen- rich manganese dioxide is reduced and the zinc becomes oxidized, while ions are being transported through conductive alkaline electrolyte. The cell reaction is:

$$Zn + 2MnO_2 \rightarrow ZnO + Mn_2O_3$$ **Equation 6.3**

6.2.1.2 Cell construction

A typical cell is designed with active materials and alkaline electrolyte contained in nickel- plated steel can. The manganese dioxide cathode powder mix is pressed against the inner surface of the steel can. With this intimate cathode-to-cell wall contact, the steel case becomes the cathode current collector and serves as the positive terminal of the cell (figure 6.3):

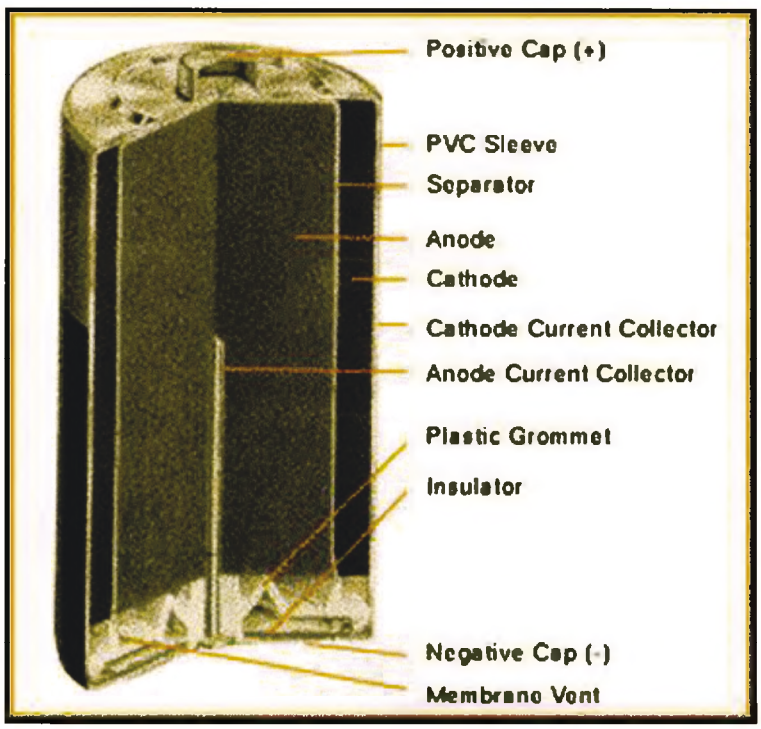

Fig. 6.3: Alkaline cell cross-section showing the battery construction including the active materials, electrodes, separator, current collectors and safety vent (Duracell).

A precise amount of the zinc anode powder is dispensed into the central cavity, located in such a manner as to ensure desired capacity and surface area. An anode current collector, welded to the external anode cap, extends through a plastic cap in the center of the anode powder mix. The separator is a highly absorbent, ion-permeable, and chemically inert material, which blocks the migration of the anode particles and prevents self-discharge of the cell when not in use. The porous nature of the anode, cathode and separator materials allows them to be thoroughly saturated with the alkaline electrolyte solution. A vent mechanism is incorporated into the plastic grommet to protect against cell rupture and damage in the event of failure or abusive conditions.

6.2.1.3 Performance characteristics

- **Voltage**: open circuit voltage (OCV) ranges from 1.5 to 1.62V. The nominal voltage is 1.5V. The operating voltage is a function of the state of discharge, load and temperature. The voltage profile under discharge is a sloping curve, as seen on figure 6.4:

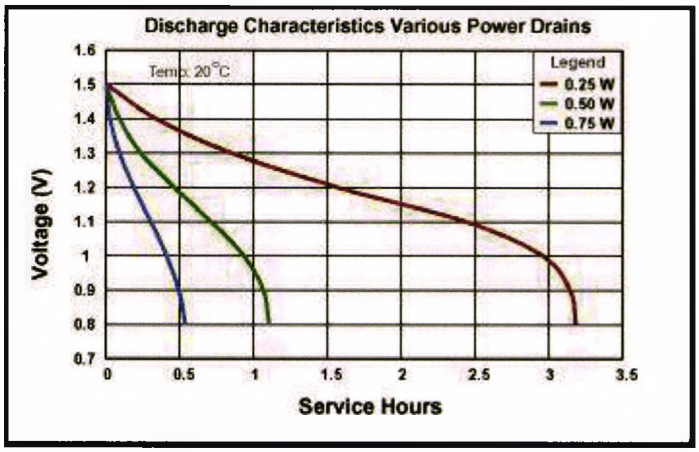

Fig. 6.4: Discharge voltage of an AAA alkaline cell at various constant power loads, showing lower discharge voltage at higher drain (Duracell).

- **Capacity**: usually expressed in Ampere-hours. In any given continuous drain application, the average load current, multiplied by the service hours, equals the rated capacity of the cell. On the following example (Fig.6.5) is shown a family of discharge capacity curves as a function of the drain for AAA (1.5V/1180mAh) alkaline cell at room temperature. From the graph is evident,

that alkaline cells are energy efficient at low discharge rates. Above 200mA constant current discharge rate, the effective capacity of the AAA alkaline cell is less than 50%. The cutoff voltage affects significantly the useful capacity, especially at high drain. It is recommended to discharge down to 0.8V/cell for full utilization of the battery capacity. Lower voltage discharge can cause hydrogen gas generation and internal cell pressure build-up, resulting eventually in venting and electrolyte leakage.

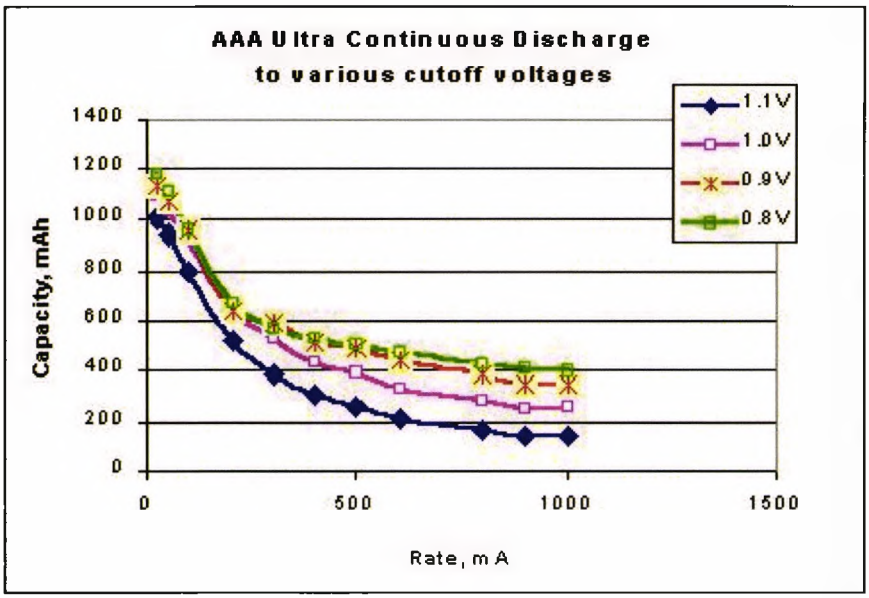

Fig. 6.5: Alkaline cell discharge capacity at constant current load, showing dramatic energy utilization penalty at high drain.

- **Temperature effect**: the alkaline system is best suited for use over a temperature range of -20°C to 54°C. For most cells, up to 75% of the rated capacity at room temperature can be delivered at freezing temperature.
- **Internal resistance**: due to the highly conductive electrolyte and compact construction, alkaline cells have relatively low internal resistance, although the "bobbin" type construction allows for lower surface area, compared to the "wound" type, used in other battery types. Also, the relatively low cell voltage is one reason to use multiple cells in series for most practical applications, causing corresponding internal resistance increase. The internal resistance

increases about 3 times from the beginning to the end of discharge. It is also reverse-proportional to temperature. In this sense, the self-heating of the cells during operation is beneficial, and a thermally isolated cavity in device is recommended.

- **Energy density**: Volumetric energy (eq. 6.2) ranges from 182 to 322 Wh/l, and Gravimetric energy (eq. 6.1) density from 91 to 130 Wh/kg, dependent on the battery size (Duracell ALKTB'98). Volumetric energy density is an important factor where battery size is the primary design consideration, while gravimetric energy density becomes important where the weight of the battery is important, such as in portable electronic devices.
- **Shelf life**: alkaline cells have long storage life. After one year of storage at room temperature, cells will provide 93 to 96% of the initial capacity. When stored for four years at room temperature, service of about 85% is still attainable. Storage at high temperature and high humidity will accelerate the degradation of the cells. At low temperature, the chemical activity is retarded and capacity is not greatly affected. Recommended storage conditions are 10 to 25°C with no more than 65% relative humidity.

6.2.2 Zinc-air

The zinc-air primary battery system is unique in that it "breathes" oxygen from the air to use as cathode reactant. The use of a virtually limitless supply of cathode reactant enables the zinc-air cell to offer some performance advantages compared to other primary battery systems. Zinc/Potassium Hydroxide/Oxygen properly describes the chemical components of this system, although "zinc-air" is the more widely used name. Zinc-air batteries include button cells, batteries, and a small number of customized battery packs. Zinc-air batteries deliver the highest energy density of any commercially available battery system, and at a low operating cost.

6.2.2.1 System Description

A zinc-air cell consists of a zinc anode, an aqueous electrolyte and an air cathode assembly. Power is derived from the reduction of oxygen at the cathode, and the oxidation of zinc at the anode. The simplified net reaction is shown below:

$$Zn + \frac{1}{2}O_2 + H_20 \rightarrow Zn(OH)_2$$ **Equation 6.4**

The zinc-air system derives its high energy density from the use of atmospheric oxygen as the cathode reactant. Compared to other systems of similar size, the use of atmospheric oxygen allows the zinc air cell to contain more zinc-anode material, which is the only material consumed during discharge. The increased amount of anode material enables the cell to offer up to 3 times more capacity than conventional zinc-anode systems, which contain oxygen within the cell in the form of manganese dioxide (as in alkaline cells) at around 60% of the cell weight. Their useful service life is limited by whichever material is consumed first. Zinc-air batteries are used in a number of consumer and industrial applications. They are best suited for applications requiring frequent or continuous use and low to medium drain applications, where high-energy density and a low operating cost are required.

Hearing aids are an ideal application for zinc-air cells because they are usually worn for up to 16 hours per day and have a low to moderate current requirement. Patient monitors and recorders, nerve and muscle stimulators, and drug infusion pumps are among the different types of medical equipment well suited for zinc-air batteries. Some telecommunication devices such as pagers are also powered by zinc-air batteries.

6.2.2.2 Performance characteristics

- **Voltage:** the nominal OCV for a zinc-air cell is 1.4 volts. Operating voltage during discharge is dependent on discharge load and temperature. Typically, operating voltage for a zinc-air cell is between 1.25 and 1.1V (fig. 6.6). The typical cutoff voltage, by which most of the cell capacity has been expended, is 0.9 volts.

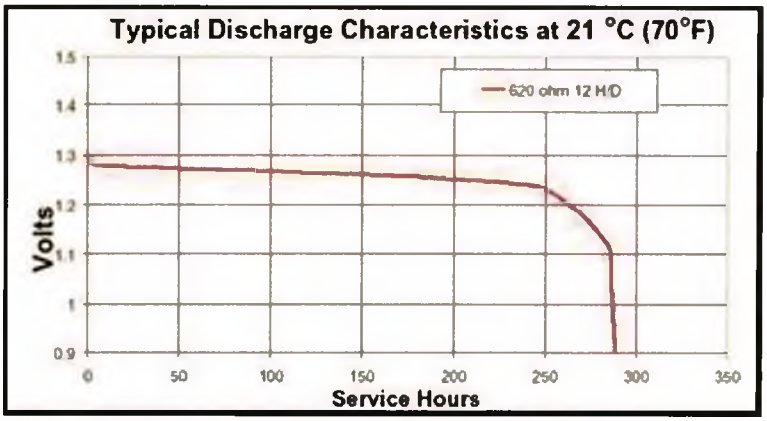

Fig. 6.6: The discharge voltage profile of zinc-air DA675 cell at constant resistance load is very flat almost to the end of service life (Duracell).

- **Energy density:** zinc-air batteries offer the highest gravimetric and volumetric energy density of any primary battery system, attributable to its use of an air electrode (cathode) which occupies very little internal volume and does not degrade throughout the discharge of the battery. The result is an increase in the volume available for the zinc anode, thus increasing the capacity. The zinc air cell has a gravimetric energy density of up to 442 Wh/kg and a volumetric energy density of up to 1673 Wh/l. This is up to three times the energy of alkaline and mercury systems. High energy is delivered under conditions of frequent or continuous use, low to medium requirements, and operating temperatures between O°C and 50°C.
- **Limiting current:** a specification or rating that is unique to the zinc-air battery. The limiting current is defined as the maximum operating current at which a battery will perform adequately at a continuous current drain. Usually the limiting current is the current at which the battery operating voltage drops to 1.1 volts per cell. This is the voltage used in specifying the "rated limiting current". This characteristic of the zinc-air battery is due to the fact that the cell can become oxygen-starved at high current drain discharges due to the rapid electrochemical utilization of the oxygen. At the limiting current, the rate of oxygen reduction is about equal to the replacement of air in the cell and the discharge current can be maintained without air starvation.

- **Pulse current capability:** many times greater than the limiting current. The average current drain during a pulse current discharge, however, must be less than the limiting current of the cell in order to maintain a constant voltage output. If the peak pulse current is increased, so that the average current is greater than the limiting current, the cell will eventually become oxygen-starved and the voltage will decline.
- **Internal impedance:** cell impedance is a critical consideration in many applications. The internal impedance of zinc-air batteries is comparable to other zinc-anode batteries of similar size.
- **Sealed shelf life:** zinc-air cells are essentially dormant until the cathode reactant, oxygen, is allowed to enter the cell. Zinc-air cells exclude oxygen during storage by means of a low-porosity tape seal place over the air holes. The cells are activated by the removal of this seal to allow oxygen to enter. The sealed storage or shelf life of a zinc-air cell has been demonstrated to retain greater than 98% or rated capacity after one year of storage at 21°C.
- **Effect of temperature:** optimum performance for zinc-air batteries is achieved at temperatures between 0°C and 50°C. At lower temperatures, a continually sloping voltage profile will be exhibited, with the degree of slope dependent on the temperature and the discharge rate. Performance at temperatures above this range may provide for increased efficiency. However, exposure to high temperatures can accelerate moisture loss, which can reduce performance. The limiting current of a zinc-air battery is also affected by temperature.
- **Effect of humidity:** relative humidity can affect the performance of a zinc air battery over long discharge periods. Moisture transfer through the air-access holes of the battery results from the difference in relative humidity between the cell and the environment. The effect of continued moisture loss or gain from the electrolyte is evidenced by shortened life or loss of power, respectively. For best results of long discharges, conditions between 35 and 80 percent relative humidity are recommended.

- **Safety:** zinc-air cells offer a means of self-venting any internally generated gases through air-access holes located on the cathode can, eliminating the possibility of cell rupture or explosion. In addition, zinc-air cells are generally considered environmentally safe and under most conditions, do not require special handling or disposal procedures.
- **Operating cost:** zinc-air cells and batteries offer a low operating cost on a per-mAh basis when used in a frequent or continuous use application.
- **Preparing batteries for use:** zinc-air cells are stored with an adhesive tape seal or in a metallized plastic pouch, which inhibits gas and vapor transfer. The batteries are ready to be used when the seal or pouch is removed, allowing oxygen from the air to enter the batteries. In most cases, nominal voltage levels are present immediately after the seal is removed.
- **Service life:** the combination of discharge demands and the effects of gas transfer determine the service life of a zinc-air cell. Since the cell is open to air during the operation, the zinc-air cell is designed to balance long life (minimum exposure to air) with power capability (maximum exposure to air). The length of service life of a zinc-air cell is inversely affected by a change is the gas transfer. When the amount of gas transfer is allowed to increase (i.e. oxygen, water vapor, etc.) the service life of an activated (unsealed) zinc-air cell decreases. Gas transfer for a zinc-air cell is controlled by a combination of factors: the number of air holes, their size and location, and the diffusion characteristics of the air electrode. The amount of gas transfer is dependent on the temperature and humidity levels of the surrounding environment. Water vapor transfer is a normal occurrence in a zinc-air cell, but operation is affected when the degree of transfer is high. The magnitude and the direction of the transfer are dependent on the difference between the vapor pressure of the water in the electrolyte and the ambient relative humidity. The electrolyte in the cell will lose water when the humidity at room temperature is below 60 percent, and will gain water at humidity levels above 60 percent. Excessive water loss can eventually cause the battery to fail because of inadequate electrolyte to maintain the discharge reaction. Excessive water gain dilutes the electrolyte necessary to maintain the discharge reaction, reducing

conductivity. A sustained water gain will eventually saturate the air cathode, causing cell failure. Oxygen and carbon dioxide gas transfer may also alter cell performance. Oxygen entering the cell may dissolve in (and diffuse through) the electrolyte, causing direct oxidation of the zinc. Carbonation of the electrolyte is the result of carbon dioxide reacting with the potassium hydroxide in the electrolyte. Both of these forms of gas transfer can affect service life, but to a much smaller degree than water transfer. The unique air-breathing property of zinc-air cells is the key to their high energy density and reserve storage nature. This factor introduces application design considerations, which do not pertain to conventional primary battery systems.

- **Air access:** when designing equipment to use zinc-air batteries, air access must be considered. Air is admitted through the holes in the positive cap of each cell. Therefore, it is important that air access to these holes not be blocked. The oxidation of a single atom of zinc provides four electrons to the external circuit. From this fact, the amount of air required per ampere-hour of capacity to be delivered can be calculated as 1.15 liters per ampere-hour at room temperature and atmospheric pressure for zinc-air cell used. It is not possible to provide hard and fast rules for designing proper air access, such as number and size of holes to be used in the equipment. However, if the limiting current is more than the average current required by the device, then sufficient air access has been provided. When zinc-air batteries are discharged well below their normal voltage cutoff, e.g. to 0.0 volts, it is possible for electrolyte to leak out of the air holes. To prevent this from occurring the device should be designed with a voltage cutoff feature that shuts the equipment off at a predetermined voltage setting.

Unfortunately, the drain capabilities of this battery chemistry are moderate, and a delay in the voltage pulse response restricts dynamic load applications. Particularly, the limited activated life (about 30 days, loaded or not) makes this chemistry suitable only for moderate, continuous loads, that utilize all the available energy within the activated life period, and where frequent replacement is not a problem.

6.2.3 Lithium

Within the last decade rapid advancements in the development and miniaturization of electronic devices have created a demand for lightweight, compact, high performance power sources which can be used under a wide range of conditions. Lithium batteries, which deliver high-energy output due to the use of elemental lithium, have become the focus of considerable attention as an optimum power source to satisfy this demand.

The term "lithium batteries" describes the family of battery systems, which use lithium as the anode, but differ in cathode material, electrolyte, cell design, and other mechanical features. Each lithium system has its own intrinsic characteristics, setting it apart from other lithium systems in terms of electrical characteristics, rate capability, energy density, operating temperature, reliability, shelf life, and safety. Lithium primary batteries are classified into three groups, depending upon the type of cathode and electrolyte used. Examples of common lithium battery systems are shown in Table 6.2:

LITHIUM PRIMARY BATTERY SYSTEMS		
SOLID ELECTROLYTE SYSTEMS	**LIQUID ELECTROLYTE SYSTEMS**	
Solid Cathode	**Solid Cathode**	**Liquid Cathode**
Iodine (I_2)	Manganese Dioxide (MnO_2) Poly-Carbonmonoflouride (CF)n Silver Chromate (Ag_2CrO_4) Iron Disulfide (FeS_2) Copper Oxide (CuO)	Sulfur Dioxide (SO_2) Thionyl Chloride ($SOCl_2$) Sulfur Chloride (SO_2Cl_2)

Table 6.2: Various primary lithium battery systems.

We considered the lithium/manganese dioxide (Li/MnO_2) system as it offers the best balance of performance: the batteries possess high energy density, excellent shelf life, long-term reliability, and relatively high rate capability over a broad temperature range.

Light in weight and compact, Li/MnO_2 batteries are ideally suited when portability is a prime requisite in equipment design.

6.2.3.1 Composition & Chemistry

- **Anode:** the anode material in Li/MnO_2 cells is pure lithium metal. Lithium, the lightest of all metals, has the highest electrode potential and offers the greatest ampere-hour capacity per unit weight. Table 6.3 illustrates the advantage that lithium offers in terms of weight and electrochemical equivalence.

ANODE MATERIAL	ATOMIC WEIGHT	AMPERE HOUR CAPACITY PER GRAM (Ah/g)
Pb	207.19	0.26
Zn	65.37	0.82
Fe	55.85	0.96
Li	6.94	3.86

Table 6.3: Lithium is light and compared to other anode materials has huge capacity advantage.

- **Cathode:** the cathode material used in Li/MnO_2 cells is a mixture of heat-treated electrolytic manganese dioxide and conductive agents blended together for high conductivity. The conductivity of the MnO_2 cathode results in higher initial cell voltage and operating voltage during discharge than that achieved when using highly-resistive active cathode materials, such as polycarbon-monofluoride. The thermodynamic stability of this specially processed MnO_2 cathode ensures high reliability and performance, even after very long periods of storage.
- **Electrolyte:** the electrolyte in Li/MnO_2 cells is an organic solvent mixture into which an alkali metal salt is dissolved. This solution is a stable, non-pressurized medium, which balances the attributes of reliability, long life, performance, and safety. High ionic conductivity and low viscosity permit efficient cathode utilization over a wide range of temperatures, even at high rates of discharge.
- **Cell reaction:** the cell reaction involves the oxidation of lithium metal at the anode to produce positively charged lithium ions (Li^+) and electrons (e^-). Li^+

ions go into the solution and diffuse through the electrolyte and separator to the cathode. Electrons travel through the external circuit and arrive at the cathode where MnO_2, Li^+ ions and electrons combine. The MnO_2 is reduced from the tetravalent (Mn_{IV}) to the trivalent state (Mn_{III}). The solid discharge reaction product remains in the cathode. No gases are evolved during discharge to cause a pressurized condition. The total cell reaction is:

$$\mathbf{Li\ Li^+ + e^-\ Mn_{IV}O_2 \longrightarrow\ Li^+ + e^-\ Mn_{III}O_2(Li^+)} \qquad \textbf{Equation 6.5}$$

The theoretical voltage of the total cell reaction is approximately 3.5 volts. The actual open circuit voltage is lower, typically 3.1 to 3.3 volts.

6.2.3.2 Construction

Three structural designs of Li/MnO_2 cells satisfy wide range of today's electronic needs for small lightweight, portable power sources.

- **Coin (button) cells:** a selection of flat, coin-shaped Li/MnO_2 cells are available for applications requiring small, thin, long-life batteries, such as memory retention, watches, calculators, remote control units, medical equipment, electronic games, and many other low current drain electronic devices. A manganese dioxide cathode pellet faces a lithium anode disc. The electrodes are separated by a non-woven polypropylene separator, impregnated with electrolyte. The cell is crimp-sealed, with the can serving as the positive terminal and the cap serving as the negative terminal.
- **High rate spiral-wound cylindrical cells:** spiral wound cylindrical cells are designed for high-current pulse capability (up to 5A), as well as for continuous high rate operation (up to 1.2A). The lithium anode and the cathode are wound together with a microporous polypropylene separator inter-spaced between thin electrodes to form a "jelly roll." In this way, high surface area is achieved and rate capability is optimized (figure 6.7).

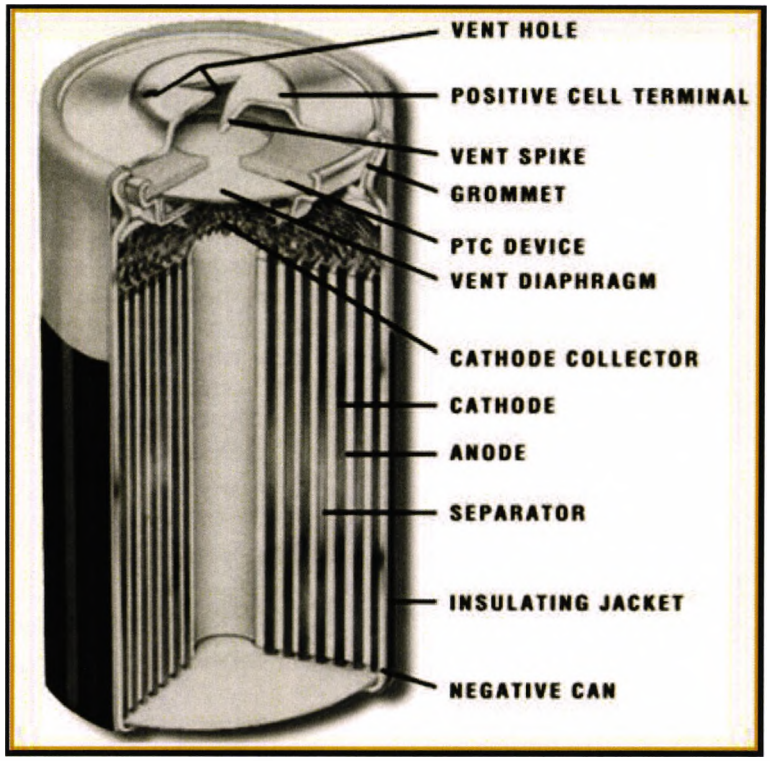

Fig. 6.7: Spiral wound cylindrical cell construction – here low impedance is achieved by the large surface area of the electrodes (Duracell).

High rate spiral-wound cells are used in a wide range of devices requiring high-current pulses and/or very low temperature operation. High rate spiral-wound cells contain a safety vent mechanism to relieve internal pressure in the event of severe mechanical abuse. High rate cells also contain a resettable PTC (Positive Temperature Coefficient) device, which limits current flow and prevents the cell from overheating if accidentally short-circuited.

- **Bobbin-type cylindrical cells:** bobbin cells contain a central lithium anode core surrounded by a manganese dioxide cathode, separated by a polypropylene separator impregnated with electrolyte solution. The increasing demand for extra long shelf life and very high energy density has inspired the development of Li/MnO_2 bobbin cells. The bobbin-type design maximizes the energy density due to the use of thick electrodes. However, unlike the spiral-wound cell design, electrode surface area is very limited. This restricts the usage of these cell types to very low drain applications. Bobbin cells are particularly suited for memory back-up applications that do not require the availability of replacement cells in the consumer or industrial market.

6.2.3.3 Performance Characteristics

- **Voltage:** the nominal voltage of Li/MnO_2 cells is 3.0 volts, twice that of conventional alkaline cells due to the high electrode potential of elemental lithium. Consequently a single Li/MnO_2 cell can replace two alkaline cells connected in series. The operating voltage of the battery during discharge is dependent on the remaining capacity, discharge load and temperature (fig. 6.8).

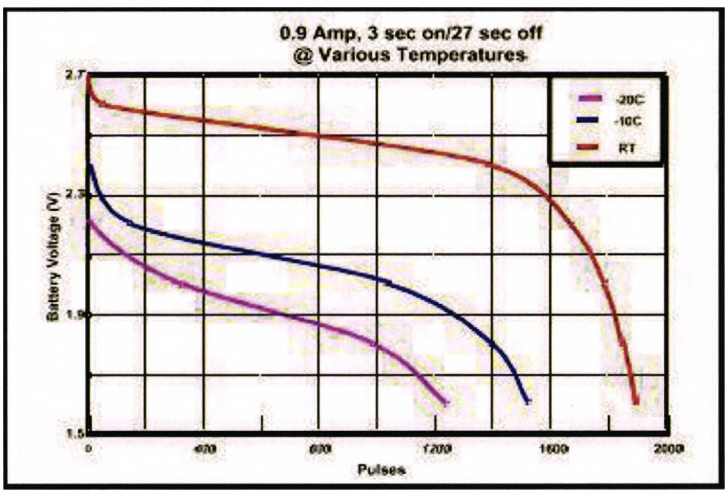

Fig. 6.8: LiMnO2 DL 123 discharge profiles at various temperatures, showing that the battery voltage drops lower and the slope is steeper at lower temperatures, resulting in shorter runtimes (Duracell).

The voltage profile of Li/MnO_2 cells at low loads is relatively flat throughout most of the discharge, with a gradual slope near the end of life. The sloping profile towards the end of life can be used in certain applications, such as utility meters and security devices. The gradual drop-off in voltage can serve as a state-of-discharge indicator to show when the battery is approaching the end of its useful life. Incorporating a low voltage indicator into equipment circuitry provides a way of alerting users to replace the battery before it drops below the minimum voltage.

- **Energy density:** The theoretical gravimetric energy density of the lithium/poly-carbonmonofluoride system, Li/(CF)n, is over 2,000 Wh/kg when the fluorocarbon used for the cathode is produced under optimum conditions. By comparison, the theoretical gravimetric energy density of the Li/MnO_2 system is 914 Wh/kg. Comparing energy densities, one must consider the influence of cell size, internal design (bobbin or spiral-wound configuration), discharge rate, and temperature conditions, as these parameters strongly impact performance characteristics (fig. 6.9).

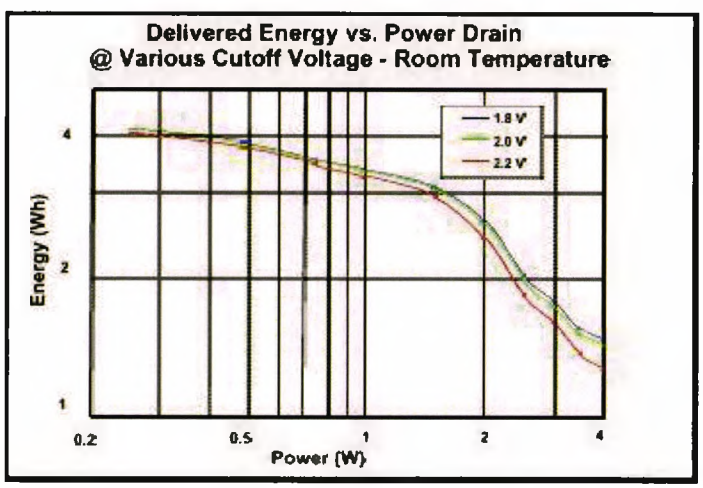

Fig. 6.9: Energy utilization of $LiMno_2$ DL123 cell at various constant power loads and different cut-off voltages (Duracell).

As a general rule, energy density decreases with decreasing cell size since the percentage of inactive materials, such as cell containers, take up proportionately more of the total cell weight and volume. Due to the use of thick electrodes, bobbin-type Li/MnO_2 cylindrical cells have slightly greater energy density (up to 1.2 times as much) than spiral wound Li/MnO_2 cells of similar size. The table in Appendix 7 compares the energy density of various bobbin cells under conditions of rated load and temperature. As shown, energy density increases with increasing cell size.

- **Capacity:** Li/MnO_2 cells are offered in a variety of cell sizes and capacities. Coin cells range from 75 to 600 mAh; spiral-wound cells are available in 900 and 1,400 mAh; and bobbin cells range from 650 to 1,900 mAh.

- **Effect of temperature:** Li/MnO_2 cells are capable of performing over a wide temperature range. The temperature range recommended for each cell type is a function of cell construction and seal design. Although –20 to +60°C is the range in temperature recommended for optimum efficiency, Li/MnO_2 cells are being used in applications ranging from –40 to +70° C.
- **Internal impedance:** the conductivity of organic electrolytes used in lithium cells is about 100 to 300 times less than aqueous electrolytes used in zinc anode cells. Consequently, lithium batteries are generally higher in internal impedance than batteries using aqueous electrolytes. The impedance of Li/MnO_2 cells varies with cell structure and size. Typically, impedance decreases with increasing cell size and electrode surface area. Li/MnO_2 spiral-wound cells utilize high surface area electrodes in a "jelly roll" configuration to achieve low impedance and high current carrying capability.
- **Shelf life:** in order to withstand extreme fluctuations in temperature and humidity conditions and perform after long periods of storage, a battery must have a precise balance of cell chemistry and internal and external hardware. Li/MnO_2 batteries have superior capacity retention characteristics, with capacity over 97 percent after five years at room temperature. Li/MnO_2 batteries are designed to store well under a range of environmental conditions and to perform at high current pulse drains after lengthy storage periods. Unlike liquid cathode lithium systems, such as lithium- thionyl chloride, voltage delays do not pose a problem. The absence of a voltage delay ensures immediate start-up of battery-powered devices even at very low temperatures. Our application is allowed to sit idle for a long period of time between uses. Having a battery which can tolerate this intermittent usage pattern is therefore very important. While many battery systems do not tolerate such applications, Li/MnO_2 batteries deliver equivalent energy even after long periods of storage.

6.3 Rechargeable battery types

Rechargeable batteries are reversible, and are reused multiple (up to thousands) times. Typically, rechargeable batteries have lower energy density, but excellent rate capability, flat discharge voltage profile and lower cost when used over extended period of time. For

many applications, where the battery service life is limited to a few days on a single charge (mobile phones, notebook computers), and the user has access to mains power, rechargeable batteries are the preferred choice.

6.3.1 Nickel-Cadmium

The NiCd batteries have a nominal voltage of 1.2V, typical range 1.35 – 1V in discharge and 1.2-1.6V in charge mode, depending on state of charge, load rate and temperature. The charging regime is typically constant current, and different methods are used for charge termination. Most common are -dV/dt (negative charge voltage slope at the end of charge, dT/dt (rate of temperature raise at the end of charge), or by time to acquire full capacity. The discharge voltage profile is very flat, approximately 1.2V. The internal resistance is very low, making this chemistry the preferred choice for high-drain applications, including transportation, power tools, radio transmitters and robots. Fast discharge up to 10C rate (C rate stands for 1-hour charge or discharge) and 4C (15 min.) fast charge rate are common. The energy density is about half of that of the newer nickel metal hydride chemistry (NiMH), which is replacing NiCd in most applications. One more reason for this trend is the so called "memory effect", a voltage depression over time, to which NiCd batteries are particularly sensitive. A reversible drop in voltage and loss of capacity occurs when a NiCd battery is partially discharged and recharged repetitively without the benefit of a full discharge. During this cycling, the discharge voltage and capacity gradually decrease. On a subsequent full discharge, the discharge voltage is depressed, compared to the original full discharge. Because the cell appears to "remember" the lower capacity, the voltage depression phenomenon is often referred to as "memory effect". The extent of the voltage depression and capacity loss depends on the depth of discharge and can be avoided by discharging the battery to the appropriate cutoff voltage. Environmental concerns related to disposal of the heavy metal Cadmium are causing the ban of this battery type in most countries.

6.3.2 Nickel-Metal Hydride

The charge methods and discharge characteristics of NiMH cells are very close to those of NiCd. The charged state OCV for both chemistries varies from 1.25 to 1.35V. On

discharge, the nominal voltage is 1.2V, and typical cutoff voltage is 1V. Typically, when the current is higher and the temperature lower, the operating voltage will be lower. This is due to the higher IR drop that occurs with increasing current and increasing cell internal resistance at low temperatures. However, at moderate discharge rates (C/5, which is used to evaluate the nominal capacity), the effect of temperature on the cell capacity is minimal. The NiMH batteries have low internal resistance, because they are manufactured with thin plate electrodes, which offer large surface area and good conductivity. The internal impedance remains relatively flat during most of the discharge. Towards the end of discharge, the impedance increases, due to the conversion of the active materials to a non-conductive form.

The gravimetric energy density for NiMH cells is 80 Wh/kg and the volumetric energy density 200 Wh/l, compared to 45 wh/kg and 70 Wh/l for NiCd. The delivered energy does not vary significantly with increasing power. It is dependent on the cutoff voltage and can be increased by discharging to lower voltages. However, the battery should not be discharged too low (less than 0.9V), as the cell can be damaged. The recommended cutoff voltage is 1V/cell. When string of cells are connected in series, the cell with the lowest capacity will reach a lower point of discharge compared to the others. The more cells are connected in series, the higher the probability for one cell to be over-discharged and even go to a voltage reversal. Extended over-discharge will lead to elevated internal cell pressure, opening of the safety vent and leakage.

Optimum temperature performance is obtained between 0 and 45°C. The performance characteristics of the battery are moderately affected at higher temperatures. At lower discharge temperatures, performance decreases more significantly, caused primarily by internal resistance increase.

The state of charge and capacity of NiMH batteries decreases during storage, due to self-discharge of the cells. Self- discharge results from the reaction of residual hydrogen in the battery with the positive electrode, as well as the reversible decomposition of the positive electrode. The rate of self-discharge is dependent on time and temperature. Typical capacity loss is 20% per month at 20°C, 10% at 0°C and 70% at 45°C. After long storage, the cell can be restored to full capacity by repeated charge/discharge cycles.

The memory effect for NiMH is much less pronounced compared to NiCd (less than 5% in worst cases) and usually performance loss is not perceptible.

6.3.3 Lead Acid

Lead acid batteries are widely used as car starting or electrical vehicle power source, as well as for stationary backup power and military applications. The electrode materials are lead (negative) and lead oxide (positive), and the electrolyte is a sulfuric acid aqueous solution. Lead acid batteries feature very good rate capability, tolerance to overcharge and long cycle life. The nominal discharge voltage is 2V, ranging from 1.8 to 2.2V, dependent on the discharge current, state of charge and temperature. The maximum charge voltage can reach 2.6V, but is usually limited to 2.4V per cell to prevent electrolyte decomposition and gassing. The typical charging regime is C/10 constant current with time limit. Trickle charge (C/50) is used to compensate for self-discharge and keep the batteries fully charged.

Last two decades, maintenance-free hermetic lead acid batteries are being offered, where the hydrogen and oxygen gases, generated at the cathode and anode during charge, are recombined to water with the help of a catalyser.

Due to the low gravimetric and volumetric energy density, and also environmental problems associated with lead disposal, this chemistry is not commonly used in portable electronic devices today.

6.3.4 Lithium-ion

The lithium-ion chemistry is currently the most promising commercially available technology for small rechargeable batteries. The energy density doubled over the last decade and is currently approaching 400 Wh/l, 200 Wh/kg. The nominal discharge voltage is 3.6V or 3.7V depending on the cathode material and the range is from 4.2V to 3.2V. The charging regime requires constant current (up to 1C rate) with voltage limit of 4.2V. A typical charger automatically transitions from constant current to constant voltage mode, when the battery voltage approaches 4.2V, and the voltage is maintained at that level while the charging current drops exponentially (see fig. 6.10). In about 2 hours in constant voltage mode, the charging current drops to less than C/10 and the charge is terminated. The total charge time is in the range of 3-4 hours, dependent on the constant current rate.

Because of safety hazard associated with the formation of lithium metal on the anode when overcharged, it is a standard to use electronic protection circuit (a MOSFET switch in series with the battery) to cut off the charging if dangerously high (4.3V) battery

voltage is detected. The same circuit usually provides under-discharge protection at 2.4V to prevent cell degradation, if the device does not provide adequate cutoff (in the range of 3-3.5V).

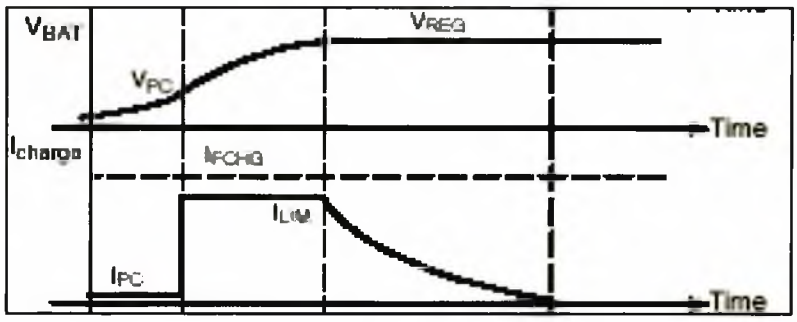

Fig. 6.10: Li- ion charging profile, including preconditioning (PC), constant current mode (**I**lim) for the first hour, and constant voltage (**V**reg) mode afterwards.

A safety PTC device (Polymer Temperature Cutoff or Positive Temperature Coefficient, both correct) is incorporated in the top of the aluminum battery can and connected in series with the cell to prevent excessive current in case of short circuit. This device is temperature dependent and will lower the cutoff current level at high temperature. Once activated, the PTC device will increase its internal resistance multiple times and stay open until the short circuit is removed, and will reset to low resistance after that. In normal operation, the Li- ion cell does not contain Li metal and is safe to use. The self discharge of less than 5% per month at room temperature and the high discharge voltage makes this chemistry a preferred choice versus NiMH. The internal resistance is low, and comparable with 3 NiMH cells in series for the same (3.6V) output. The high battery cell voltage is a critical advantage for portable electronic devices. The typical variety of voltages for microcontrollers and logic (5V; 3.3V; 2.5V; 1.8V), analog circuits as power and audio amplifiers (12V;3V), and motors (5V;2.8V) makes this chemistry perfectly situated for either step-up (boost) or step-down (buck) voltage conversion, including DC/DC and linear regulators, without the need for combined step-up/step-down (buck/boost) converters as for lower voltage chemistries. This is the reason for the Li-ion chemistry dominance on the portable telecom and computing market today.

6.4. Hybrid batteries

The elevated power and energy demands of our targeted portable electrical pH control system challenge both primary and rechargeable batteries. As shown above, primary batteries are known for their high energy density at low rate of discharge, and rechargeable batteries - for their high power capabilities. A hybrid system, involving primary battery charging a rechargeable battery, can combine the best of both chemistries and provide highly flexible and efficient power solution. Specifically, the need for high drain with intermittent usage pattern and autonomous operation can be met by a hybrid design.

6.4.1 Principle

A hybrid system utilizes a high capacity primary battery as an energy source for the rechargeable battery, which acts as the principle power source for the device. The primary battery indirectly powers the device through the rechargeable source (see fig.6.11). This enables a low-power battery not only to operate a high drain device, but also more efficiently deliver the available energy powering the device.

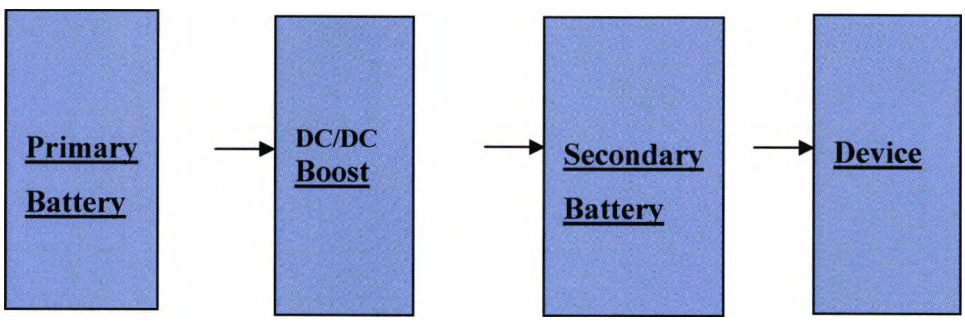

Fig.6.11: Hybrid system block diagram, showing a high-capacity primary battery charging a high-power secondary battery via voltage converter, and the secondary battery in turn powering an electronic device with intermittent high load.

Hybrid solutions typically involve alkaline or zinc-air batteries on the primary side, and NiCd, NiMH, lead acid or lithium-ion batteries on the secondary side, which powers the device. A typical hybrid implementation for a portable electronic device is shown on fig. 6.12. The circuit consists of a primary battery, boost voltage converter, Li-ion charge controller, and a Li-ion rechargeable cell. Due to the two-stage voltage regulation – first

boost from the range1.6V- 3V up to 5V, and than charge in the range 3.2V-4.2V, the efficiency is low. Also, the discharge current of the primary battery is not limited, and when the voltage of the rechargeable battery is less than 4.2V, the only available current limit is on the secondary side of the boost converter, resulting in varying primary current with voltage and inefficient primary battery energy utilization. We have investigated opportunities to optimize the hybrid circuit and to produce a highly efficient power solution.

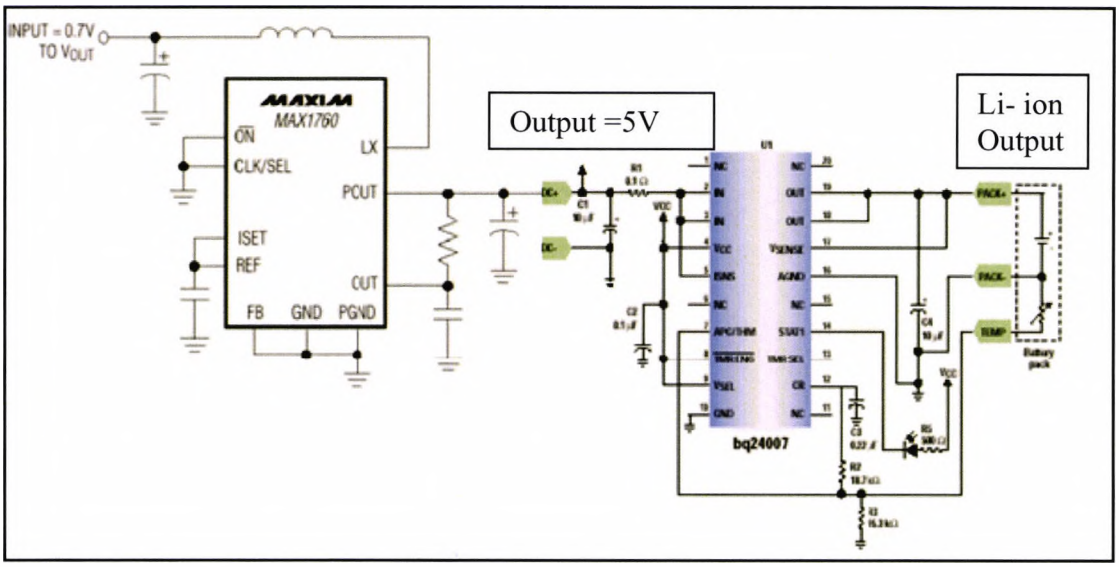

Fig. 6.12: A typical hybrid circuit, including a voltage boost converter and a charge controller.

6.4.2 A novel hybrid power concept

In the hybrid power system developed here, a boost DC/DC converter, Li-ion battery charger and controller are combined into one electronic circuit (Klein, 2002). Testing has demonstrated the feasibility of this design solution as a way to use convenient and familiar primary power batteries for high loads and extend runtime. The system is based on Li-Ion or Li-Polymer rechargeable cells. The charging voltage for these two chemistries is conveniently related to battery state of charge in a sufficiently wide voltage range (as shown on fig.6.10 before) that is adequate for a simple electronic circuit to recognize. This allows to tune the output voltage of the DC/DC converter to a level, corresponding to the desired state of charge (3.9V to 4.1V = about 70-90 % state of charge).

Two new and unique features separate this hybrid power concept from the existing art. The first is that the rechargeable battery never gets fully charged, just levels up to the output voltage of the converter. The charging current exponentially drops to virtually zero, hence the quiescent current of the circuit is very low (a few tens of uA). By not fully charging the Li-ion battery and reducing by an average of 20% the maximum continuous runtime of the power system, the following benefits are achieved:

- The need for an additional charger integrated circuit (IC) is eliminated, since the accuracy of the charging voltage at the end of charge is not critical. The DC/DC converter output voltage accuracy (typically 2.5%) can satisfy the charging voltage accuracy requirements, thus reducing cost, complexity and efficiency losses.
- Lower self-discharge rate of the rechargeable cell (because of the lower charge voltage - 4V average instead of 4.2V for full charge).
- Higher energy efficiency of the rechargeable cell (at the end of charge, rechargeable batteries dissipate heat – energy losses which are now avoided).
- Damage from long storage is eliminated (if stored at full charge, the Li-ion battery will permanently lose a portion of its capacity).
- The risk to overcharge the Li-ion cell is minimized, resulting in a simplified protection circuit.

The second key feature of this hybrid system is the constant primary battery current. Most DC/DC converters allow a limit only of the output current. Constant output current at constant output voltage is referred to above as constant power type of discharge. This mode results in "*variable*" current on the primary side, increasing as the voltage of the primary battery decreases, and is *least favorable* for the primary battery.

In summary, according to this hybrid concept, the circuit limits the primary battery discharge current and the secondary battery charge voltage, thus optimizing the primary battery energy utilization while satisfying the Li-ion charging requirements.

The primary battery discharge voltage and current, and the rechargeable cell charging voltage and current profiles for one charge cycle of the hybrid system are shown on fig.6.13 and fig.6.14. The responses of the same parameters to a 5-minute high-drain load across the Li- ion cell are shown as follows on fig.6.15 and fig.6.16.

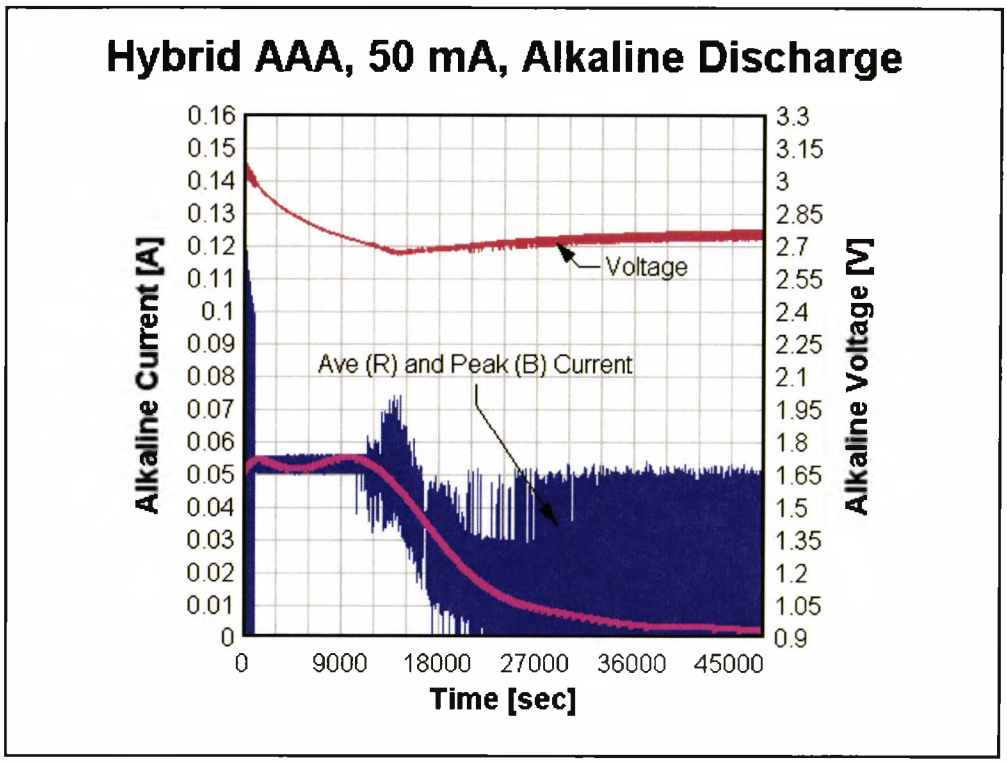

Fig. 6.13: Primary battery discharge voltage and current profiles in the hybrid circuit.

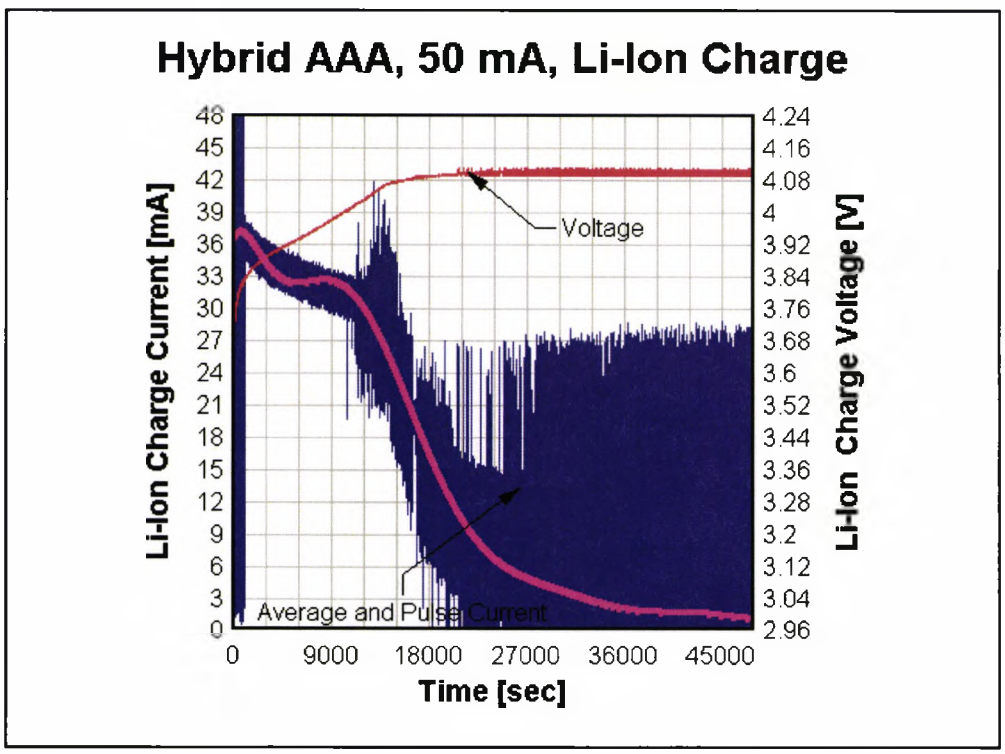

Fig. 6.14: Rechargeable battery charging voltage and current profiles in the hybrid circuit.

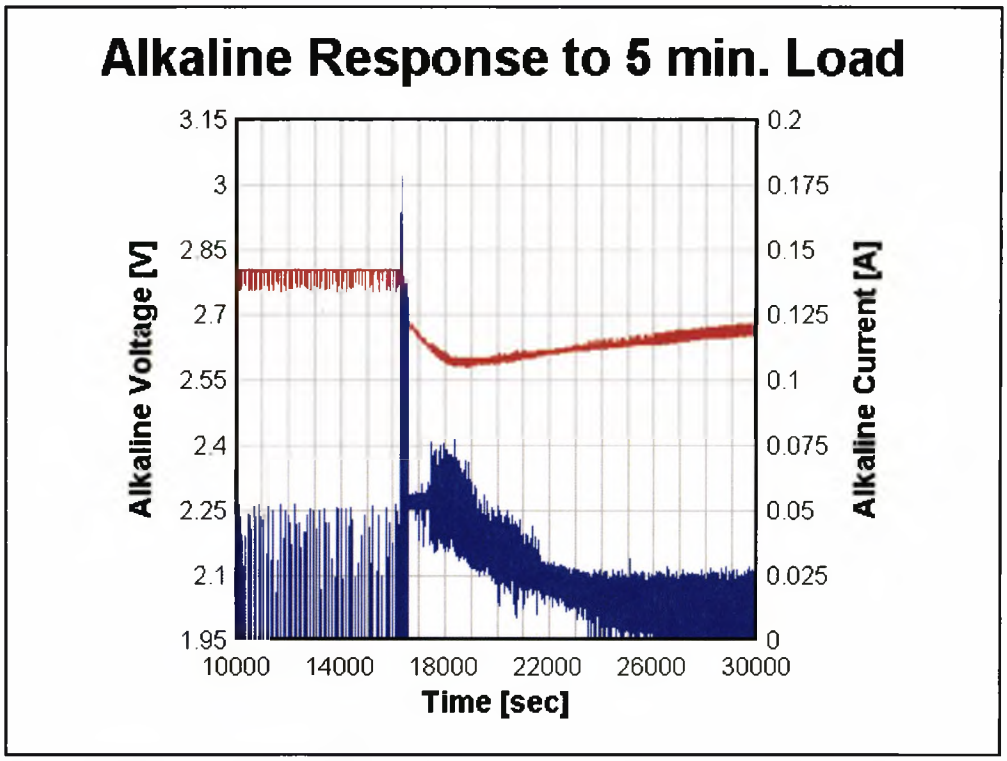

Fig. 6.15: Primary battery load voltage and current response to intermittent load on the secondary side.

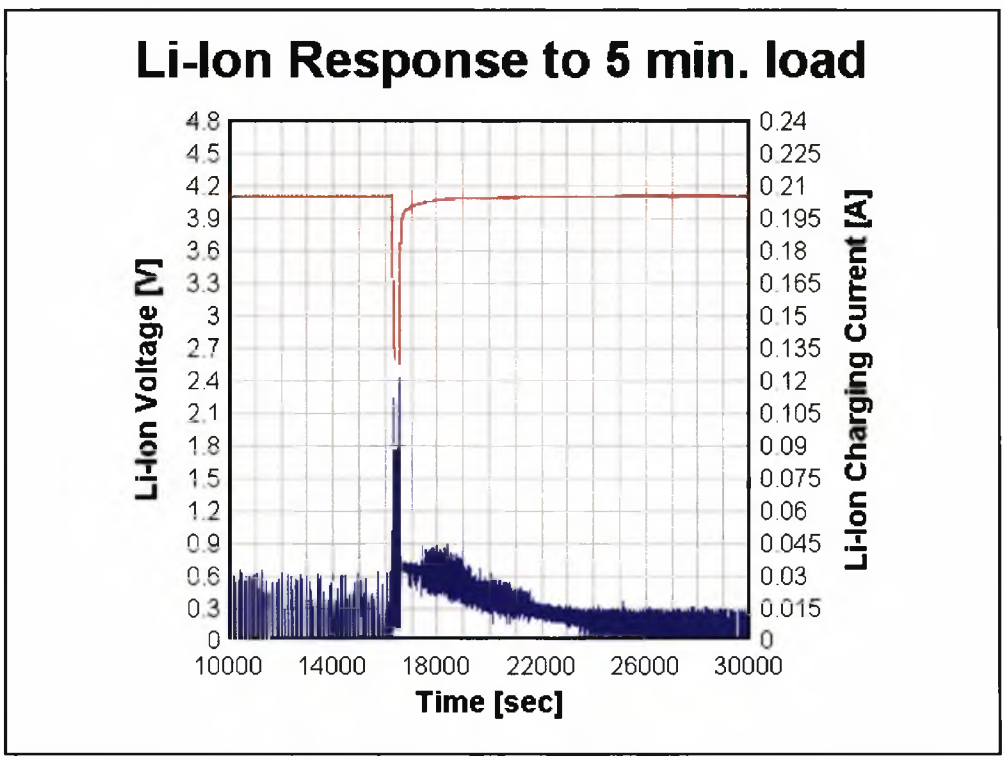

Fig. 6.16: Rechargeable battery load voltage and current response to intermittent load.

6.4.3 Hybrid circuit description

Our hybrid circuit is a low-power boost converter with *constant input current/constant output voltage* control. The system manages charging control, where the primary battery charges the rechargeable battery, which in turn provides power to the load.

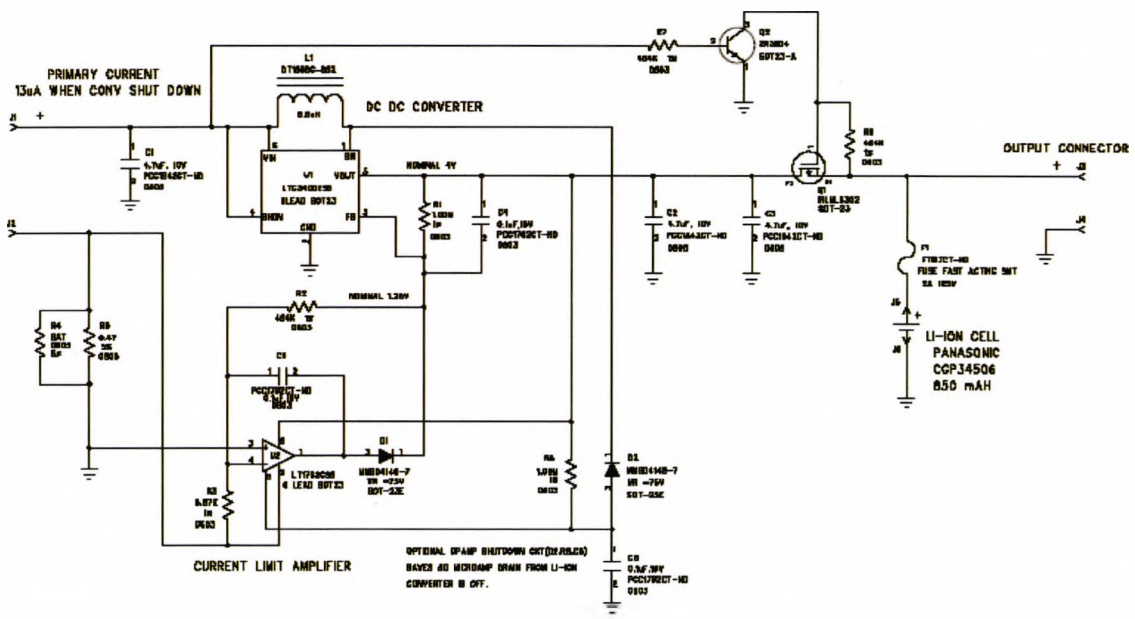

Fig. 6.17: Hybrid circuit diagram, showing all electronic components and their connections to create a very efficient voltage booster/Li-ion charger (shown expanded in Appendix 10).

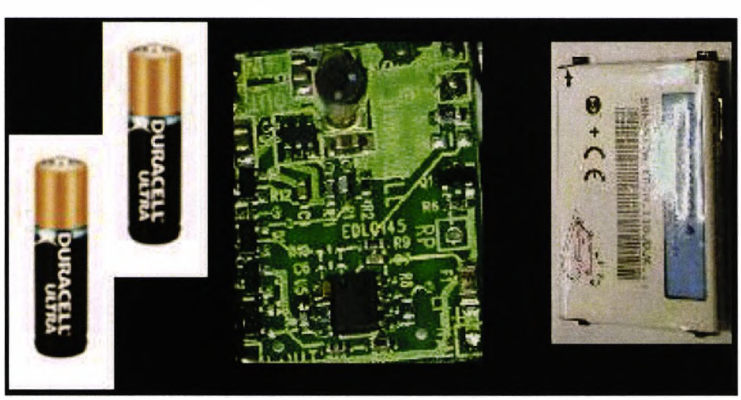

Fig. 6.18: Hybrid circuit prototype (30x40 mm) used to demonstrate the concept and measure performance characteristics.

The circuit (fig.6.17, and expanded in Appendix 10) includes a DC-DC boost converter, a primary current sense resistor and a current limit comparator, and a charge cutoff switch. In addition, over-current fuse protection for both the charge and the discharge paths of the Li- ion cell is provided. This circuit was prototyped (fig. 6.18) to demonstrate the feasibility of the hybrid approach. A rechargeable Li- ion prismatic cell (Panasonic 1000 mAh/3.7V) was attached to the hybrid circuit board and charged by 2x AA Duracell alkaline cells (2800 mAh/1.5V). At constant primary current of 50 mA, over 90% of the rated primary battery energy was transferred to the rechargeable cell and hence to the load.

6.4.3.1 Boost conversion

We used the step-up (boost) DC/DC converter LTC 3400 from Linear Technology. Other devices could also be used, for example, MAX 1765 from Maxim. The external components for the converter include an inductor (6.8 uH), which is selected for optimal conversion efficiency. The input voltage range of the LTC 3400 is from 0.7 to 5.5V. The output voltage is adjusted at the feedback input (FB) of the converter to equal an internal voltage reference (1.25V), when the output voltage is 4.0V. The output voltage should remain all the time higher than the input voltage of the converter to avoid high inrush current to flow through the Shottky diode from input to output. For the output voltage range of the Li-ion battery of 3.2-4.2V, which will satisfy the device needs, the input (primary battery) voltage should not exceed 3.3V. This can be achieved by using 2 alkaline cells in series or a single $LiMnO_2$ cell.

6.4.3.2 Primary current control

The control circuit includes a primary current comparator using an operational amplifier having adjustable primary current sensing resistor, which should have a very low value for minimum voltage drop (or IR losses) across (0.25 Ohm x 100 mA). The very low (25 mV average) IR drop is amplified and compared to the internal reference voltage (1.25V) of the DC/DC converter at the feedback input. The diode prevents interference between the voltage control and the current control circuits. In this way, the output voltage signal and the input current signal, coming through the diode, are summed at the feedback input of the converter, without interference in-between, on a "largest-only" basis, and compared

to the internal reference voltage. The system reacts to whichever of the signals first reaches 1.25V, and stops the converter switching, thus reducing the output voltage.

6.4.3.3 Low voltage cutoff

The Li-ion cell is connected to the output of the DC/DC converter through a MOSFET switch. This circuit prevents discharge of the Li-ion cell backwards through the output of the DC/DC converter, when the primary battery reaches the low voltage cutoff level (set to 1.4V for two alkaline cells in series). The system primary cutoff voltage can be tuned to a desired level for one or two cells in series of the selected battery chemistry. If the input voltage is less than 1.40V, the converter is shut down to save power, and the charge path is cut off. If the input is more than 1.45V, the DC/DC converter turns on and the circuit resumes charging. Charge turnoff removes the load from the primary battery, and the voltage of the primary battery recovers, turning the charge on again. The switching and hence charge will continue at an attenuated duty cycle until all of the available energy of the primary battery for the chosen voltage cutoff is transferred to the rechargeable battery.

This is another advantage of this hybrid solution, as normally any energy from the battery after cutoff is not utilized.

6.4.3.4 Optimized circuit for maximum efficiency

There are several important parameters to optimize in the hybrid power system design:

- **Energy of the primary battery**: sufficient for the desired total runtime of the device.
- **Energy of the rechargeable cell**: sufficient for the desired continuous runtime of the device for 1 cycle.
- **Power of the rechargeable cell**: must be adequate to handle the device peak power.
- **Charge Rate**: to achieve optimum primary battery utilization and satisfy the desired intermittent performance of the device.

In the next paragraphs, these and other aspects of the hybrid design are addressed in more detail.

6.4.3.4.1 Energy of the primary battery

The utilization of the primary battery capacity, and hence the related energy, is dependent on the primary current rate. On fig. 6.5 above was shown the capacity vs. drain graph for AAA alkaline cells. From the graphs is evident, that lower drain and lower cutoff voltage maximize the utilization. The hybrid circuit is optimized for both. It is interesting to note that the advantage of the premium battery (with low internal resistance) is not important for the hybrid implementation, and the use of cost-effective cells is feasible.

Very low drain can yield very high energy from the alkaline cells, but the DC/DC converter is not very efficient at this low rate. A good rule of thumb is to use 50-100 mA rate for both high energy and good converter efficiency.

Also, the Li-ion charge time is related to the primary battery rate, corrected for the voltage conversion ratio and the converter efficiency:

$$I_{ch.} = I_{disch.} \text{ x Efficiency x } V_{in}/V_{out} \qquad \textbf{Equation 6.6}$$

For example, if two alkaline cells are used in series (average discharge voltage 2.5V) at 100 mA, the average charging voltage of the Li- ion cell is 3.8V, and the converter efficiency is 90 %, the average charge current from Equation. 6.6 is:

$$\mathbf{I_{ch} = 100x0.9x2.5/3.8 = 59.2\ mA}$$

For a 600 mAh Li-ion cell, it will take about 10 hours to fully charge. The charging current varies with the changes in the primary and secondary voltages. When the charge enters the constant output voltage mode the charging current drops exponentially with time. As our pH controller device usage pattern is "intermittent", the predominant charging mode will be at very low current, and the primary energy utilization will be better than estimated using the value of the set constant primary current limit.

Discharge current of 100 mA for AA and 50 mA for AAA alkaline cells is recommended to maximize energy utilization. Two cells in series will charge two times faster, and the converter efficiency also improves at higher input voltage (fig. 6.15). The use of three cells in series is not allowed, as the input voltage exceeds the output and can cause hazardous condition.

6.4.3.4.2 Primary battery fuel gauging

The remaining energy versus voltage graphs for the widely available AA Duracell Ultra alkaline cells at 50 mA and 100 mA continuous discharge current are shown on fig.6.19. These values should be used on a "per cell" basis, and if two cells are used in series, the voltage should be doubled.

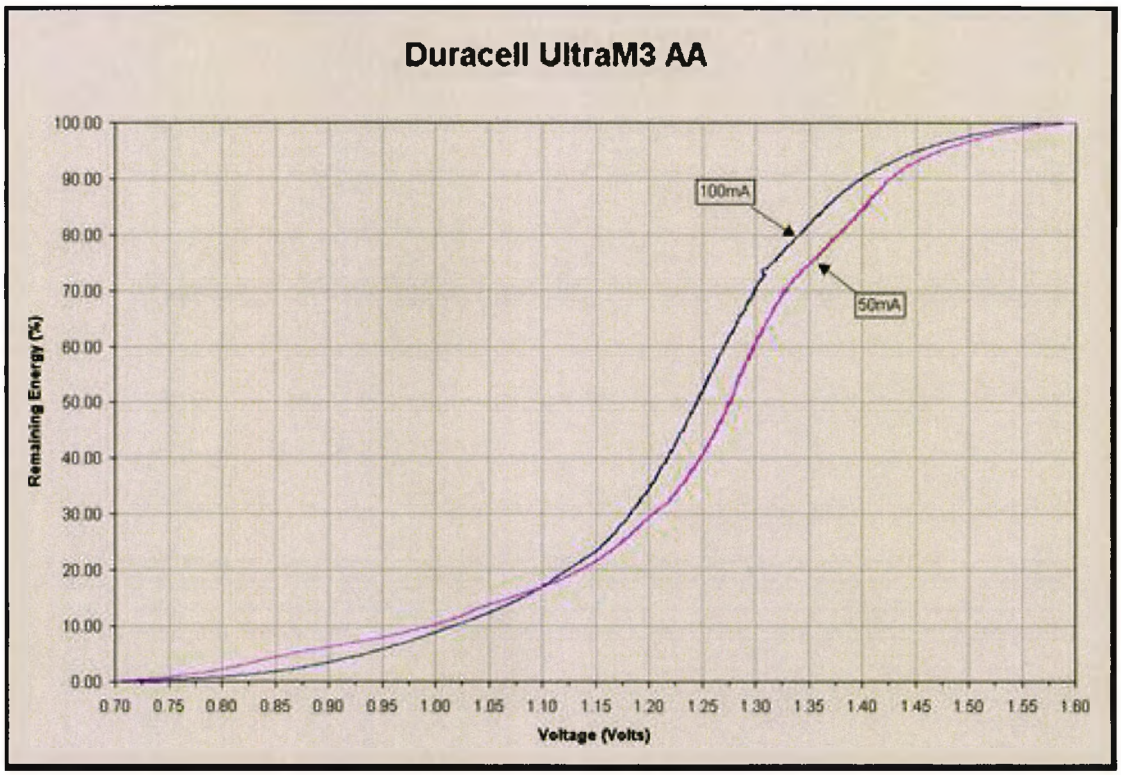

Fig. 6.19: Primary battery fuel gauge calibration curve for two typical discharge current settings.

This data can be used for an approximate fuel gauge only. Despite the constant discharge current control of the hybrid circuit, the real device usage is intermittent, and the discharge current will vary over time between zero and the set limit, affecting the voltage value. Also, long periods of inactivity will allow the primary cells voltage to recover. Different makes and types of batteries will have different discharge characteristics as well. This will inevitably cause inaccuracies in the remaining energy measurement. A

low-battery warning can be implemented at about 1V/cell, where the remaining energy is 5-10%.

From the graphs, three points of interest are derived and shown on table 6.4 below. These values can be used to design a four-bar fuel gauge, typical for portable devices.

Voltage at Specific			
Remaining Capacity [V]:	75%	50%	25%
UltraAA_100mA	1.32	1.25	1.16
UltraAA_50mA	1.35	1.27	1.17
CoppertopAA_100mA	1.32	1.25	1.16
CoppertopAA_50mA	1.34	1.27	1.16
UltraAAA_100mA	1.3	1.22	1.14
UltraAAA_50mA	1.32	1.26	1.17
CoppertopAAA_100mA	1.3	1.22	1.15
CoppertopAAA_50mA	1.33	1.26	1.18

Table 6.4: AA&AAA alkaline cells remaining energy versus battery voltage.

6.4.3.4.3 Charge rate

The optimization of the charge time is a compromise between efficiency, size and price from one side, and performance from the other. In order to accelerate the charge, when the rechargeable battery is close to a discharged state, a voltage-related rapid charge rate could be implemented in the converter design. As the Li-ion charge voltage is raising fast in the 3V-3.6V region, the high rate charge lasts for a short time only and does not deteriorate greatly the primary battery utilization.

6.4.3.4.4 Converter efficiency

The circuit diagram from fig. 6.17 was optimized for efficiency and cutoff voltage, as shown on fig. 6.20 below (and expanded in Appendix 10).

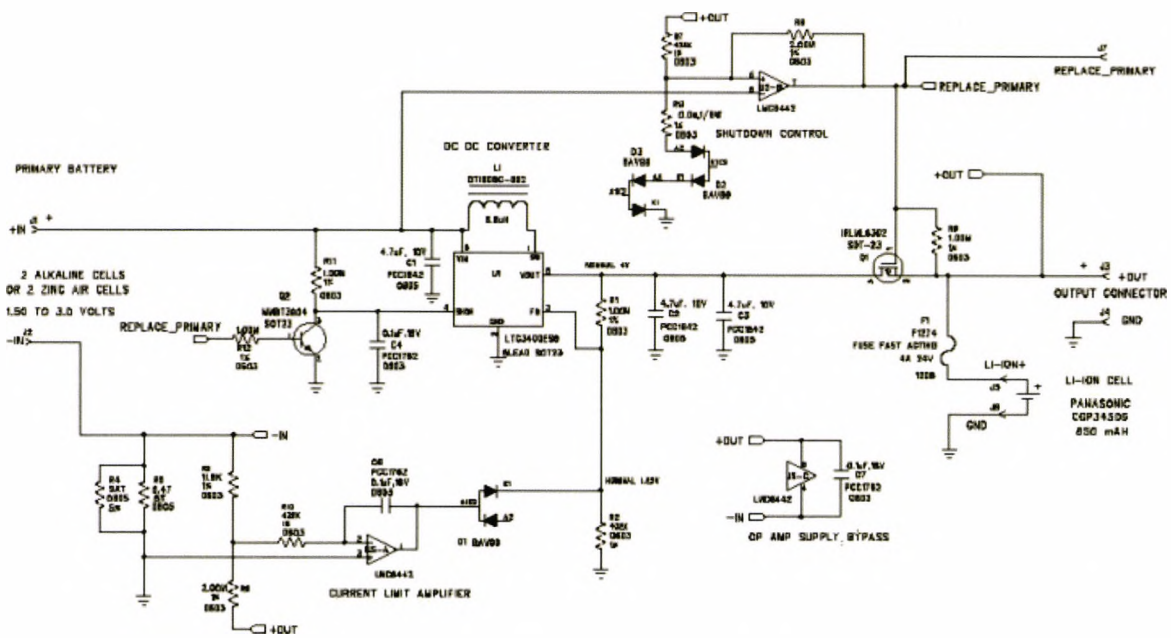

Figure 6.20: Hybrid circuit diagram (Version 2).

Efficiency test of the so modified hybrid circuit was carried out at different input voltage and current values. The primary and rechargeable battery utilization was not accounted for

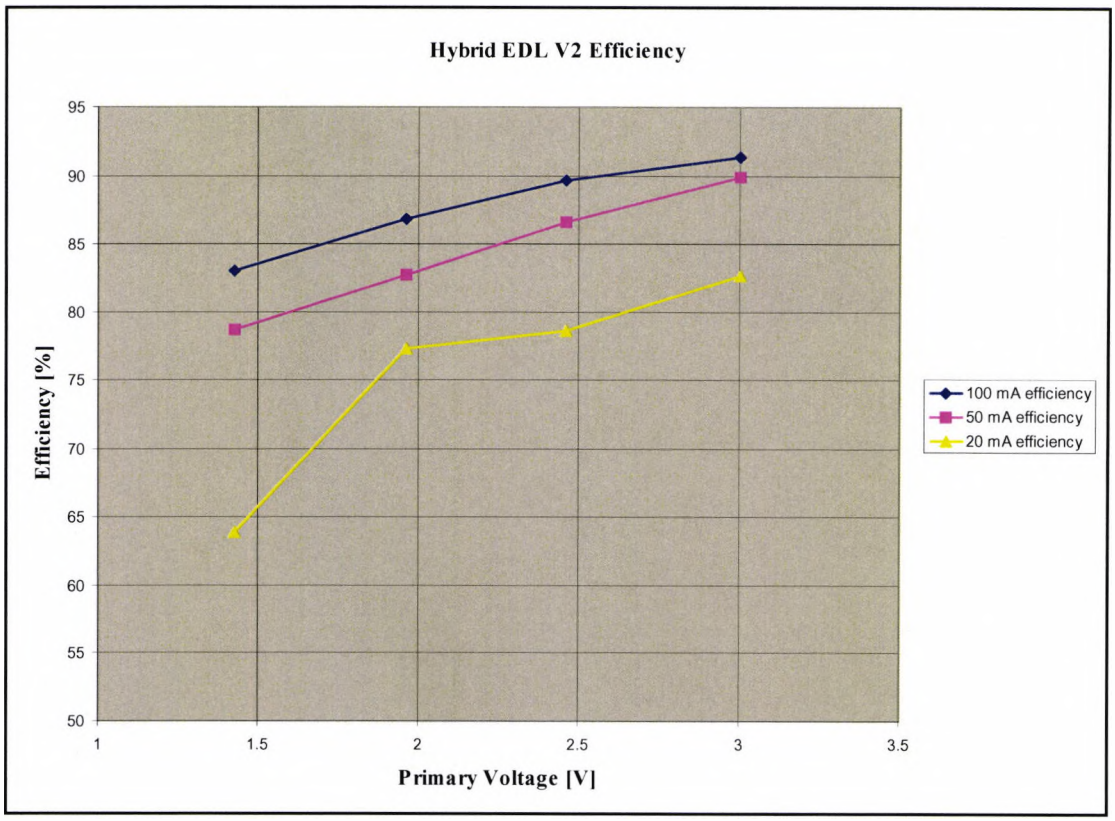

Figure 6.21: Converter efficiency for the second version of the hybrid circuit (not including battery efficiency).

in this test, only the electronic circuit efficiency. The primary constant current limit was set sequentially at 100 mA, 50 mA and 20 mA. The efficiency graph is shown on fig. 6.21.

6.4.3.4.5 Power of the rechargeable cell

In a hybrid powered devices, compared to a rechargeable-only powered, smaller Li-ion battery can provide the necessary peak power, and thanks to the permanent charging, may be sufficient for satisfactory device performance. The size, weight and cost savings could be utilized to offset the hybrid implementation cost.

Typical maximum load for Li-ion cells is 2C rate. The peak current capability depends on the internal resistance of the cell and can exceed the average drain many times.

6.4.3.4.6 Energy of the rechargeable cell

The energy of the Li-ion cell is selected to satisfy the continuous device runtime. This should normally cover the longest active period in intermittent usage, and the cell should charge during inactive periods to near full strength.

6.4.3.4.7 Testing Run time with Simulated Load

The device continuous runtime depends on the rechargeable cell energy, and the total runtime – on the primary battery energy. If the device is charged in advance, we can benefit from both before replacing batteries. However, in this case there will be a delay, before the device becomes operational again after use.

A testing protocol was created to simulate typical pH controller load interaction with the above hybrid system. In table 6.5 below are results in 2 different intermittent modes, with 2 different hybrid boards, set at 50 mA and 110 mA constant primary current, using 2x AA Duracell Ultra M3 cells in series. It is important to note, that in constant voltage charge mode, which takes place most of the time, especially when simulating 3 minutes active periods, the current drops exponentially and the average may be much lower than in constant current mode, as explained previously.

Board 1 (110mA)	**Board 2 (50mA)**
Test Sequence	
16hr rest	16hr rest
150hr 4mA (standby)	150hr 4mA (standby)
Active (200mA) to 3.2V	Active (200mA) to 3.2V
Rest overnight	Rest overnight
Active (200mA) to 3.2V	Active (200mA) to 3.2V
Results:	
150hr standby (2.36Wh)	150hr standby (2.26Wh)
3:28 Active (2.58Wh)	2:29 Active (1.82Wh)
0:18 Active (0.22Wh)	1:53 Active (1.37Wh)
Total active time 3:46	Total active time 4:22
Total energy 5.16 Wh	Total energy 5.45 Wh

For comparison, the same type cells were discharged without the hybrid circuit, directly on a tester in constant current mode:

Continuous load results:	
Continuous load (200mA)	Continuous load (200mA)
6:14, 4.55Wh	8:12, 5.86Wh
Continuous low-rate drain (66mA)	Continuous low-rate drain (33mA)
5.05Wh	6.01W
2xAA M3 at 110mA cont. to 0.8V	2xAA M3 at 50mA cont. to 0.8V
5.53Wh	6.67Wh

Intermittent procedure:

Active (200mA) 3min. every two hours eight hours a day;
Standby (4mA) the rest of the time.
2xAA M3 Ultra

Board #	**1 (110mA)**	**2 (50mA)**
Total Active Time (hr:min)	2:24	2:48
Total Standby Time	284hr	331hr
Total Energy	5.9Wh	6.8Wh
Test Duration	12 days	14 days

Table 6.5: Test results, generated using two prototype hybrid circuit boards and a simulation test procedure.

Both systems reached a 3.2V cutoff during the 16hr 4mA standby simulation. The numbers reported above include data up to the last successful 3min/ 200mA drain.

The numbers above are about the best performance that one could expect from two AA alkaline cells. One reason is that most of the time the batteries were running at a < 10 mA drain rate, as the current drops exponentially after every active period. Another contributor is the energy, "squeezed" from the alkaline cells after cutoff, as explained in the circuit description paragraph (4.3.3).

6.4.3.4.8 AC charging

AC charging of the Li-ion cell is possible to accommodate within the hybrid system, by connecting in parallel the output of the AC charger and the output of the hybrid circuit to the Li-ion cell. In this case, when the battery charging voltage equals or exceeds the output voltage of the hybrid circuit (4V), the last will stay idle and not drain the primary battery. Additional circuit modifications could be implemented to disable the hybrid converter when AC power is present. In case that AC fast charge is desirable, an over-voltage protection circuit should be used in conjunction with the Li-ion cell.

6.4.3.4.9 System fuel gauging

One drawback of the hybrid circuit is the initial delay, needed for the Li- Ion cell to get enough charge to operate the device, especially after replacing the primary battery. A good solution to this problem is to monitor the primary battery voltage in the device (through fuel gauge, low-battery warning and cutoff) and prevent further discharge of the secondary cell. In this way, when the primary battery is flat, and the rechargeable battery is still nearly fully charged, the device will prompt the user to replace the battery or suspend operation. After replacing the primary battery, the device will be immediately ready to use. The rechargeable battery could be incorporated in the device and not be visible or known to the user.

6.4.3.4.10 Integration and cost

As described above, a low current DC/DC converter, in the range of 20-100 mA, is needed for this application. The implementation of the hybrid circuit in a miniature, low-power IC, is desirable to further improve the efficiency, and reduce complexity and cost. A modified boost converter can incorporate most of the functionality and the associated external components (probably except the inductor and the current sensing resistor).

Summary

In this chapter, we reviewed different primary and rechargeable battery systems, and their suitability for providing power to a portable remote pH controller. Primary battery systems have attractive energy densities and shelf life, but suffer limited output power and low efficiencies at high drain. Rechargeable batteries provide excellent output power, but suffer lower energy densities. Combined with their limited shelf life and significant self-discharge, the need for external (usually AC) power for regular recharge is a must. A hybrid power solution provides a better combination of high energy density and high power output, and allows for low-maintenance autonomous operation. We developed and tested a highly efficient and simple self-controlled analog hybrid circuit, which can provide the necessary power supply for the pH controller over extended periods of time using widely available standard cost-effective alkaline batteries.

In the next chapter, we shall focus on the development of an electrically powered pH controller, as an alternative to the existing pH regulators using chemical energy as a control media. Electrolysis-based pH modulation with feedback closed loop control is used for on- line pH control. Battery powered electrochemical controllers using optical or electrical pH feedback signal are developed and their performance evaluated.

CHAPTER 7: ELECTRICAL PH-CONTROLLER

Introduction

This chapter relates to the original method of electrical feedback control of the hydrogen ion concentration (pH) in aqueous solutions and the development of instrumentation for automatic control with potentiometric or spectrophotometric feedback.

Automatic devices for the control of pH, based on the above principles, exist, as discussed in Chapter 2. A pH electrode continuously senses the condition of the analyte solution. A controller monitors the signal and, when required, activates reagent pumps and valves to add pH-balancing chemicals until the pH set point is achieved.

However, pH control has been recognized as a very difficult problem because of its nonlinearities and time-varying characteristics. Many different strategies like proportional integral (PI) controllers, nonlinear pH neutralization based on fuzzy logic and multi-component reagents with auto-regressive influent composition are being developed to improve the controller overall performance, time response and stability.

Instrumentation for chemical pH control is also known as (pH-stat). Particular reference is made to the following patents: CH-89-01-11-U (1989); JP-91-11-08-A2 (1990); KR-90-12-22-Y1 (1990). These methods employ the addition of buffer solutions to the sample volume under control and potentiometric feedback for automatic regulation.

Systems of this type suffer from the complexity of the operational mechanism, slow time response and changes of the sample chemical composition. They are not useful for field applications including on-line, low maintenance chemical sensor conditioning methods, i.e. those using ion-selective electrodes.

It has been demonstrated that electrolysis in aqueous solution at a potential difference for practical purposes above 2.3V generates hydrogen gas at the surface of the cathode and oxygen gas at the surface of the anode, thus modulating the ion concentration equilibrium towards increase in the cathode area and decrease around the anode (Battery Reference Book, Bitrode Corporation, 1989). The use of electrolysis as means of pH modulation was developed further as a method for feedback electrical pH control. According to the method, a voltage corresponding to a desired set pH value is applied to the input of the instrument, and the last responds by biasing the controlled aqueous media to the set pH and maintains this value.

7.1 Objective

The primary objective of our method is to produce automatic on-line pH control in aqueous solutions without the addition of buffer reagents.

The existing pH-control methods using addition of chemicals to the solution are complex to implement and require mechanical valves, pumps, and reagent reservoirs (also a safety concern). The response is slow and non-linear. The chemical composition of the solution changes. Electrical pH control simplifies the instrumentation, allows more flexible control and does not require as much maintenance.

Another objective is to control the pH of particular point or area of the sample. With chemical control, a mechanical mixer is used to homogenize the solution and the added chemicals, and the whole solution changes pH. Only a small area or volume of interest is much faster to control, for example the surface of an ion-selective sensor membrane, using an adjacent to the surface pH modulation electrode.

7.2 Method description

The instrumentation for pH control designed in this study differs from that previously used for pH modulation (Bourilkov, 1996) in that a feedback control system is implied, including a pH measurement device and a pH modulation device in the closed feedback control loop. This approach allows the setting of a particular value of pH (its corresponding voltage) at the input of the control system so that the electrical bias needed to equalize the values of the set and real pH can be readily applied.

Negative feedback electronic systems that behave in the way described above exist, as described in Chapter 5. Depending on the parameter that produces the feedback signal (voltage or current) they are usually constant voltage or constant current negative feedback systems. In electrochemistry, both systems are largely applied as potentiostats and galvanostats. The suitability of these systems for the purpose of pH control will be investigated.

Our instrument consists of an electrical voltage or current source, providing an appropriate ionic current flow through an electrochemical cell, characterized in that the current source is feedback-controlled by the electrical signal, proportional to the pH in the point or area of control. The feedback signal is generated either by an electrochemical pH electrode or spectrophotometer configured as optical pH sensor (Chapter 4). In the last case a colorimetric pH indicator is dissolved in the sample solution. A fibre optic colorimetric

probe (Smith, 1986; Mooney, 1993; Grattan, 1989, 1994, 1996; Mouaziz, 1993; Badini, 1994; Kurata, 1995; Fneer, 1996) or a color video camera is used to monitor the controlled area and provide a pH-correlating signal. This approach was initially targeted to ion-selective sensors conditioning, but could be expanded and applied for chemical process control, and other cases where pH control in aqueous environment is required.

7.3 Examples

The novel approach to pH control can be implemented in a variety of applications, where traditionally chemical control is used.

The following systems illustrate some of the preferred forms of the method of realization. Both potentiostatic and galvanostatic approaches to electrolysis biasing, and electrochemical or optical pH sensing in the feedback control loop have been used.

7.3.1 System 1: Electrical current source (galvanostat) controlled by potentiometric hydrogen ion-selective glass electrode feedback

A source of constant electrical current (I) is connected to a three-electrode electrochemical cell (fig. 7.1). The current through the cell is independent of the solution conductivity within certain limits and controlled by a closed-loop feedback system, including a glass-membrane ion-selective electrode and an operational amplifier. The system generates as much current as necessary through the cell until the potential of the pH electrode versus ground equals the voltage value of the control signal, which corresponds to a certain pre-set pH. The potential difference between the working and the counter electrodes depends on the solution conductivity and is restricted by the compliance voltage of the galvanostat, which is the 4V Li-ion battery power supply voltage. The time response is not strongly dependent on the solution conductivity, as the electrolysis rate is primarily a function of the electrolyte current, which is maintained constant within the galvanostat control range. The maximum output constant current I_{max} for a given output compliance voltage V_{max} is:

$$\mathbf{I_{max} = V_{max}/R_{cell}} \qquad \textbf{Equation 7.1}$$

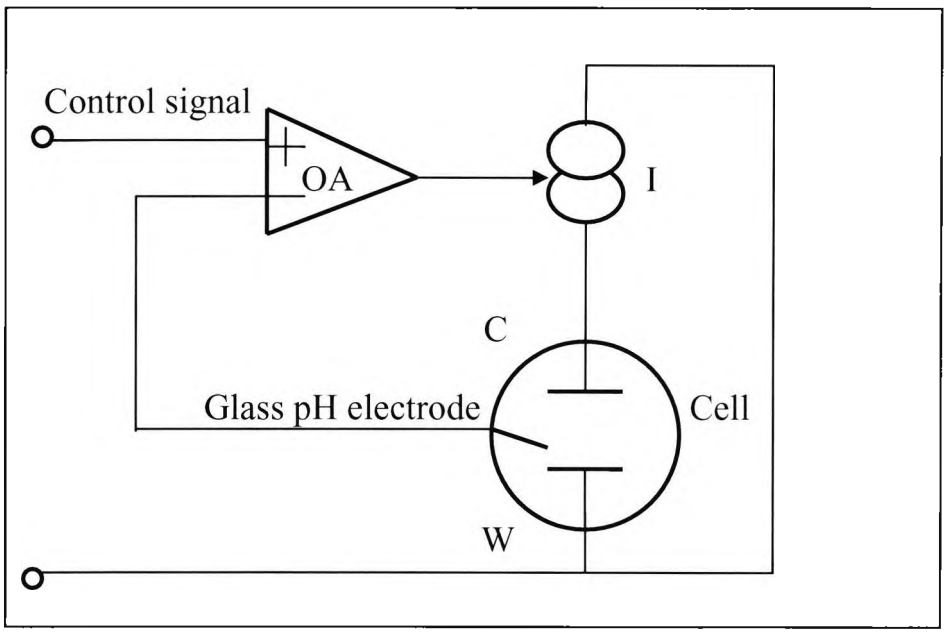

Fig. 7.1: Galvanostatic pH-controller, where the voltage feedback control signal results in a current-type regulator response.

7.3.2. System 2: Electrical voltage source (potentiostat) controlled by potentiometric hydrogen ion-selective glass electrode feedback

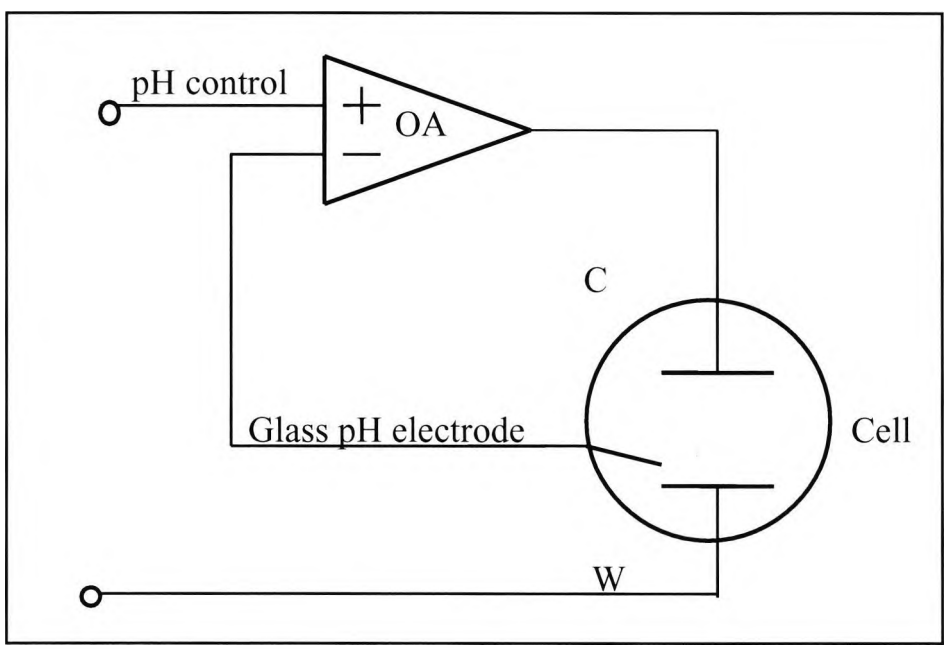

Fig. 7.2: Potentiostatic pH-controller where the voltage feedback control signal results in a voltage-type regulator response.

An electrochemical three-electrode cell is enclosed in a potentiostatic feedback-controlled system, with a difference from the classical potentiostat being that the voltage RE is replaced by a hydrogen ion-selective electrode and the system control responds to the pH value at the reference point, rather than the RE potential (fig. 7.2). In this case, the potential difference between the WE and the CE is independent of the solution conductivity, but the current flowing across varies. The time-response of this system will normally be slower than that of Example 1 if the solution conductivity is low, but could be faster if the conductivity is high. Advantage of this method is the precise voltage control over the cell, which also allows for control of the electrochemical side-reactions.

7.3.3 System 3: Electrical voltage or current source, controlled by optical fibre colorimetric pH sensor feedback

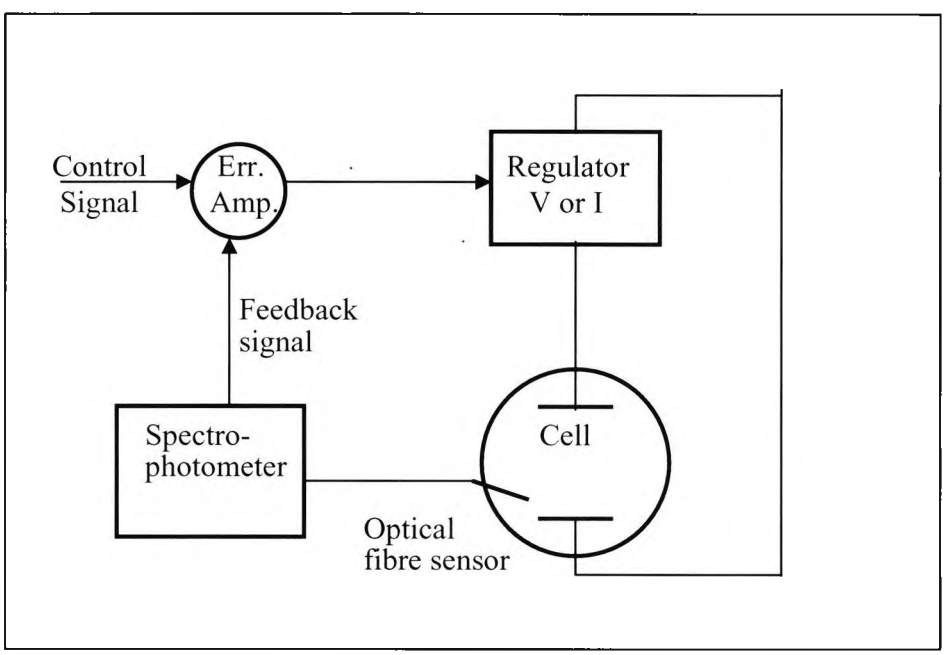

Fig. 7.3: pH-controller using optical fibre chemical sensor to provide feedback signal to the error amplifier.

This system is similar, in principle, to the previous two, but the feedback loop is closed by an optical pH-meter, including an optical fibre colorimetric pH-sensor and spectrophotometer, converting the colour changes into an electrical control signal (fig. 7.3). Advantage of this design is that the optical sensor is immune to electrical interference, caused by the electrical current flowing through the cell, and also that the miniature dimensions of the optical fibre will allow for pH control in a particular point of the internal volume of the cell.

The approach shown above allows for the development of sensors and measurement methods for *in-situ* real time monitoring of the composition and flux of species in sea water, especially the dissolved "greenhouse" gases, using on-line combined optical and electrochemical methods. An infrared/visible optic fibre spectrophotometer in conjunction with novel probes, representing electrochemically conditioned gas-permeable membrane sensors using optical absorption and fluorescence, could be developed and adapted for measurement of the concentration of "greenhouse effect" pollutants. A variety of gases (of interest that are) dissolve in water, including CO_2, NH_3, CH_4, NOx, H_2S, O_2 as well as pH, turbidity, prediction of total organic carbon (TOC), and chemical oxygen demand (COD), can be measured as described in detail in our INCO-COPERNICUS EC project proposal (A System for *in-situ* .., 1996). Measurements in the sea could be performed *in-situ* over a range of depths to investigate concentration distribution, flux and seepage in the atmosphere.

The development of this approach could create a range of effective chemical sensors and instruments able to monitor the concentration of several major greenhouse gases in depth to at least 200 meters. Such instrumentation can allow for an *in-situ*, on-line study of the oxic/anoxic interface, suboxic zone and the anoxic part of the sea. The above sensors and instruments may be incorporated in a monitoring system which gathers and correlates data about the gases of interest from a range of probes distributed over a geographical region for on-line real time distributed sensing. The system would be based on the optical fibre sensing approach combining the use of membrane techniques for separation of the selected gases from the water with thin permeable sol-gel based sensitized layers incorporating chemical indicator dyes tailored to the range of gases under study. The sensors could be further developed for the sea environment and remote operation under pressure. In the case of acidous and basic gases, the monitoring approach is based on pH control in the sample solution and from both sides of a gas-permeable membrane in the sensor. This could possibly be realized by the use of optically controlled, battery powered pH regulators, connected respectively to a pair of electrodes externally and internally to the volume of the probe. This technique allows for remote wireless reversible control and reset of the sensors and obviates the use of additional chemical reagents for preconditioning and cleaning of the probe, which would otherwise prevent the possibility of *in-situ* measurement without sophisticated sampling and conditioning instrumentation.

Because of the complexity of the seawater composition and possible interference between the measurands, broad band optical spectroscopy (300nm - 1200nm) may be used. Miniature diode array spectrometers and high luminescence LED (light emitting diode) sources are suitable to investigate the differences in the optical responses of the dyes to the various gases of interest. The *in-situ* application of such sensors in depth is possible because of the very low signal attenuation by the optical fibres in the chosen range and their intrinsic immunity to electromagnetic noise. The spectrometer and control instrument may be placed on a ship, for example, and could measure remotely the sensor response. The chemical reactions in the sensor head depend dramatically on the pressure, and to ensure proper measurements, several different sensing approaches could be developed. These range from the very robust direct absorption and fluorescence measurement techniques using the sensitive edges of optical fibres to the delicate gas-permeable membrane probes with many options for conditioning and control. The promising sol-gel technology for preparation of sensitive and selective thin layers, applied at the edge or as coating of an optical fibre, could be implemented as well.

A mathematical analysis of the resulting spectral data could enhance the power of this approach relatively easily. In particular, artificial intelligence-based classification methods (deconvolution) could be employed to differentiate between overlapping spectral detail and determine the presence of unknown species. Such work will involve the use of neural networks, Bayesian methods of analysis and fuzzy logic methods already under development.

7.3.4 System 4: Process control for metals extraction

This is a specific application of the optical-feedback pH-control system for a metal-extraction column (fig. 7.4). Water containing metal ions is flowing through a preconcentration column, filled with silica-gel incorporating an ion-selective ligand. When a certain level of preconcentration is reached, the pH control system is activated to selectively extract the metals of interest at the corresponding pH values. At this stage a colored pH-dye is mixed with the water stream. The optical sensor in this case is a color video camera focused to sense the color changes in the solution volume where control is exercised and provide a pH-related voltage feedback signal. By control of the voltage or current across the two polarization electrodes and by reversing the polarity of the control voltage, a wide range of stable pH levels could be achieved.

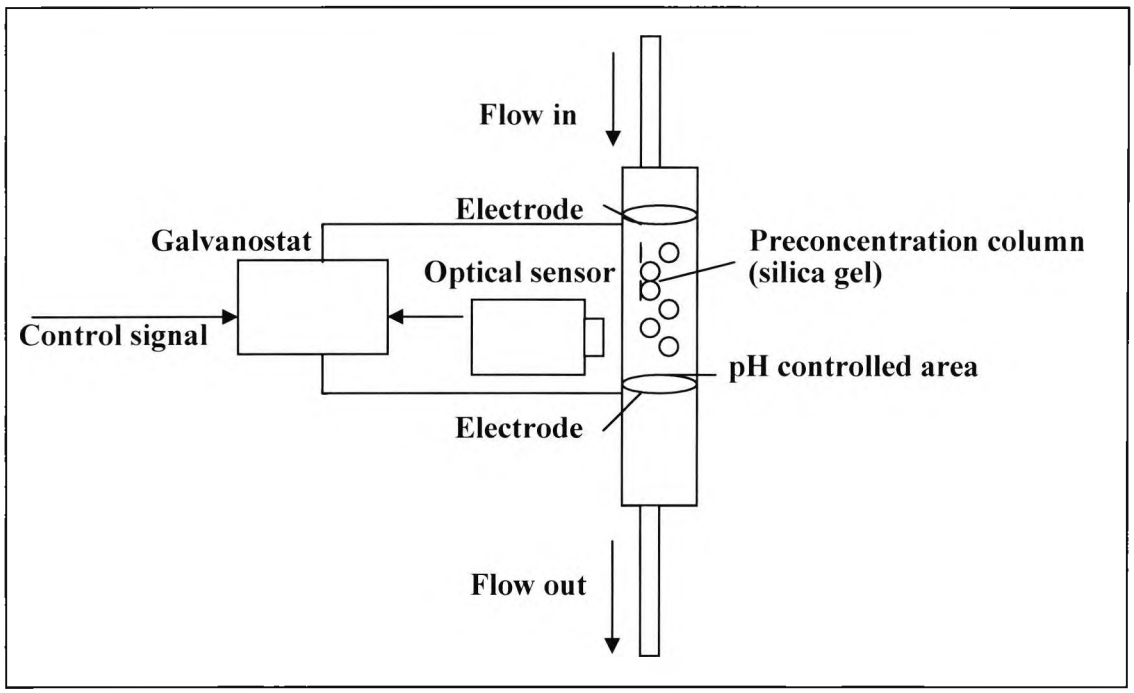

Fig. 7.4: Block diagram of an optical pH-controller for metal extraction, where the optical feedback is responsive to volumetric color change.

Summary

In this chapter, we described in more detail the principle of operation of the electrical pH controller and developed ideas for practical implementations. Realizations of different systems were discussed, based on potentiostatic and galvanostatic controlled electrolysis, and practical circuits were developed. Examples using electrochemical or optical pH sensor feedback were demonstrated. Apparatus for environmental sensing and *in-situ* water monitoring was attempted, including project applications for EC-funding.

Based on the above system principles, practical pH control instrumentation was designed, and experiments involving ion-selective sensor conditioning, control with a chemical pH sensor and control with an optical pH sensor were carried out as described in the next chapter. The colour indicator spectral characteristics and the performance of the prototype pH controller were tested against the targeted specifications.

CHAPTER 8: EXPERIMENTAL

Introduction

In this chapter are presented the experiments carried out to demonstrate the feasibility of the new method and targeted applications. First, pH modulation was used in an open-loop system for conditioning of an optical ammonia sensor. Traces of ammonia in water were measured successfully. Second, a closed-loop feedback controller was prototyped, using alternatively a glass electrode pH sensor and an optical colorimetric pH sensor. The spectrum of a universal pH indicator was evaluated for the purposes of optical pH control. Voltage signal proportional to pH was successfully used in the feedback loop of a potentiostatic and galvanostatic controllers. The response time, accuracy and power consumption of the controller are discussed.

8.1 pH modulation for ammonia sensing

Sensing of dissolved ammonia, using ion-selective electrodes, is one area where pH control is critical. To convert the dissolved ammonia species from ionic to gaseous form, pH control of the solution is required. Instead of controlling the pH of the whole sample volume, as with chemical control, electrical pH modulation can quickly and accurately bias pH to the desired value only in the proximity of the sensor membrane. This is especially valuable for remote on-line environmental monitoring.

8.1.1 Sensor design

In order to implement the pH-modulation techniques described in Chapter 2 to condition an optical fibre ammonia sensor, the following sensor head was designed (fig.8.1) and prototyped (fig. 8.2).

A Teflon gas-permeable membrane, shown as a roll on the above figure, was used to separate the internal sensor solution from the external sample solution. The cathode is constructed of a stainless steel grid with surface area of 10 cm^2, enclosing the front side of the sensor, to generate by electrolysis basic environment in this area.

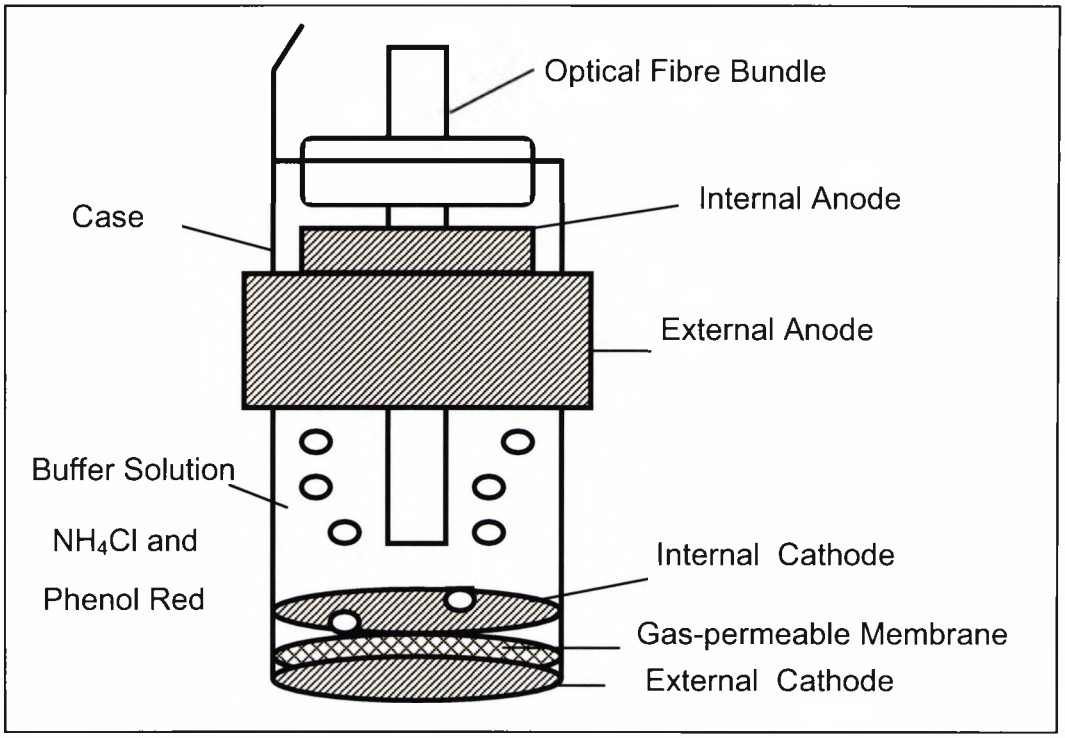

Fig 8.1: Construction of an optical fibre Ammonia Sensor with electrical control.

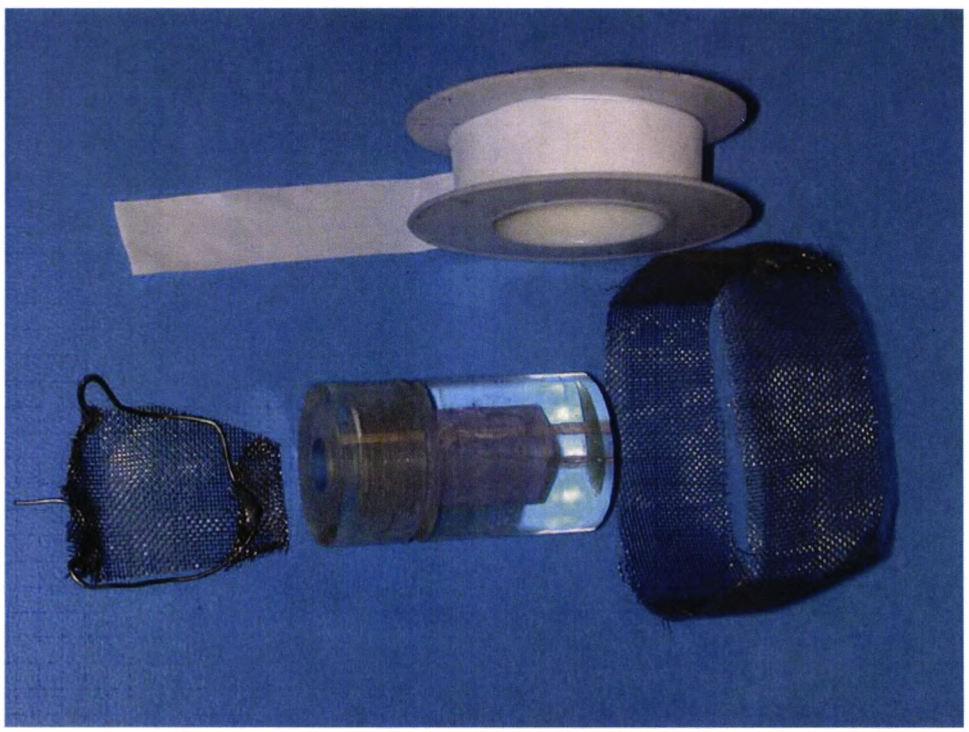

Fig. 8.2: Our sensor prototype (D=25mm; L=44mm), using stainless steel grid and Teflon membrane.

The anode represents a high surface area (50 cm^2) stainless steel grid cylinder, incorporated externally in the upper part of the sensor, where the created acidic environment will be far enough away not to influence the conditions in the near-membrane sensing area. The inside volume of the sensor is filled with a buffer solution containing ammonium chloride (NH_4Cl) and phenol red at pH = 5.6. Inside this solution is placed the sensing end of an optical fibre colorimetric pH sensor, using a dual fixed-wavelength interrogation method (Fneer, 1996). We used this previously developed optical sensor as part of the new experimental setup. According to this previous work, pH in the measured sample was increased manually by adding drops of sodium hydroxide to the solution, stirring and measuring with an external glass-electrode pH meter. At pH = 10, the ionic ammonia turns to its gaseous form and penetrates the membrane, thus increasing pH of the internal sample.

The electrical pH modulation approach allows automatic and remote, low-maintenance operation. It is more convenient to supply electrical current to the two biasing electrodes with the help of a battery power supply and control electronics, rather than conditioning the external sample with the addition of chemicals. Valuable benefit is the reversibility of operation, permitting reset of the sensor to its original condition by voltage polarity reversal and self-cleaning by pulsing higher current to the electrodes. Sensing of more than one measurand is also made possible at different pH values, creating opportunity for remote controlled *in-situ* smart sensing.

8.1.2. Experimental results

The described above optical pH sensor is based on color measurement of a pH indicator (Phenol red, Appendix 3), dissolved in the internal sensor volume. The measurement method is based on a dual wavelength approach, making the pH sensor a self-referenced device. An optical signal in the green visible range is responding to the indicator color and hence pH changes. Both the green and the additional infrared signals respond to common changes of different nature (temperature, voltage offset) of the sensor. The ratio of the two optical signals, which represents the measured value, is shown on fig. 8.3 as a function on the changes of pH inside the sensor. The phenol red operational range of substantial color change is from the initial pH = 5.6 of up to approximately pH = 8. The instrument colorimetric response is not linear, except in the near proximity of pH = 6.5.

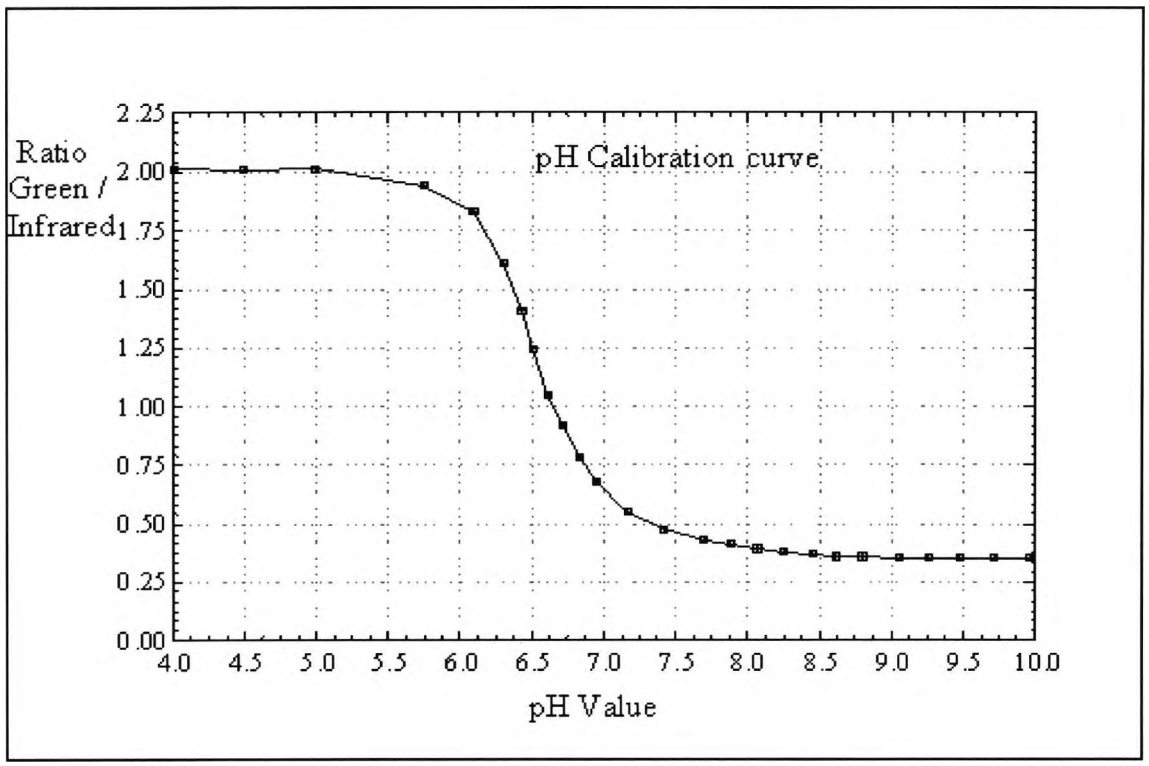

Fig. 8.3: Optical sensor response as a function of pH.

For this experiment, the existing prototype optical ammonia sensor was modified as shown on fig. 8.1 and fig. 8.2 and tested with external electrical pH modulation. Internally to the sensor, the existing optical pH meter was used. To demonstrate the operation of the electrical pH modulation method in this practical application, the sensor was immersed in a water solution of 1 ppm ammonium chloride and constant electrical current was applied to the cell from a galvanostatic source set at 2 mA (compliance voltage 4V). The measured current density through the external cathode was 0.2 mA/cm^2. This was repeated for concentration of 10 ppm. The time response of the sensor for both concentrations is shown on fig. 8.4. Because of the very low biasing current and extremely low ammonia concentration, the time response was slow and saturation was not achieved. The results show that the signal (S) rate of change over time (t), i.e. dS/dt, could be used for measurement of traces of ammonia or early environmental pollution detection.

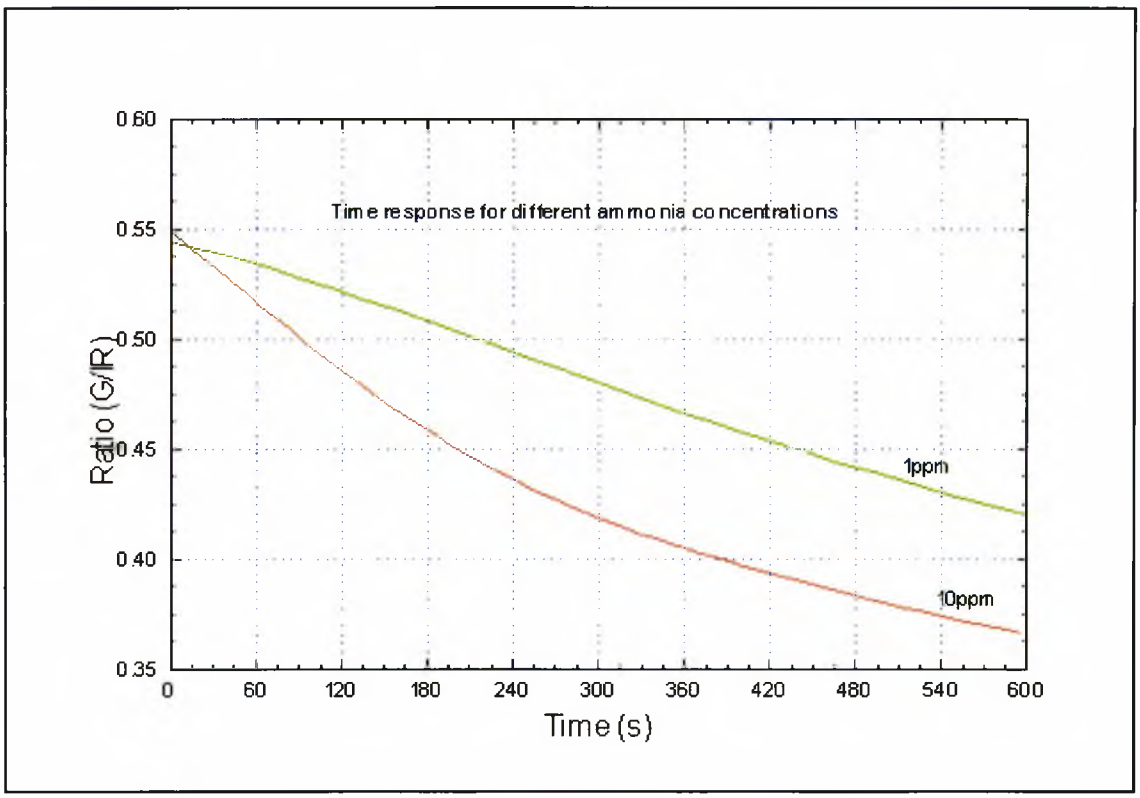

Fig. 8.4: Optical sensor time response to different concentrations of ammonia.

In this experiment, the PD was generated by direct electrical means - in an all-optical system such a PD could be produced by photovoltaic conversion of an optical signal from a laser diode source, to avoid electrical power transmission in the system, as described in our INCO – COPERNICUS project proposal description. In case that the optically generated bias is not sufficient, a local battery power supply, mounted on the sensor and optically controlled, should be used.

The described here ammonia sensor was conditioned by electrochemical pH modulation without interference between conditioning current and measurement signal, as the optical fibre-based internal pH sensor is immune to the effect of the electrical field distribution through the solution. As demonstrated in Chapter 4, electrochemical pH electrodes are strongly influenced by the applied electrical field, and have proved to suffer significant limitations for this application. It must be emphasized that, as shown, this sensor is still not reversible, because the ammonia gas is dissolved again after passing through the membrane to form ammonium ions, thus causing a change in the sensor internal pH. This means that the measurement system requires calibration before every use (which can be

carried out automatically under computer control) and the sensor internal volume is refilled after saturation. However, the accumulative effect of ammonium ions in the internal volume of the sensor is useful for trace ammonia measurement, when the time constant is not critical. The addition of electrodes to the internal sensor volume and internal pH modulation in proximity of the inner side of the membrane is one approach to achieve reversibility.

8.2 Electrochemical pH control system

The concept of electrical pH modulation was demonstrated by conditioning the ammonia sensor as described above. The next step according to the set objectives is to accurately control and maintain pH by electrical bias. The method of pH modulation, although useful in some applications, allows only to shift pH in the desired direction, but not to maintain a precisely set value as required in pH-controllers. To achieve this goal, a closed loop negative feedback control system is needed. To investigate the concept of electrical pH control system, an electrochemical controller - a potentiostat AMEL Model 551, and a pH meter CORNING model 320 as a reference - were the building blocks used for this prototype instrumentation. The electrochemical cell consisted of a stainless still grid WE and CE of 10 cm^2 and 3-in-one combination pH electrode immersed in 200 cm^3 of 1M solution of NaCl. The two-electrode electrochemical cell was connected to the potentiostat output via relay switch, as shown on fig.8.5. The pH electrode was immersed in proximity to the WE surface in the cell solution, and the recorder output of the pH sensor was connected through a sample and hold circuit to the RE input of the potentiostat.

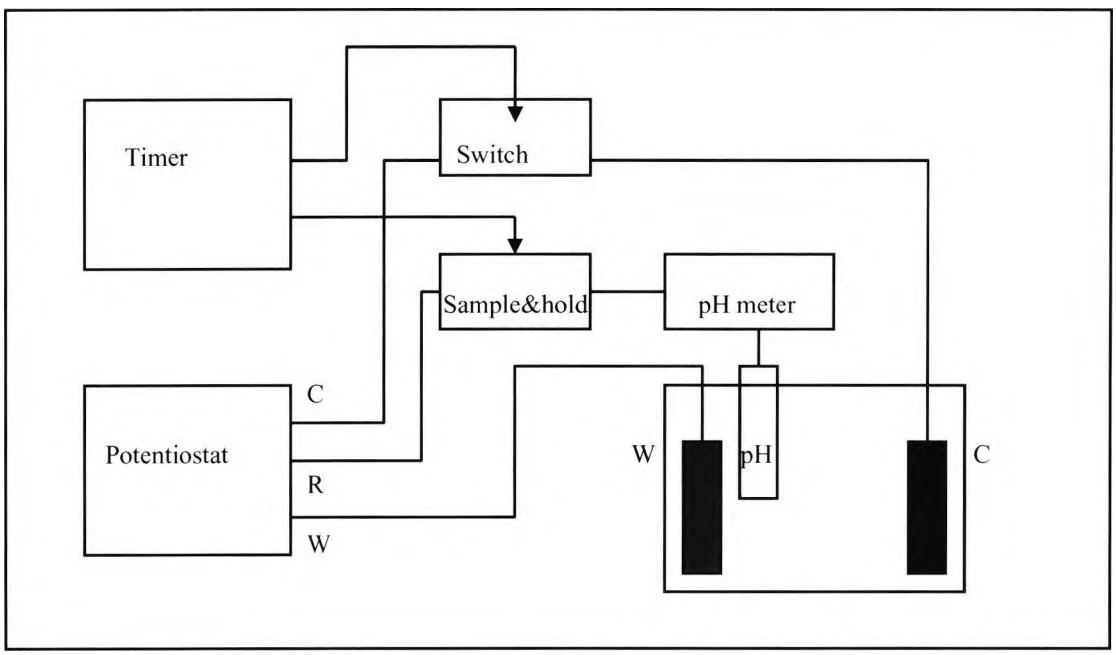

Fig. 8.5: Electrical pH controller, based on a time sequence of measurement and control periods.

Timer control was used as shown on fig. 8.6a to drive the potentiostat output and input switching, in a way that they are out of phase and do not overlap in time, to avoid electrical interference between bias and measurement, as electrochemical pH sensor was used. The system was in rest when both the potentiostat input voltage was set to zero, and pH of the solution in the cell equalled 7, the point where the pH meter recorder output was calibrated to zero volts. If potential of either polarity was set at the potentiostat input, the instrument worked out the corresponding pH (measured by the pH meter as a voltage offset of 59.16 mV for each unit of pH at 25°C – see Chapter 3). The potentiostat output biased the electrochemical cell until the voltage at the output of the pH meter equaled the set input voltage (this is when the set and measured pH equalize). Depending on the polarity of the set voltage, the working electrode was the anode when producing oxygen in its surroundings and hence pH lower than 7, or the cathode when generating hydrogen and pH higher than 7. As the pH measurement electrode was located in proximity to the working electrode, the pH meter output produced negative feedback voltage to keep the system in control. It was observed that potential difference above 2.7V between the working and counter electrodes caused significant (over 1%) error in the pH measurement

and the pH meter displayed "out of range" warning above 4V biasing voltage. The standard output compliance voltage of the potentiostat used was 30V (of either polarity), and thanks to the high gain of the error amplifier, a small difference between the set and measured pH was causing the maximum output voltage to swing. For this reason, the pH biasing action and the measurement were separated in time for one of the experiments (fig.8.6a) and for another option (fig.8.6b) the potentiostat output voltage was restricted to 2.7V by using battery power supply.

The control system timing and pH time response in the controlled media to an input step signal of one pH unit is shown on fig. 8.6a for the switching version, and on fig. 8.6b for the restricted output voltage option. The switching cycle period was 30 s, with 10 s active regulation and the potentiostat output connected to the cell, 10s waiting for the time constant of the pH meter glass electrode to settle, 9s for pH measurement sampling time and 1s pause. Without stirring of the solution the pH electrode response was about 50% of the set value in one cycle and within 90% in three cycles with 10% overshooting. The restricted output voltage regulator was considerably slower, but responded smoothly and allowed for more accurate control. Also, this method allowed better control over side reactions on the electrodes, other than generating hydrogen and oxygen.

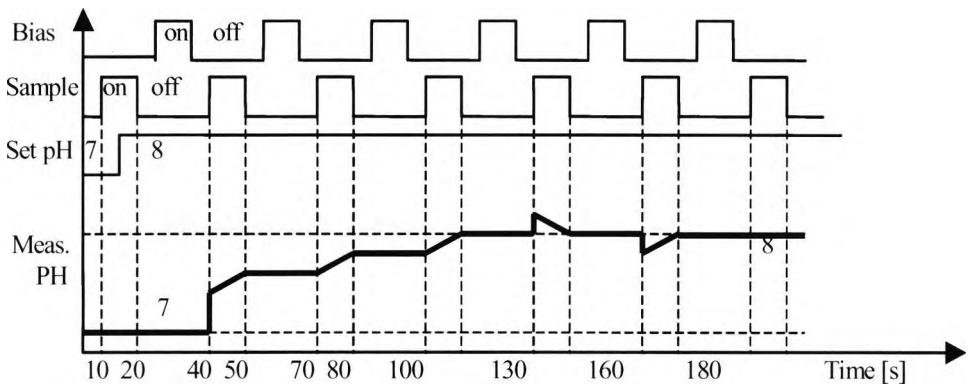

Fig. 8.6a: Time- divided bias/measurement control approach.

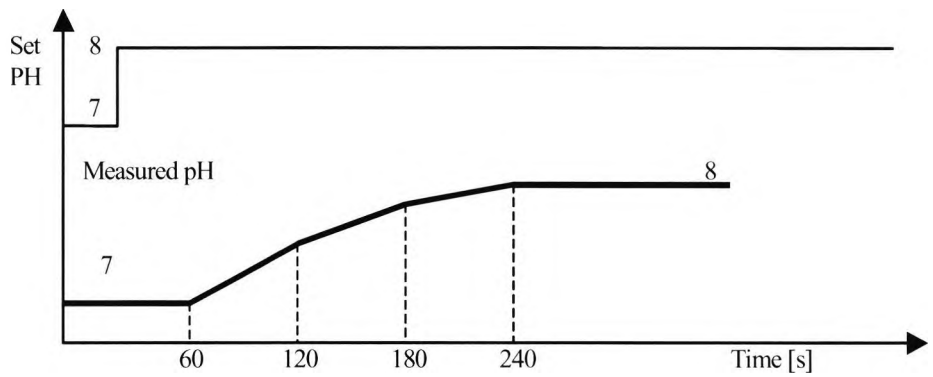

Fig. 8.6b: Continuous bias control.

8.3 Optical pH control system

8.3.1 Universal pH indicator

Optical pH sensing in the feedback loop of the controller was our preferred method, in order to avoid interference from the biasing electrolytic current and the PD gradient in the solution. In this way, timing and switching of the control and measurement loops were not necessary.

The optical method used was based on measurement of the color changes of a pH indicator dye, dissolved in the solution. Phenol red, which was used in the ammonia sensor described above, as most color pH indicators (listed in Appendix 3), is useful in a relatively narrow pH range (approximately from 6 to 8, as evident from fig 8.2). To investigate the optical feedback pH control system in a wider pH range, a universal pH indicator was used (Gornovski, 1974) covering the pH range from 2 to10. In 50 cm^3 pure alcohol 10 mg phenolphthalein, 20 mg methyl red, 30 mg methyl yellow, 40 mg bromthymol blue and 50 mg thymol blue were dissolved, then 0.1 N sodium hydroxide was added until the solution is yellow in color (pH=6).

8.3.2 Indicator spectra

To evaluate the universal indicator spectra as a function of pH, a spectrophotometer (Novaspec 4049, range 350-900 nm) was used. The pH-related color changes in the indicator solution were measured and recorded. The results were stored from the "recorder" output of the spectrophotometer by a custom made data acquisition system, consisting of Keithley DAS 800 12 bit A/D board and a PC. The integration time was set to one second for good noise averaging. The solution in the measurement sample cell was 1M NaCl. A few drops of the universal indicator solution were added to the cell. Samples with different pH (4, 5, 6, 7, 8, 9, and 10) have been prepared externally in a larger vessel with the addition of orthophosphoric acid and sodium hydroxide. The optical spectra of the samples were evaluated in sequence scanning through the spectrophotometer range of 350-900 nm. The results are shown on Figure 8.7 (plot from the raw data in Appendix 8).

Fig.8.7: Universal pH Indicator Spectra.

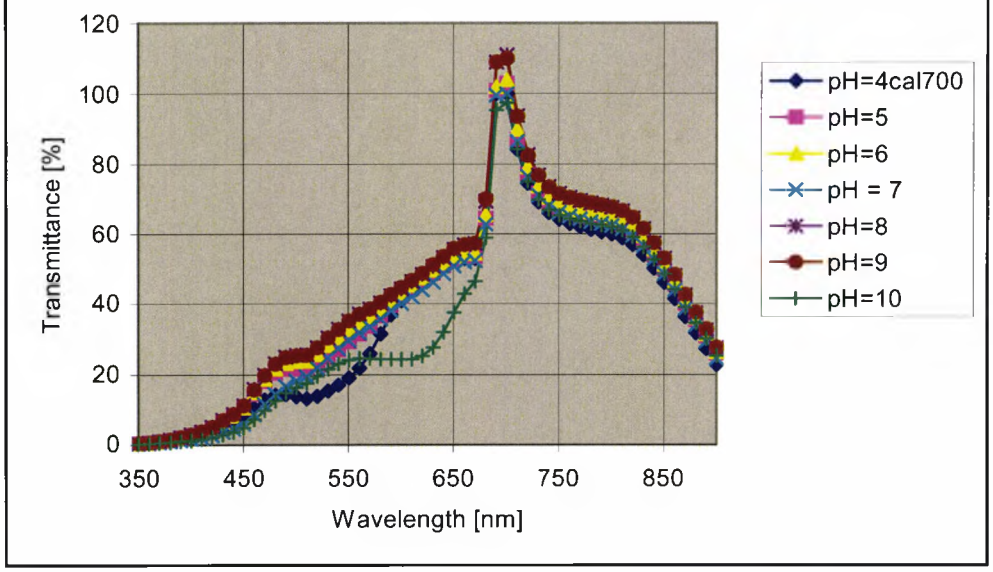

Fig.8.8: Indicator Normalized Spectra.

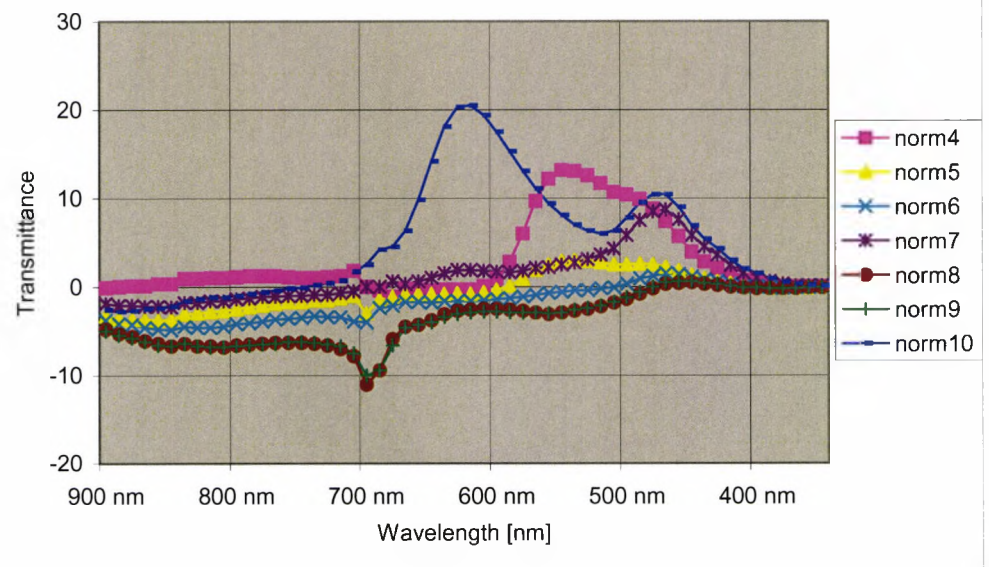

To eliminate the absorption of the sodium hydroxide solution fraction from the signal, all the measured values were subtracted from those obtained for pure 1M NaCl solution without indicator. The resulting indicator normalized spectra (Figure 8.8, plot from the normalized data in Appendix 8) shows better the relative change of the solution optical transmittance as a function of pH. The data series (norm 4 to norm 10) represent the normalized data for pH values from 4 to 10.

Fig.8.9: Indicator pH Response.

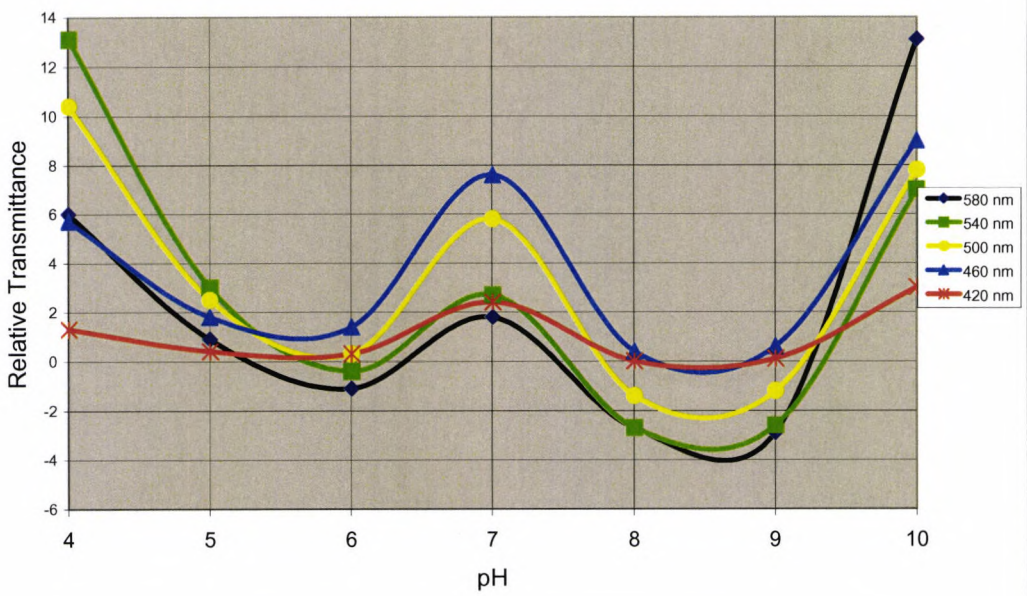

A better way to present the indicator spectral response is to plot the relative optical transmittance as a function of pH for a range of wavelengths (fig.8.9).

As the optical response of the pH indicator solution is not monotonic in a range larger then 1 – 2 pH units for any wavelength measured, single wavelength measurement is not sufficient to measure pH in a wide range. Such measurement is restricted only to small biasing steps. Multi- wavelength measurements based on the unique combination of spectral responses and data analysis can allow for wider range feedback signal generation, although it is complex and requires the use of the data in Appendix 8 for the creation of look-up-through tables stored in a ROM, and embedded microprocessor control.

8.3.3 Performance of optical feedback pH control system

To investigate an optical feedback pH control system, the setup of fig. 8.10 was used:

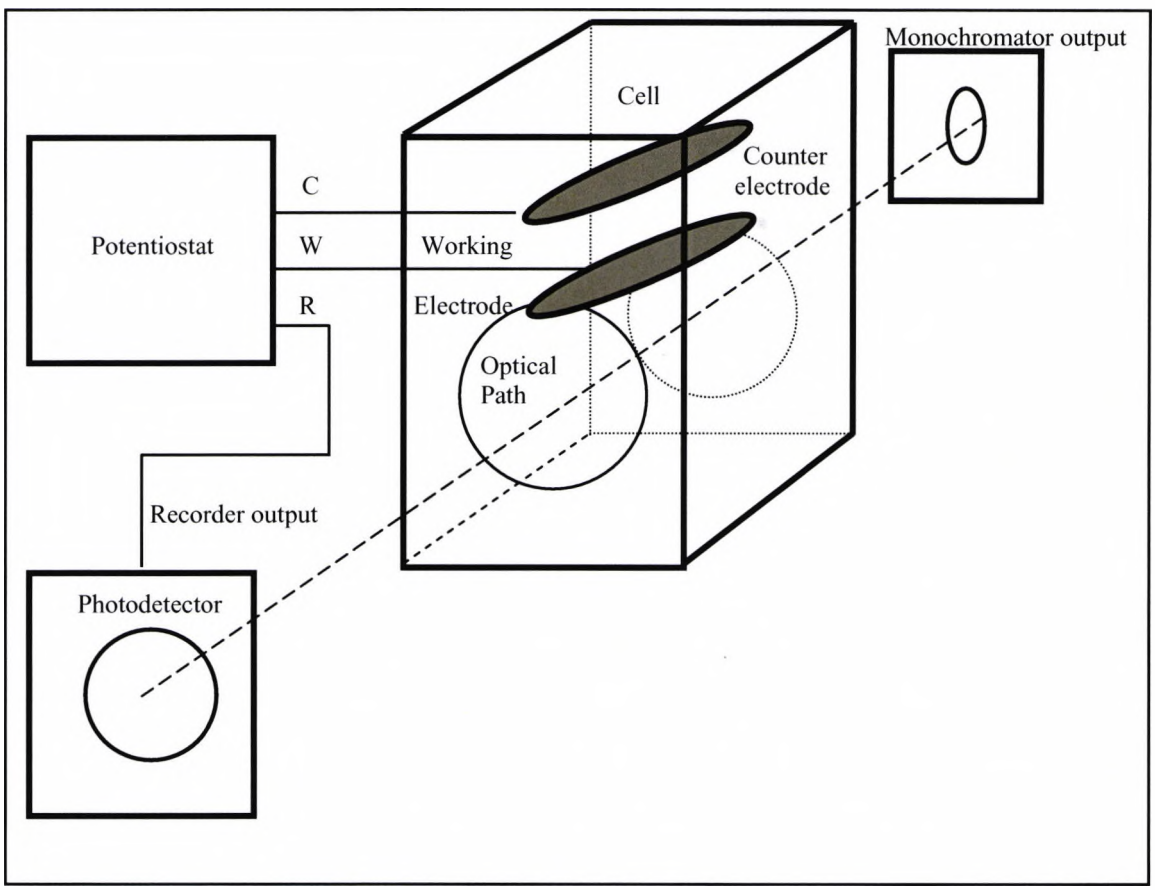

Fig. 8.10: Optical cell (10x10x40mm) with internal electrochemical modulation electrodes designed to demonstrate the optical feedback pH control method.

The spectrophotometer standard sample cell (4 cc cuvette) was modified to an electrochemical cell. Two platinum wire electrodes were placed inside the sample, the working electrode located as close as possible above the optical window, without obstructing the optical path, and the counter electrode, set as far as possible, close to the top of the probe. With this layout the influence on the optical transmission of the aerosol caused by the hydrogen and oxygen gas generated during operation was avoided. The "recorder" output of the spectrometer was used to provide a pH-related negative feedback signal. A single wavelength measurement at 500 nm was used, where the indicator response is monotonic over a restricted pH range from 7 to 8 according to the spectral response shown on fig. 8.11.

Fig. 8.11: Reversible pH dynamic response; pH from 7 to 8.

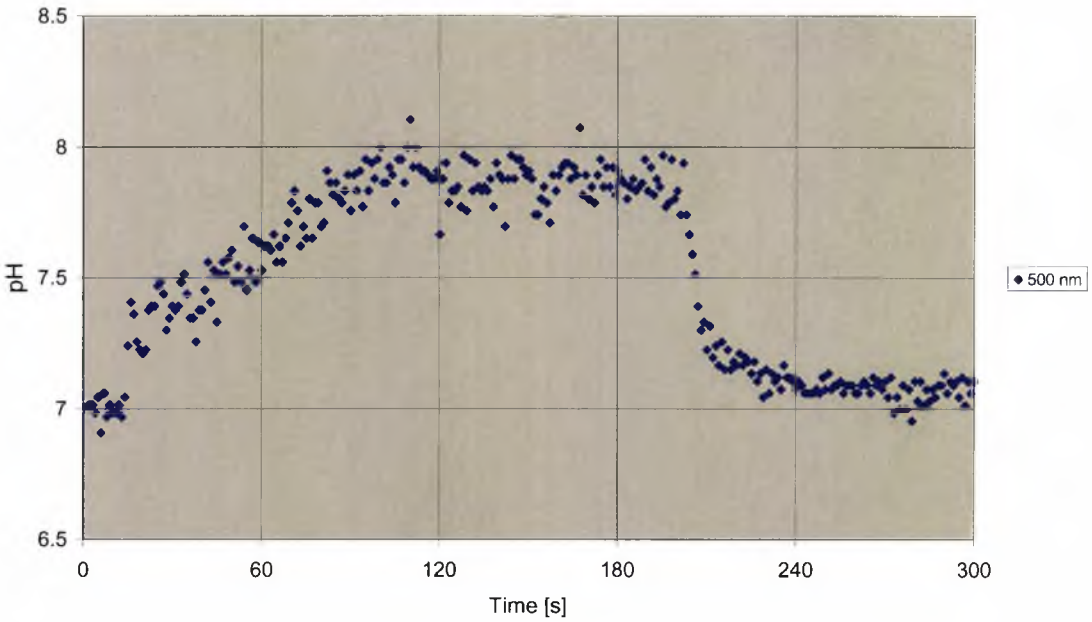

For reversible operation, bipolar power supply was used for the potentiostat output power amplifier. Two Li-ion rechargeable batteries, both charged in advance to 4V by the hybrid circuit (described in Chapter 6) attached to them, with two AA alkaline batteries in series at the input side. The maximum output voltage of the potentiostat was reduced by two p-n junction's bias voltage of the silicon power transistors in Darlington configuration (about 0.6-0.7V per junction, average of 1.3V). In this way, the output compliance voltage of the potentiostat was reduced to 2.7V of either polarity, which was previously identified to be the preferred safe limit. The potentiostat output current (flowing between the two electrodes in the sample cell) was limited to 20 mA, to avoid excessive internal gassing and interference of the gas bubbles with the solution optical properties.

Fig.8.12: Reversible pH dynamic response; pH from 4 to 5.

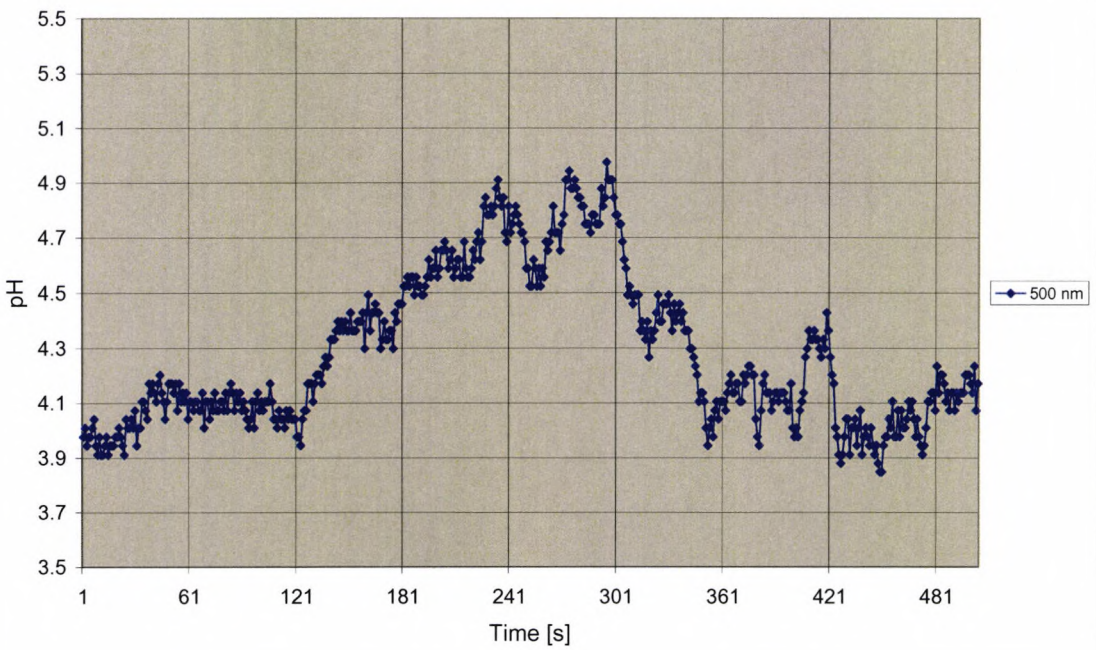

During operation, the regulator was maintaining minimum error voltage between the potentiostat input voltage and the spectrophotometer output voltage, by applying constant current within the output voltage and cell resistance limits. This mode could be referred to as constant current (CC) of 20 mA with limited output voltage of 2.7V, or galvanostatic/voltage limited mode of operation.

The reversible dynamic response of this system to a step of 1 pH unit bias is shown on fig.8.11. The spectrophotometer recorder output was calibrated to 1V at 100% transmittance and pH = 7, and the potentiostat set voltage was calibrated according to the indicator pH response for the wavelength used. A voltage step, corresponding to a set pH = 8, was applied to the potentiostat input at t = 0 s, and returned to pH = 7 at t = 180 s. The data show two times faster response from pH8 backwards to pH7 (60 s), versus the initial transition from 7 to 8 (120 s), possibly due to different gassing rate for hydrogen and oxygen at this potential. The system response was also tested in the acidic range, using solution with initial pH = 4. The universal indicator response in the pH 4 to 5 range at wavelength of 500 nm is also monotonic, and in the same direction as from 7 to 8 (according to fig. 8.9). The reversible dynamic response of the regulator to a step input voltage, corresponding to a change from pH = 4 to pH = 5 and back to pH = 4, is shown on

fig. 8.12. The output voltage of the spectrophotometer was recalibrated to 1V at 100 % transmittance and pH = 4, and wavelength of 500 nm. The system was in rest at t = 0 s, when the potentiostat input was set to a voltage corresponding to pH5, and returned to pH4 at t = 300 s.

The time response ratio of 2:1 remained the same as above for pH = 7. The transition from pH 4 to pH 5 took place in approximately 240 s, and from pH 5 to pH 4 in about 120 s, although the absolute time duration was two times longer compared to the neutral solution. The aerosol generation in the solution was the main source of noise in the signal, but contributed for steering of the solution and accelerated the dynamic response.

Fig. 8.13: Controller Time Response; pH from 8 to 7.

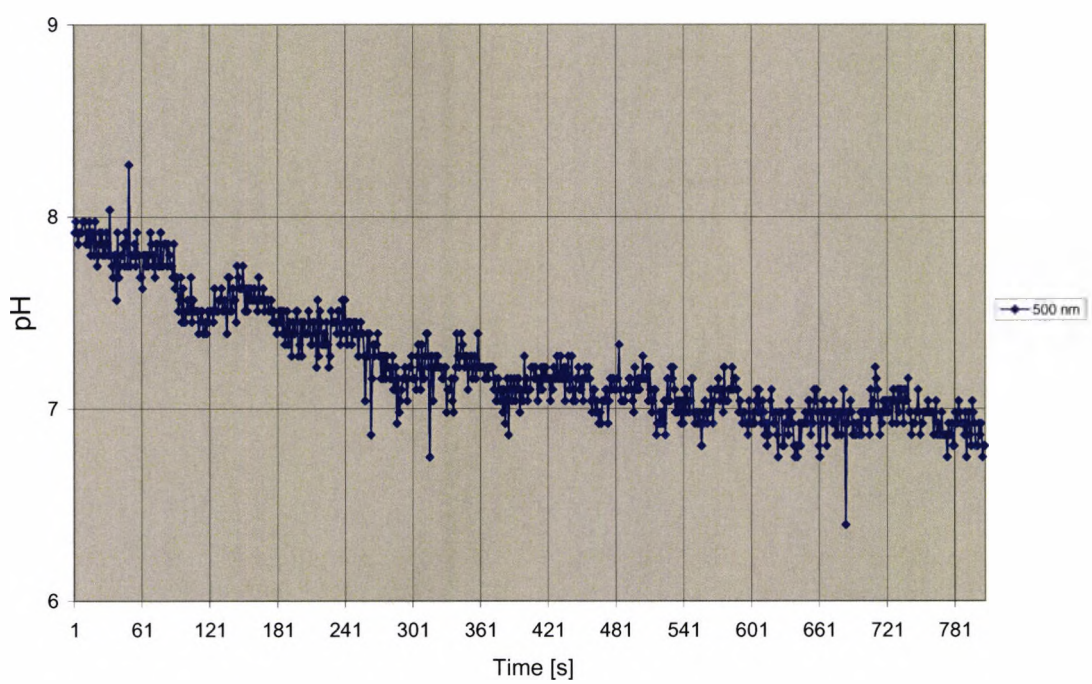

To compare "galvanostatic" versus "potentiostatic" mode of operation, the potentiostat was set in constant voltage (CV) mode. In this case, the current was dependent on the potentiostat output voltage and the solution conductivity, the electrodes surface area and polarization. The regulator was controlled by voltage, and automatically applied the necessary current to maintain control. On fig. 8.13 is shown the time response in potentiostatic mode for the transition from pH8 to pH7. The average current was 2mA.

The time response (approximately 500 s) was significantly slower than the same transition in CC mode.

Fig. 8.14: Controller Time Response; pH from 5 to 4

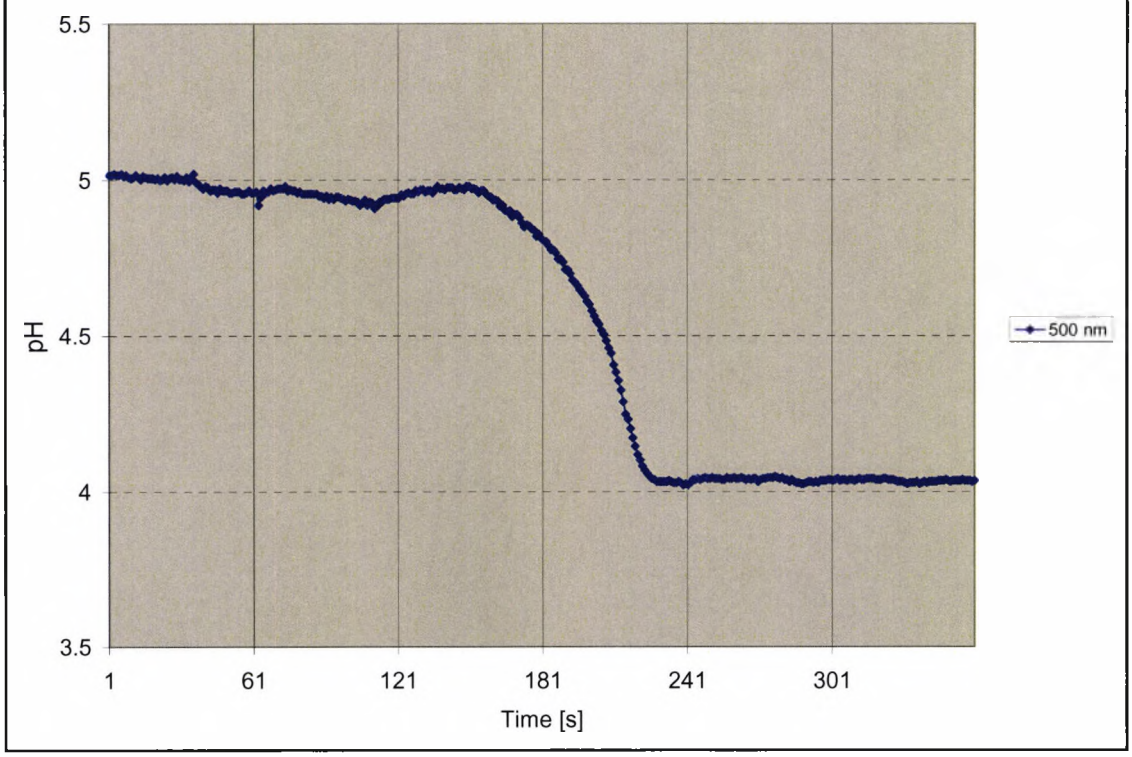

Measurement in the same mode was repeated in acidic environment (transition from pH5 to pH4). The higher solution conductivity resulted in higher average current (260mA), and the time response (approximately 60 s) was much faster (fig. 8.14). At this high rate, less noise was observed in the signal.

The results show that the controller speed is related to the mode of regulation and the value of the electrical current through the solution. The cell conductivity limits the current at certain maximum output voltage of the regulator, which in turn is limited by the electrochemistry of the cell. In potentiostatic mode, the current is a function of the cell conductivity, but the electrochemical reactions control is good. In galvanostatic mode, more predictable speed of response is achievable, at the expense of variable output voltage.

Summary

In this chapter were reported experimental results, demonstrating practical applications of the method of electrical pH control in aqueous solutions. First, open loop electrical pH modulation was applied for optical ammonia sensor conditioning. This method was successfully used for measurement of traces of dissolved ammonia in water. Next, a closed feedback electrolysis control system, using a glass pH electrode sensor, was tested with a step pH disturbance of one unit, using switching and continuous control. The disturbance of the pH measurement by the electrical current through the solution was overcome by the use of optical pH sensor. A universal pH indicator was evaluated in a wide pH range (4-10), and used as a colorimetric dye in the optical sensing path. The pH-related voltage feedback from the optical pH sensor was successfully used in the control loop of the electrochemical controller in both galvanostatic and potentiostatic modes. The time response, accuracy and power consumption of the controller were measured and discussed. Next, the main conclusions of this research are made, based on the method theory and practical confirmation of the applicability for chemical sensing by optical techniques.

9. CONCLUSIONS

9.1 Summary

The subject of the research program was pH measurement and control in aqueous solutions. Chemical and optical methods for pH measurement and instrumentation for pH control have been investigated. Practical applications were developed and tested.

The work began with a critical review of the existing methods of electrochemical pH sensing and chemical pH control, and as a result the research was focused on a novel approach to electrochemical pH modulation, based on electrolysis in aqueous solutions. An application for ammonia optical fibre sensor conditioning was successfully demonstrated. A smart multivariable sensing approach, based on reversible electrical pH conditioning, was investigated and recommendations developed. The electrical pH modulation method was further developed to the next level – an accurate reversible pH control, where the desired pH value can be preset and maintained over time. Both electrochemical and optical feedback systems were developed and prototyped. The advantages of the optical approach were demonstrated. The spectrum of a universal pH color indicator was evaluated and calibration tables for wide pH range operation produced. The electrolysis controller mode of regulation and the output parameters as voltage, current and time response were optimized, considering the biasing and measurement requirements and interference limitations.

9.2 Accomplishments

The main achievement of the investigation was the development of a novel method for electrical pH control in aqueous solutions, which overcomes many drawbacks of the chemical methods applied today. By the use of a closed loop feedback electrolysis regulator, reversible pH control to a preset pH was achieved. In a review of the existing electrochemical controllers, i.e. potentiostats and galvanostats, with their characteristics and limitations, analogy between voltage, current and electrolysis (pH modulation) regulators was established. The new method of electrical pH control in aqueous solutions was demonstrated with an electrochemical controller (combined potentiostat/galvanostat). The last was modified in such a way that the regulated parameter was the pH of the interrogated media, instead of the reference electrode potential (potentiostat), or the electrical current flowing through the electrochemical cell (galvanostat). A comprehensive collection of regulation examples was developed. Various control modes were investigated including constant voltage, constant current, and combined pH feedback regulated

controllers. The results of this work were published in a number of relevant papers, reports and patents over the period during which the research was carried out. They are listed in Appendix 9.

In order to develop a controller with a closed loop pH-related negative feedback, two alternative pH measurement approaches were investigated:

- Electrochemical pH meters based on a hydrogen ion-selective glass electrode.
- Optical pH sensors based on colourimetry, including optical fibre pH sensors and sol-gel optical sensors.

The advantages and drawbacks of the two approaches were compared and discussed, and prototype instruments were designed and tested. The electrochemical feedback controller provided stable operation in a wide pH range, although interference with the electrical field caused by the electrolytic current was observed. A limit of the maximal bias voltage across the controlled solution was established in order to save the accuracy of the pH measurement and control. The voltage limit restricted the maximal ionic current through the solution at a given solution conductivity and surface area of the modulation electrodes, and hence the speed of operation. It was found that the minimum output voltage to generate significant pH modulation in aqueous solutions for pH control with practical time response is 2.3V, and the interference with the measurement is negligible at compliance voltage limited to 2.7V at the regulator output. This is a suitable voltage range for a Li-ion rechargeable battery, which has a 4.2V- 3V discharge range, but reduced with the voltage drop across the power amplifier output transistors could be accurately adapted to the ideal requirements.

To maximize the energy utilization of a battery power supply for a remote *in-situ* pH sensor/controller, a hybrid circuit using high-energy primary batteries in combination with a rechargeable battery was developed. The hybrid power supply combines the convenient discharge voltage range and high current rate capability of the Li-ion battery with the high energy density at low drain rate and low-maintenance convenience of the widely available AA alkaline battery. In this way, an independent from AC, low-maintenance operation was achieved, where the replacement of the alkaline batteries could be combined with the modulation electrodes and optical sensor head renewal.

A pH controller was configured as time-sequenced switching and sampling device, thus separating in time the bias and measurement processes, and was prototyped and tested. It was found that this method eliminates the electrical interference problem and speeds up operation, although the control response is a pulse rather than smooth voltage change.

An optical pH sensing approach has been developed in order to avoid the electrochemical sensing interference problems and reduce the controller response time. The optical spectral response of a universal wide-range pH color indicator was evaluated for the purpose of pH control. An on-line spectrophotometer-based colorimetric pH measurement instrument was developed to provide a pH-related feedback signal. Especially designed electrochemical cell was placed in the spectrophotometer cuvette, where the universal pH indicator was dissolved in the controlled aqueous solution. This prototype instrument demonstrated the feasibility of the optical feedback control approach and gained significant advantages in reliability and response time versus the electrochemical approach.

9.3 Recommendations for future development

The problem of the non-monotonic pH indicator spectral response was discussed. Future development based on multi-wavelength interrogation and digital signal processing of the response signal for individual point signature identification is suggested.

Also, the investigation of the electrical field influence on the chemical reactions in the pH-controlled solution is of great importance for every particular application. The side reactions of the electrolysis pH control need further investigation. The potentiostatic method allows for precise voltage control and is recommended, when a specific operating voltage range is required. In the opposite case, when the operating voltage is not an issue, but the controlled solution conductivity is low, e.g. pure water, the galvanostatic method with higher compliance voltage gives better results.

The hybrid power supply system can be developed for fuel cell applications, when the last becomes a viable portable power source. A tempting idea is to use the pH controlled cell in a reversible manner, as a very low-rate fuel cell, that can charge the rechargeable battery over extended period of time, especially in sea water environment. Monitoring can be performed using intermittent protocol with a very low duty cycle. The direction of the charge/discharge process could be reversed under control. Large biasing current can be

supplied from the rechargeable battery to the electrochemical cell for a short time to control pH and perform the necessary measurements, followed by a long rest/charge period. Such operation can free the system from power supply maintenance until the electrolytic cell and sensors need reconditioning.

It is well understood that the seepage of greenhouse gases from the sea surface contributes considerably to increases in their concentration in the atmosphere. Enhanced tools for the sea water monitoring contribute for better understanding the mechanism of generation of the "greenhouse effect" gases, both natural and created by man activities. This allows for recommendation of measures for restriction or modernization of certain industries and for prediction of the global impact of climate changes in the future.

The pH sensing and control approach considered herein could find interesting applications in environmental control and particularly seawater monitoring by the use of optical fibre colorimetric sensors, based on VIS-IR light absorption, using ion-sensitive dyes. The measurement selectivity of dissolved species could be achieved in several ways:

- Separation by gas-permeable and ion-selective membranes.
- Use of chemically sensitive dyes either in liquid form or entrapped in the network of sol-gel layer, applied to the sensing end of optical fibres.
- Applying electrical potentials to electrodes placed in key areas in the sensor as to control the ion concentration and pH and to allow reversible two-way gas permeation, selectivity and sensitivity calibration.

Such measurements help to estimate the global impact of the released gases from the sea surface and recommend measures for the reduction of particular pollution sources.

10. REFERENCES AND BIBLIOGRAPHY

10.1 Papers, books and reports

1. Alloway, B.J. and Ayres, D.C. (1993). Chemical Principles of Environmental Pollution, *Chapman and Hall.*
2. Andreev P., Bourilkov J. (1985) Low Frequency Instrumentation for Potentiodynamic Studies, *Communications of the Department of Chemistry*, Bulgarian Academy of Sciences, Vol.18, Number 1.
3. Andreev P, Bourilkov J, Tonchev D. (1990) A New General Purpose Potentiostat, *41st ISE Meeting*, Prague, Proceedings I, Tu-3.Atkins, P.W. (1990) Physical Chemistry, *Oxford University Press.*
4. Atmatzidis, P.A. (1993) Development of a Prototype Ammonium Ion Monitor, MPhil Thesis, City University, London.
5. Attridge J.W., Leaver K.D. and Cozens J.R. (1987) Design of a Fibre- optic pH Sensor with rapid Response, *J. Phys. E: Sci. Instrum.* 20 No 5 (May 1987) pp. 548-553.
6. Badini, G.E. (1994). Investigation of a Porous Glass-like Substrates for use in Fibre Optic Chemical Sensors, *PhD Thesis,* City University, London.
7. Belz, M., Boyle, W.J.O.,.Klein, K.F. and Grattan, K.T.V. (1996) Smart Sensor Approach for a Fibre-Optic-based Residual Chlorine Monitor, *Internal City University Report.*
8. Belz, M.(1996) Measurements on Sol Gel samples prepared by Janusz Pokorowski , *Internal City University Report.*
9. Bourilkov J, Iltchev N, Banov B (1992) Wideband Power Operational Amplifier, *Journal of Radio, Television and Electronics*, Bulgaria, June, pp. 8-10.
10. Bourilkov J., Iltchev N., Banov B. (1992) Wideband Potentiostat, *Fourth European Conference on Electroanalysis*, Noordvijkerhout, Holland, May 31 - June 3, Proceedings p.14.
11. Bourilkov, J.T., Fneer, M., Boyle, W.J.O., Grattan, K.T.V. and Palmer, A.W. (1996) Dissolved gas sensing based on composite optical fibre and electrochemical techniques, *Proceedings of the Applied Optics Divisional Conference of The Institute of Physics*, pp. 449-454, Reading, UK.
12. Bourilkov J., Belz M., Boyle W.J.O., Grattan K.T.V. (1998) Electrical pH Control in Aqueous Solutions, *Conference on Process Monitoring Applications of Fiber Optic Sensors*, 4 November, Boston, *SPIE Proceedings* Vol. 3538, pp. 268 – 277.

13. Butler, T.M., MacCraith, B.D., McDonagh, C.M., 1995, Development of an extended range fibre optic pH sensor using evanescent wave absorption of sol- gel entrapped pH indicators, *SPIE Vol.2508*, 168- 177.
14. Cheng, D, 2004, Applying PID control algorithms in sensor circuits, *Sensors*, May 2004, pp.52-55.
15. Chojnacki, J. and Biernat, J.F., 1990, Application of azoles as neutral carriers in liquid membrane ion- selective pH electrodes, *Journal of Electroanalytical Chemistry*, 277, 159- 164.
16. Christian, G.D. (1980) Analytical Chemistry, *J. Wiley and Sons*, USA.
17. Desai, M. M.,Rhinehart, R.R. (1994) pH Control Using a Heuristic Model: A Pilot Scale Demonstration, *Proceedings of the American Control Conference*, Baltimore, MD, paper FM 14 - 2:50, pp. 3137-3141.
18. Ding, J.Y., Shahriari, M.R., Sigel, G.H.,Jun., 1991, Fibre optic pH sensors prepared by sol- gel immobilization technique, *Electronic Letters*, Vol. 27, #17.
19. Fneer, M., Kurata, J., Boyle, W.J.O. and Grattan, K.T.V. (1996) Optical Fibre Ammonia Sensor for Water Measurement, *Internal City University Report*
20. Frishman, G., Gabor, G. (1994) Surface Characteristics of Optical Chemical Sensors, *Sensors and Actuators B, Chem. (Switzerland)*, Vol. B 17, #3, pp. 227-232.
21. Fuh, M.- R.S., Burgess, L.W., Hirschfeld, T.B., Christian, G.D. and Wang, F.T., 1987, Single fibre optic fluorescence pH probe, *Analyst*, 112, p 1159.
22. Gornovski, I.T., Nazarenko, U.P., Nekriach, E.F. (1974) Short Handbook of Chemistry, *Naukova Dumka*, Kiev, p. 330.
23. Grattan, K.T.V., 1989, New development in sensor technology – fibre and electro-optics, *Measurement and Control*, Vol. 22, pp 165- 175.
24. Grattan, K.T.V. (1994) A Fundamental Base in Physical Science for Measurement and Analytical Instrumentation, *Measurement* 14, pp 89-101.
25. Grattan, K.T.V (1996) Many Hands Make Light Work: Optics in the Service of Instrumentation and Measurement, *Chairman's Inaugural Address, Science, Education & Technology Division, IEE*, 24.10.1996.
26. Hammer, M.J. (1994) Water and Wastewater Technology, *Prentice hall Career and Technology*, New Jersey.
27. Hampel, C.A. (1964) The Encyclopedia of Electrochemistry, *Reinhold Publishing Corporation*, p1156.

28. Heineman, R.W., Seliskar, C.J. and Richardson, J.N. (2003), Spectroelectrochemical Sensing Based on Multimode Selectivity Simultaneously Achievable in a Single Device: an Overview, *Aust. J. Chem. 2003, 56, 93-102.*
29. Henkel, N. (1996) Principles of a Representation Scheme for Modeling Optical Instrumentation, Diploma Report, City University, London.
30. Hunt, D.T.E. and Wilson, A.L. (1986) The Chemical Analysis of Water, *The Royal Society of Chemistry*, Alden Press, Oxford.
31. Jones, T.P. and Porter, M.D., 1988, Optical pH sensor based on the chemical modification of a porous polymer film, *Analytical Chemistry*, 60, 404.
32. Kirkbright, G.F., Narayanaswamy, R. and Welti, N.A., 1984, Fibre- optic pH probe based on the use of an immobilized colorimetric reagent, Analyst, 109, 1025.
33. Kimura, S.G., Matson S.L. and Ward, W.J. III(1972) Industrial Applications of Facilitated Transport, *Recent Developments in Separation Science, C.R.C. Press* Vol.1, 1972, pp. 11-25.
34. Klein, D.N., Bourilkov, J.T. (2002), Hybrid Energy Systems for Mobile Devices, *IMPACCT,* May 2, 2002, New York City, NY.
35. Klein, L.C. (1994) Sol-Gel Optics: Processing and Applications, *Kluwer Academic Publishers*.
36. Kohsick, W. (1991) A Fast Response Water Vapour and Carbon Dioxide Sensor, SPIE Vol. 1511, *Fiber Optic Sensors: Engineering and Applications*, pp.114-119.
37. Kornilov, V.M., Lavrov, I.S., Smirnov O.V. and Yaroslavski, Z.Y. (1975) Use of Electrical Treatment in Technological Purification of Water, *Journal of Applied Chemistry*, Chech, Vol. 48, #2, pp. 357-361.
38. Kurata, J. (1995) Report on the Design and Improvement of the Fibre Optic Ammonia Sensor, City University, London.
39. Lambrechts, M. and Sansen, W. (1992) Biosensors: Microelectrochemical Devices, *Institute of Physics Publishing*, Bristol, Philadelphia and New York.
40. Lee S.T., Gin J., Nampoori V.P.N., Vallabhan C.P.G., Unnikrishnan N.V., Radhakrishnan P.(2001) A Sensitive Fibre Optic pH Sensor Using Multiple sol-gel Coatings, *J. Opt. A: Pure Appl. Opt. 3 No 5* (September 2001), pp 355-359.
41. Mackison, R., Brinkworth, S.J., Belchamber, R.M., Aries, R.E, Cutler, D.J., Deeley, C. and Mould, H.M. (1992) A Demonstration of Truly Remote In-Line Near-Infrared Process Analysis, *Applied Spectroscopy*, Vol. 46, #6.

42. Mahuli, S.K., Rhinehart, R.R., Riggs, J.B. (1992) Experimental Demonstration of Nonlinear Model-based In-line Control of pH, *Journal of Process Control*, Vol.2, #3, pp. 145-153.
43. McMillan G.K. (1993) pH Measurement and Control, *Instrument Society of America,* ISBN: 1556174837.
44. Milo, Ch. And Atwater, B., 1992, Luminescent fiber optic sensor for the measurement of pH, *SPIE Vol. 1796*, pp 188- 197.
45. Michie W.C., Culshaw B., McKenzie I., Konstantakis M., Graham N.B., Moran C., Santos F., Bergquist E. and Carlstrom B., (1995) Distributed sensor for water and pH measurements using fiber optics and swellable polymeric systems, *Optics Letters*, Vol. 20, #1, pp. 103- 105.
46. Mooney, E. (1993) Applications of a Fiber Optic Probe for Colorimetric Determinations, *Proceedings SPIE*, Vol. 1796, pp. 260-271.
47. Moore R.L. (1995) Environmental Protection by the Neutralization of Wastewater using pH Control, *ISA,* ISBN: 1556175264.
48. Mouaziz, Z. (1993) Optic Fibre Sensor for pH Measurement, *PhD Thesis*, City University, London.
49. Mouaziz, Z., Briggs, R., Hamilton, I. and Grattan, K.T.V., 1993, Design and Implementation of a Fibre-Optic-based Residual Chlorine Monitor, *Sensors and Actuators B*, 11, 431- 40.
50. Mouaziz, Z, Briggs, R. and Grattan, K.T.V., 1993, Multi-Parameter Fibre Optic Chemical Sensor for the Measurement of Nitrate Ion, Ammonia and Organic Matter, *Proceedings of the Symposium on Chemical Sensors II*, The Electrochemical Society Inc., New Jersey, USA, Vol. 93- 7, 303- 316.
51. Murray, J.W., Codispoti, L.A. and Friederich, G.E. (1995) Oxidation-Reduction Environments: The Suboxic Zone in the Black Sea, *Advances in Chemistry Series*, Vol. 244, pp. 157-176.
52. Natarajan, S., Rhinehart, R.R. (1994) Implementation Techniques for an In-line pH Controller, *Proceedings of the American Control Conference*, Baltimore, MD, paper FP 14 – 4:40, pp. 3523-3527.
53. Novak J. (2002) PH Control Systems: Six Options for Small System Operators, *Water Conditioning and Purification Magazine* (October 2002).
54. Oesch, U., Brzozka, Z., Xu, A., Rusterholz, B., Suter, G., Pham, H.V., Welti, D.H., Ammann, D., Pretsch, E. and Simon W., 1986, Design of neutral hydrogen ion carrier

s for solvent polymeric membrane electrodes of selected pH range, *Analytical Chemistry*, 58, 2285- 2289.

55. Parekh, M., Desai, M., Li, H., Rhinehart, R.R. (1994) In-line Control of Nonlinear pH Neutralization Based on Fuzzy Logic, *IEEE Transactions on Components, Packaging and Manufacturing Technology*, Part A- Vol. 17, #2.
56. Parr R.A., Wilson J.C. and Kelly R.G. (1986) A Hybrid Microelectronic pH Sensor, *J. Phys. E: Sci. Instrum.* 19 No 12 (December 1986) pp. 1070-1072.
57. Peterson, J.I. (1984) Fiber Optic Chemical Sensors – a View from the Past to the Future", *Proceedings of the Symposium on Biosensors*, 15-17 Sept., LA, CA, pp. 35-39.
58. Phillips, I. and Bartlett, D.V. (1961) Permeability of Plastics, *British Plastics*.
59. Presley R. (1999) The Sometimes Maddening Science of pH Measurement, *American Laboratory News*, (June 1999).
60. Regner A., 1957, Electrochemical Processes in Chemical Industries, *Artia*, Prague pp 198-212.
61. Rogov, V.M., 1989, Electrochimicheskoe izmenenie svoistv vodi, *Livov*, Ucraine, pp 15-40.
62. Samson, P.J., Stuart, A.D. (1988) Coal Mine Methane Sensing by Optical Fibre, *Proceedings of 13th Australian Conference on Optical Fibre Technology (IREE, Aust.)*, Hobart, Tasmania, December 4-7, pp.113-116.
63. Schulthess, P., Shijo, Y., Pham, H.V., Pretsch, E., Ammann, D. and Simon W., A hydrogen ion- selective liquid- membrane electrode based on tri-n-dodecylamine as neutral carrier, 1981, *Analytica Chimica Acta*, 131, 111- 116.
64. Seitz, W.R., 1988, Chemical sensors based on immobilized indicators and fibre optics, CRC Critical Review, *Analytical Chemistry*, 19, 135.
65. Sengupta, A., Raghuraman, B. and Sirkar, K.K. (1990) Liquid Membranes for Flue Gas Desulfurization, *Journal of Membrane Science*, 51, pp. 105-126.
66. Smith, A.M. (1986) Optical-Fibre Sensors – New Opportunities for Chemical Sensing, *Electron. & Power* (GB), Vol. 32, #11, pp. 811-813.
67. Spinu, V.C., Langhans, R.W., Albright, L.D., 1999, Electrochemical pH control in hydroponic systems, *ISHS Acta Horticulturae 456*: II Modelling Plant Growth, Environmental Control and farm management in Protected Cultivation.
68. Stam, H. (1980) Membrane Separation of CO2 and H2S from Mixtures with Gaseous Hydrocarbons, Proceedings of EC Symposium on Basic Research and Industrial

Technologies for Europe "Radioactivity, Waste Management and Disposal" held in Brussels, Belgium, pp. 135-152.

69. Tang, T.B., Johannessen, E.A., Wang L., Astaras A., Ahmadian M., Cui L., Murray A. F., Cooper J.M., Beaumont S.P., Flynn B.W., Cumming D.R.S., (2002), IDEAS: A Miniature Lab-In-A-Pill Multisensor Microsystems, *RDG 130. The Scottish Higher Education Funding Council Project.*
70. Van den Berg, C.M.G (1991) Potentials and Potentialities of cathodic Stripping Voltammetry of Trace Elements in Natural waters, *Analytica Chimica Acta*, 250, pp. 265-276.
71. Van den Berg, C.M.G and Nimmo, M., Abollino, O, and Mentasti, E. (1991) The Determination of Trace Levels of Iron in Seawater Using Adsorptive Cathodic Stripping Voltammetry, *Electroanalysis*, 3, pp. 477-484.
72. Villarruel, C.A., Dominguez, D.D. and Dandridge, A. (1997) Evanescent wave Fiber Optic Chemical Sensor, *SPIE Vol. 798 Fiber Optic Sensors II*, pp. 225-229.
73. Wallace P.A., Elliot N., Uttamlal M., Holmes-Smith A.S. and Campbell M. (2001) Development of a Quasi-distributed Optical Fibre pH Sensor using a Covalently Bound Indicator, *Meas. Sci. Technol.* 12 No 7 (July 2001), pp 882-886.
74. Wallington, S.A., Labayen, T.,. Poppe, A., Sommerdijk, N.A.J.M., Wright, J.D. (1996) Sol-Gel Materials for Optical Sensing of Solvents and Metal Ions, *3rd European Conference on Optical Chemical Sensors and Biosensors, Europtrode III*, Zurich, Switzerland, March 31- April 3, 1996 p. 44. .
75. Ward, W.J. III (1972) Immobilized Liquid Membranes, *Recent Developments in Separation Science, C.R.C. Press* Vol.1, pp. 153-161.
76. Wolfbeis, O.S. and Posch, H.E., 1986, Fibre- optic fluorescing sensor for ammonia, *Analytica Chimica Acta*, 185, 321.

10.2 Project applications arising from this work

77. Boyle, W.J.O, Grattan, K.T.V, Bourilkov, J.T., Belz, M, On-line Waste Water Monitoring Based on Optical Fibre Chemical Sensing Techniques and Artificial Intelligence Analysis – Proposal submitted to the Fourth Framework Programme for Research and Technological Development and Demonstration of EC (1994-98), Theme III (Measurements related to the needs of society), Second call (Deadline 15.11.95).

78. W.J.O. Boyle- Development of Optical Fibre Based Sensors for Chemical Monitoring in Extreme Environments – Case for an extension of SERC Advanced Fellowship B/91/AF/1406 "Environmental Sensing for the Water Industry Using Fibre Based Techniques", to the Clean Technology Unit of the EPSRC.
79. Bourilkov, J.T, Boyle, W.J.O, Grattan, K.T.V, (1996) A System for In-Situ Monitoring of Greenhouse Gases Distribution in the Anoxic Zones of the Black Sea, Proposal for Cooperation in Science and Technology with CCE/NIS (INCO-COPERNICUS-1995/96).

10.3 Publications of systems

80. Aqua-Tonic Counter Top AT-500 Water Ionizer, Natural Solutions Environmental, Inc, www.naturalsolutions1.com
81. Battery Reference Book, 1989, Bitrode Corporation.
82. Burleson's J.P. Controllers: Dupla pH set; Dupla pH/MP; Tunse pH.
83. CO_2, Carbonate hardness, etc., Booth G., 1993, www.lvld.hp.com
84. Corning, 1993, Guide to pH measurement.
85. Chamberlin, 1995, Absolute SPA Services, Service Industry Publications.
86. Chemtrol: 6000 Integrated Controller, 3000 Programmable Controller, 350 ppm/ORP/pH Controller, 320 ppm/ORP/pH Controller, 210 ORP/pH Controller (Sanitizer Control).
87. Determination of Anions and Cations, Transitional Metals, Other Complex Ions and Organic Acids and Bases in Water by Chromatography, HMSO Publication Centre, London, 1990.
88. ETUS: CPU-MOD/T Treatment System – A system for removal/recovery of heavy metals from process wastewater streams.
89. Introduction to pH, Omega Engineering, www.omega.com
90. Iotronic products, Measurement and Process Controller for Chlorine CL s2381 (Drinking Water Treatment); Measurement and Process Controller for use with open electrode type sensors (Min Type- Control of Alloy Baths, Max Type- Desalination of cooling Towers); Process Analyzer & Controller PAA (Process Control); pH measurement and control with pH s2380 (Drinking water Treatment and Food Processing).
91. ISFETs, New Tools for Water Quality Monitoring, THORN EMI Central Research Laboratories.

92. Pacific Northwest Garden Supply, 1996, How to maintain proper pH levels.
93. PH Control 2 Relay LED Panel Mount, Pulse Instruments, www.pulseinstrument.com
94. REMCO Engineering: pH Controller/Recorders (Environmental water systems and controls).

10.4 Patents cited

95. Electrical pH Control, Japan, JP 91-11-08-A2 (3250309), 28.02.1990.
96. PH Photoelectrochemical Control, China, CH-89-01-11-U (2030721), 1.11.1989.
97. PH Control, Korea, KR-90-12-22-Y1 (9011233), 17.02.1990.
98. Bourilkov, J. T., Klein, D.N., Rotondo, J., Gillette CO, US 20030155887, WO200371651, Hybrid Power Supply, USA, February 2002.
99. Bourilkov, J. T., Klein, D.N., Rotondo, J., Gilicinski, A.G., Gillette CO, US 2004/0174072, Fuel Cell Hybrid Power Supply, USA, filed March 5, 2003, Pub. Date September 9, 2004.

APPENDIX 1: DISSOLVED CO_2 LEVELS [PPM] IN WATER VS. PH/KH

The rise in pH that occurs when KH is added is balanced to a degree by the dissolved CO_2 in water. CO_2 forms small amounts of carbonic acid and hydrogen carbonate that tend to reduce pH. This mechanism gives a way to regulate pH. If the pH of a solution is determined primarily by the carbonate buffering system, then the relation of pH, KH and dissolved CO_2 is fixed. A change of either KH or CO_2 sets the pH (Chapter 2, p.15).

pH/KH	2	3	4	5	6
6.6	15	23	30	38	46
6.7	12	18	24	30	36
6.8	9	14	19	24	28
6.9	7	12	15	19	23
7	6	9	12	15	18
7.1	5	7	9	12	14
7.2	4	6	8	9	11
7.3	3	4	6	7	9
7.4	2.4	3	5	6	7
7.5	1.9	2.5	3.5	5	5
7.6	1.5	2	2.4	3	4
7.7	1	1.5	2	2.5	3
7.8	0.9	1.1	1.5	2	2
7.9	0.6	0.9	1	1.2	1.6
8	0.5	0.7	0.9	1	1.2

APPENDIX 2: TABLE OF STANDARD REFERENCE ELECTRODE POTENTIALS AT DIFFERENT TEMPERATURES

Additional electrode systems which meet the requirements for reference electrodes and their potentials at different temperatures (Hampel, 1964), as referred to in Chapter 3, p5.

Electrode	Temperature (°C)	Electrode Potential (abs. volt)	
H_2 (ideal, 1 atm) | HCl (ideal, m = 1)	zero at all temperatures by definition		
Ag | AgCl | HCl	0	0.2365	
	25	0.2224	
	50	0.2043	
Ag | AgBr | HBr	0	0.08168	
	25	0.07132	
	50	0.05668	
Ag | AgI | HI	25	−0.15230	
		E^0 (sec leg)[1]	E^*
Hg | Hg_2Cl_2, KCl (satd) | buffer solution	25	0.2412	0.2415
Hg | Hg_2Cl_2, KCl (1N)	25	0.2801	—
Hg | Hg_2Cl_2, KCl (1N) | salt bridge	25	—	0.283
Hg | Hg_2Cl_2, KCl (0.1N)	25	0.3337	—
Hg | Hg_2Cl_2, KCl (0.1N) | salt bridge | buffer solution	25	—	0.3356
Hg | Hg_2Cl_2, HCl [metastable]	25	0.26796	
Hg | Hg_2Cl_2 | HCl [stable]	5	0.27290	
	25	0.26823	
	45	0.26104	
Pt | QH_2, Q | HCl[2]	0	0.71798	
	25	0.69976	
	40	0.69865	

[1] All data in this table refer to aqueous solutions.
[2] Q = p-benzoquinone ($C_6H_4O_2$).

APPENDIX 3: ACID/ALKALINE INDICATORS

The color changes only over a limited pH range. The choice of the appropriate indicator for every particular application (see Chapter 4, p.3) depends on the pH range of measurement or control. To cover wider pH measurement range, composite indicators (as developed in Chapter 8) with adjacent ranges and spectrally matching colors are used. Below is shown a list of the most used indicators and their pH ranges starting from acid to base.

Cat No.	Indicator	Transition interval Colour change	Indicator solution (preparation)
1398	Malachite green oxalate (C.I. No. 42000)	0.0 - 2.0 Yellow Green-blue	0.1 g in 100 ml water
1310	Brilliant green (C.I. No. 42040)	0.0 - 2.6 Yellow Green	0.1 g in 100 ml water
15935	Eosin yellowish (C.I. No. 45380)	0.0 - 3.0 Yellow Green fluorescence	0.1 g in 100 ml water
15936	Erythrosin B (C.I. No. 45430)	0.0 - 3.6 Orange Red	0.1 g in 100 ml water
15944	Methyl green (C.I. No. 42590)	0.1 - 2.3 Yellow Blue	0.1 g in 100 ml water
15945	Methyl violet (C.I. No. 42535)	0.1 - 2.7 Yellow Violet	0.1 g in 100 ml ethanol (20 %)
623	Picric acid (C.I. No. 10305)	0.2 - 1.0 Colour-less Yellow	0.1 g in 100 ml ethanol (70 %)
5225	Cresol red	0.2 - 1.8 Red Yellow	0.1 g in 100 ml ethanol (20 %) or dissolve 0.04 g in 1.05 ml sodium hydroxide solution (0.1 mol/l) and make up to 100 ml with water
1408	Crystal violet (C.I. No. 42555)	0.8 - 2.6 Yellow Blue-violet	0.1 g in 100 ml ethanol (70 %)
5228	m-Cresol purple	1.2 - 2.8 Red Yellow	0.04 g in 100 ml ethanol (20 %) or dissolve 0.04 g in 1.05 ml sodium hydroxide solution (0.1 mol/l) and make up to 100 ml with water
8176	Thymol blue	1.2 - 2.8 Red Yellow	0.04 g in 100 ml ethanol (20 %) or dissolve 0.04 g in 0.86 ml sodium hydroxide solution (0.1 mol/l) and make up to 100 ml with water
8682	p-Xylenol blue	1.2 - 2.8 Red Yellow	0.1 g in 100 ml ethanol (50 %) or dissolve 0.04 g in 0.98 ml sodium hydroxide solution (0.1 mol/l) and make up to 100 ml with water

Cat No	Indicator	Transition interval Colour change	Indicator solution (preparation)
11473	2,2',2",4,4"-Pentamethoxy-triphenylcarbinol	1.2 - 3.2 Red Colourless	0.1 g in 100 ml ethanol (96 %)
15934	Eosin bluish (C.I. No. 45400)	1.4 - 2.4 Colour-less Fluorescent pink	0.1 g in 100 ml water
2282	Quinaldine red	1.4 - 3.2 Colour-less Pink	0.1 g in 100 ml ethanol (60 %)
3464	2,4-Dinitrophenol	2.8 - 4.7 Colour-less Yellow	0.1 g in 100 ml ethanol (70 %)
3055	Methyl yellow (C.I. No. 11020)	2.9 - 4.0 Red Yellow-orange	0.1 - 0.5 g in 100 ml ethanol (90 %)
3022	Bromochlorophenol	3.0 - 4.6 Yellow Blue-violet	0.1 g in 100 ml ethanol (20 %) or dissolve 0.04 g in 0.69 ml sodium hydroxide solution (0.1 mol/l) and make up to 100 ml with water
8122	Bromophenol blue	3.0 - 4.6 Yellow Blue-violet	0.1 g in 100 ml ethanol (20 %) or dissolve 0.04 g in 0.6 ml sodium hydroxide solution (0.1 mol/l) and make up to 100 ml with water
1340	Congo red (C.I. No. 22120)	3.0 - 5.2 Blue Yellow-orange	0.2 g in 100 ml water
1322	Methyl orange (C.I. No. 13025)	3.1 - 4.4 Red Yellow-orange	0.04 g in 100 ml ethanol (20 %) or 0.04 g in 100 ml water
1323	Methyl orange solution		
1359	Mixed indicator 4.5 acc. to Mortimer	4.3 - 5.2 Red Blue	
8121	Bromocresol green	3.8 - 5.4 Yellow Blue	0.1 g in 100 ml ethanol (20 %) or dissolve 0.04 g in 0.58 ml sodium hydroxide solution (0.1 mol/l) and make up to 100 ml with water

Cat No.	Indicator	Transition interval Colour change	Indicator solution (preparation)
3465	2,5-Dinitrophenol	4.0 – 5.8 Colour-less – Yellow	0.05 – 0.1 g in 100 ml ethanol (70 %)
6279	Alizarinsulfonic acid sodium salt (C.I. No. 58005)	4.3 – 6.3 Yellow – Violet	0.1 g in 100 ml ethanol (50 %) or 0.1 g in 100 ml water
6076	Methyl red (C.I. No. 13020)	4.4 – 6.2 Red – Yellow-orange	0.1 g in 100 ml ethanol (96 %)
6078	Methyl red sodium salt (C.I. No. 13020)	4.4 – 6.2 Red – Yellow-orange	
6130	Mixed indicator 5	4.4 – 5.8 Red violet – Green	250 ml
3024	Chlorophenol red	4.8 – 6.4 Yellow – Purple	0.1 g in 100 ml ethanol (20 %) or dissolve 0.04 g in 0.94 ml sodium hydroxide solution (0.1 mol/l) and make up to 100 ml with water
5312	Litmus (C.I. No. 1242)	5.0 – 8.0 Red – Blue	4 g in 100 ml water
3025	Bromocresol purple	5.2 – 6.8 Yellow – Purple	0.1 g in 100 ml ethanol (20 %) or dissolve 0.04 g in 0.74 ml sodium hydroxide solution (0.1 mol/l) and make up to 100 ml with water
3023	Bromophenol red	5.2 – 6.8 Orange-yellow – Purple	0.1 g in 100 ml ethanol (20 %) or dissolve 0.04 g in 0.94 ml sodium hydroxide solution (0.1 mol/l) and make up to 100 ml with water
6798	4-Nitrophenol	5.4 – 7.5 Colour-less – Yellow	0.2 g in 100 ml ethanol (96 %) or 0.08 g in 100 ml water
3033	Bromoxylenol blue	5.7 – 7.5 Yellow – Blue	0.1 g in 100 ml ethanol (96 %)
1016	Alizarin (C.I. No. 58000)	5.8 – 7.2 Yellow – Red	0.5 g in 100 ml ethanol (96 %)

Cat No.	Indicator	Transition interval Colour change	Indicator solution (preparation)
3026	Bromothymol blue	6.0 – 7.6 Yellow – Blue	0.1 g in 100 ml ethanol (20 %) or dissolve 0.04 g in 0.64 ml sodium hydroxide solution (0.1 mol/l) and make up to 100 ml with water
7241	Phenol red	6.4 – 8.2 Yellow – Red-violet	0.1 g in 100 ml ethanol (20 %) or dissolve 0.04 g in 1.13 ml sodium hydroxide solution (0.1 mol/l) and make up to 100 ml with water
6794	3-Nitrophenol	6.6 – 8.6 Colour-less – Yellow-orange	0.3 g in 100 ml ethanol (96 %) or 0.08 g in 100 ml water
1369	Neutral red (C.I. No. 50040)	6.8 – 8.0 Blue-red – Orange-yellow	0.3 g in 100 ml ethanol (70 %)
13857	4,5,6,7-Tetrabromo-phenolphthalein	7.0 – 8.0 Colour-less – Purple	0.1 g in 100 ml ethanol (96 %)
5225	Cresol red	7.0 – 8.8 Orange – Purple	0.1 g in 100 ml ethanol (50 %) or dissolve 0.04 g in 1.05 ml sodium hydroxide solution (0.1 mol/l) and make up to 100 ml with water
6246	1-Naphtholphthalein	7.1 – 8.3 Brownish – Blue-green	0.1 g in 100 ml ethanol (96 %)
5228	m-Cresol purple	7.4 – 9.0 Yellow – Purple	0.04 g in 100 ml ethanol (20 %) or dissolve 0.04 g in 1.05 ml sodium hydroxide solution (0.1 mol/l) and make up to 100 ml with water
8176	Thymol blue	8.0 – 9.6 Yellow – Blue	0.04 g in 100 ml ethanol (20 %) or dissolve 0.04 g in 0.86 ml sodium hydroxide solution (0.1 mol/l) and make up to 100 ml with water

Cat No.	Indicator	Transition interval Colour change	Indicator solution (preparation)
8682	p-Xylenol blue	8.0 – 9.6 Yellow – Blue	0.1 g in 100 ml ethanol (50 %) or dissolve 0.04 g in 0.98 ml sodium hydroxide solution (0.1 mol/l) and make up to 100 ml with water
7233	Phenolphthalein	8.2 – 9.8 Colour-less – Red-violet	0.1 g in 100 ml ethanol (96 %)
7227	Phenolphthalein solution (1 % in ethanol)		
7238	Phenolphthalein solution (0.375 % in methanol)		
8175	Thymolphthalein	9.3 – 10.5 Colour-less – Blue	0.1 g in 100 ml ethanol (50 %)
1331	Alkali blue (C.I. No. 42765)	9.4 – 14.0 Violet – Pink	0.1 g in 100 ml ethanol (96 %)
6776	Alizarin yellow GG (C.I. No. 14025)	10.0 – 12.1 Light-yellow – Brownish-yellow	0.1 g in 100 ml water
1016	Alizarin (C.I. No. 58000)	10.1 – 12.1 Red – Purple	0.5 g in 100 ml ethanol (96 %)
1307	Titan yellow (C.I. No. 19540)	12.0 – 13.0 Yellow – Red	0.1 g in 100 ml ethanol (20 %)
4724	Indigo carmine (C.I. No. 73015)	11.5 – 13.0 Blue – Yellow	0.25 g in 100 ml ethanol (59 %) or 1 g in 100 ml water
6810	Epsilon blue	11.6 – 13.0 Orange – Violet	0.1 g in 100 ml water

APPENDIX 4: TRANSMISSION RANGE OF OPTICAL FIBRES MADE OF DIFFERENT MATERIALS

The development of inexpensive, high quality optical fibres for the communications industry has provided the main component for the optical fibre chemical sensors (Chapter 4, p.3).

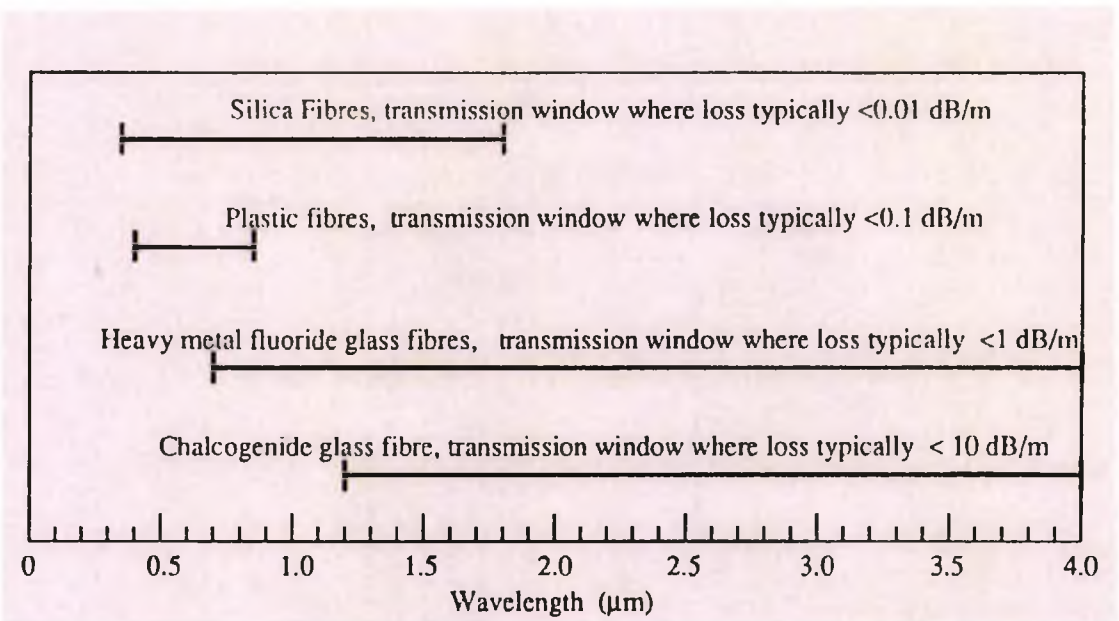

APPENDIX 5: MEASUREMENT PRINCIPLES USING FIBER OPTIC CHEMICAL SENSORS

Optical sensors are constructed by coupling a reagent to a transparent porous surface (the sensor head) at the tip of an optical fibre (Frishman, 1994). The sensor head, including the immobilized reagent, is either a part of the optical fibre or a particle attached to it physically by means of a membrane or optical glue (Chapter 4, p.).

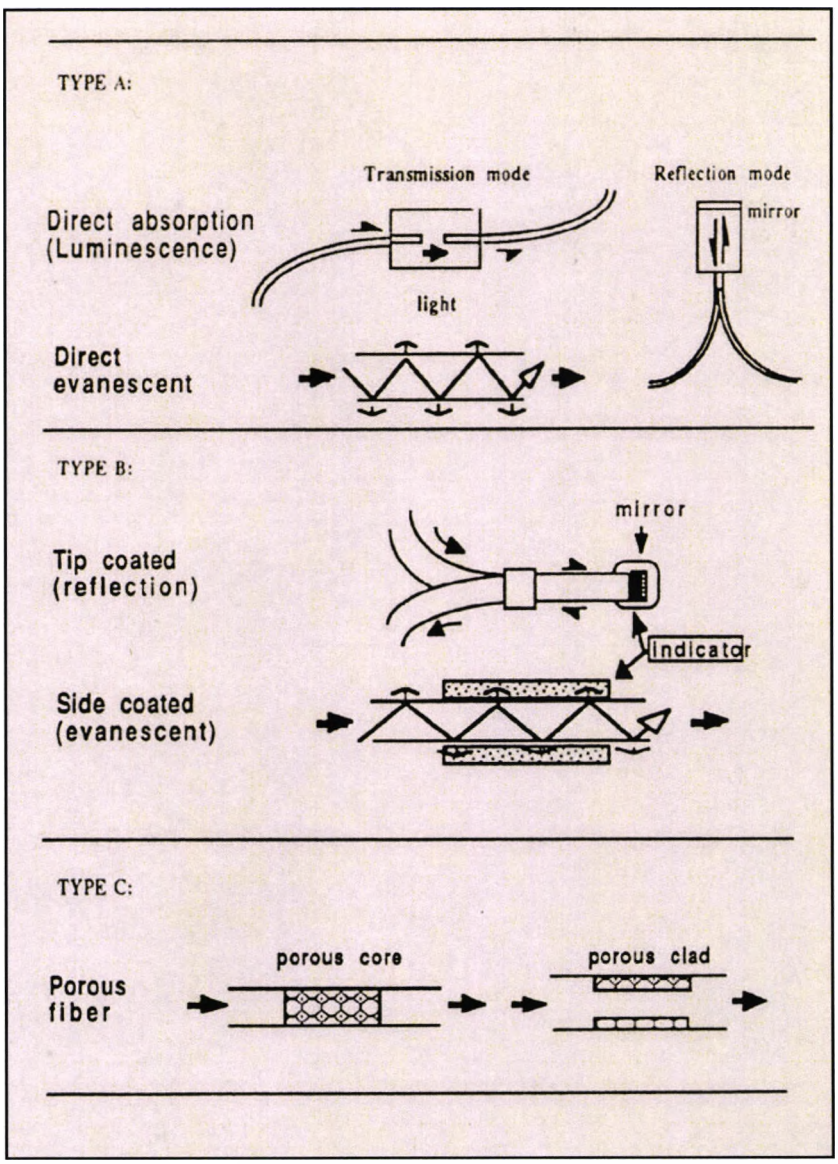

APPENDIX 6: EMISSION SPECTRA OF VARIOUS DOPED SILICA OR SILICA-TITANIA SOL-GEL THIN FILMS

The sol-gel process is applicable to preparing glass-like structures which can be used in optical fibre chemical sensors, as reviewed in Chapter 4, p9. Further in Chapter 4, p.17, different materials are studied as colorimetric or fluorometric additives to sol-gel sensor heads. The graph below shows the fluorometric response of different doped sol-gel thin films.

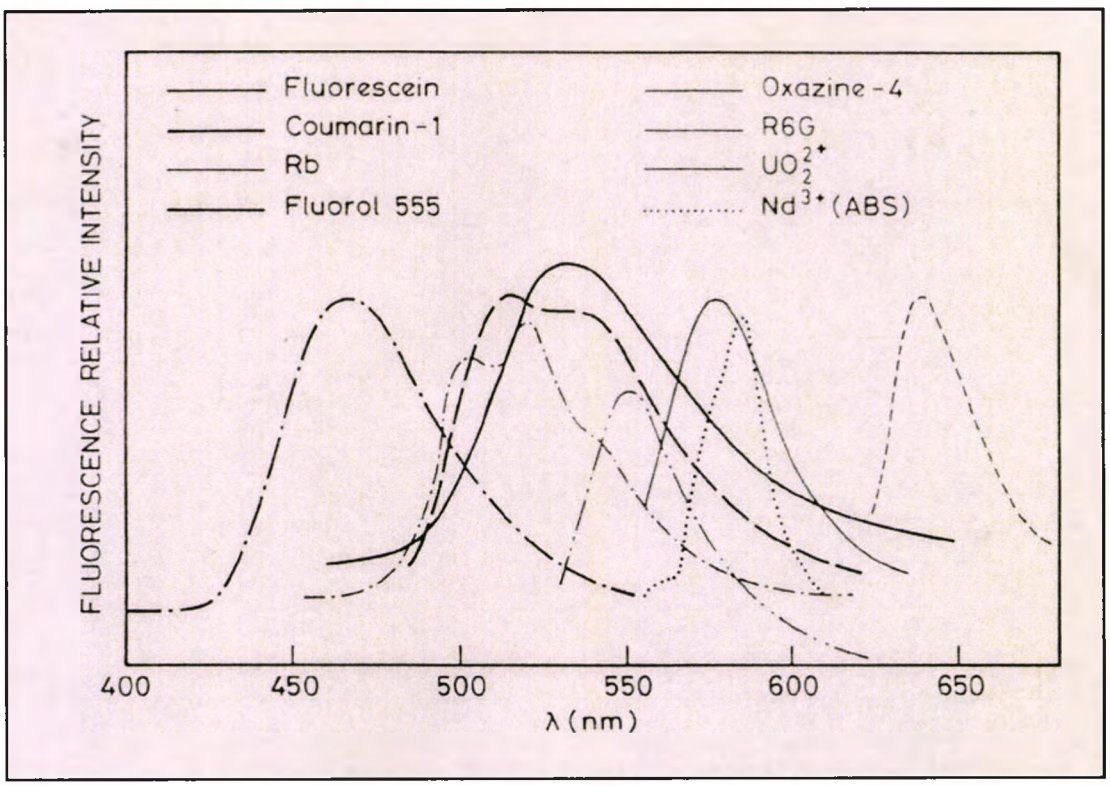

APPENDIX 7: TABLE OF VOLUMETRIC AND GRAVIMETRIC ENERGY DENSITY OF VARIOUS DURACELL ® MICROLITHIUM™ BOBBIN CELLS

The increasing demand for extra long shelf life and very high energy density has inspired the development of Li/MnO_2 bobbin cells. The bobbin-type design maximizes the energy density due to the use of thick electrodes (Chapter 6, p. 126).

	ENERGY DENSITY			
Battery type	**Volumetric**		**Gravimetric**	
	Wh/in.3	**Wh/L**	**Wh/lb.**	**Wh/kg**
DL1/2AAL	**7.5**	**456**	**95**	**209**
DL2/3AL	**9.4**	**574**	**132**	**291**
DLAAL	**10.9**	**668**	**149**	**329**

APPENDIX 8: UNIVERSAL PH INDICATOR

The spectral response of a universal indicator (Gornovski, 1974) was measured vs. pH, using a custom designed optical cell with electrochemical control, as described in Chapter 7, p. 9. The results in the table below are in mV, measured at the recorder output of the spectrophotometer (Novaspec 4049, range 350-900 nm).

Wavelength	pH=4cal700	pH=5	pH=6	pH = 7	pH=8	pH=9	pH=10	wat. C700
900 nm	22.8	26	26.5	24.6	27.5	27.7	25.3	22.7
890 nm	27.3	30.9	31.5	29.4	32.6	32.8	30.1	27.3
880 nm	31.7	35.5	36.1	33.9	37.4	37.6	34.5	31.8
870 nm	36.3	40.1	41	38.6	42.5	42.6	38.9	36.4
860 nm	41.4	45.5	46.5	43.9	48.1	48.3	44.1	41.7
850 nm	46	50	51.2	48.6	53	53	48.5	46.3
840 nm	50.1	54.1	55.5	52.8	57.4	57.4	52.6	51
830 nm	53.9	57.8	59.4	56.6	61.5	61.5	56.2	54.8
820 nm	56.9	60.7	62.5	59.5	64.6	64.7	59.1	57.9
810 nm	58.8	62.5	64.3	61.4	66.6	66.6	61	59.8
800 nm	59.9	63.5	65.2	62.4	67.6	67.7	62	61
790 nm	60.5	64	65.8	63	68.2	68.3	62.5	61.7
780 nm	61.2	64.5	66.3	63.5	68.8	68.9	63	62.4
770 nm	62	65.1	66.9	64.3	69.5	69.6	63.6	63.2
760 nm	63	65.8	67.7	65.1	70.4	70.3	64.3	64.1
750 nm	64.2	66.9	68.7	66.2	71.5	71.4	65.3	65.2
740 nm	66.1	68.6	70.4	68	73.5	73.4	66.9	67.1
730 nm	69.1	71.7	73.6	71.1	76.8	76.7	69.8	70.2
720 nm	74.5	77	79.1	76.4	82.7	82.4	75	75.7
710 nm	84.2	87	89.9	86.5	93.8	93.5	84.3	86
700 nm	100	103	104	100	111	110	97.5	100
690 nm	100	101	102	99.6	109	109	95.4	99.6
680 nm	64.5	64.5	65.5	62.8	69.3	70	58.9	63.4
670 nm	52.9	53.5	54.4	52.4	57.2	57.3	46.4	52.7
660 nm	52.9	53.4	54.3	52	56.9	56.9	42.8	52.6
650 nm	52.2	52.6	53.6	50.8	55.6	55.8	37.6	51.8
640 nm	50.4	50.9	51.7	48.6	53.2	53.5	32	50.1
630 nm	48.3	48.7	49.6	46.1	50.7	51.1	27.7	48
620 nm	46.1	46.6	47.4	43.9	48.4	48.7	25.3	45.8
610 nm	43.7	44.4	45.3	42	46.3	46.6	24.4	43.8
600 nm	40.9	42.1	43.2	40.1	44.3	44.6	24.3	41.8
590 nm	36.9	39.6	41	38.1	42.3	42.6	24.4	39.7
580 nm	31.5	36.6	38.6	35.7	40.2	40.4	24.4	37.5
570 nm	25.9	33.7	36.5	33.5	38.5	38.5	24.5	35.6
560 nm	21.8	31.5	34.7	31.8	37.1	37	24.6	34
550 nm	19	29.3	32.8	29.7	35.1	35.1	24.1	32.2
540 nm	17	27.1	30.5	27.4	32.8	32.7	23.1	30.1
530 nm	15.3	25	28.3	24.8	30.4	30.3	21.6	27.9
520 nm	13.8	22.8	25.7	21.9	27.7	27.6	19.5	25.5
510 nm	13.1	21.3	23.9	19.5	25.6	25.5	17.5	23.8

500 nm	13.7	21.6	23.8	18.3	25.5	25.3	16.3	24.1
490 nm	14.3	21.6	23.3	16.7	25	24.8	14.7	24.2
480 nm	14.1	20.4	21.7	14.4	23.1	22.9	12.5	22.9
470 nm	12.8	18	18.7	11.5	19.9	19.7	9.8	20.2
460 nm	10.5	14.4	14.8	8.6	15.8	15.6	7.2	16.2
450 nm	7.8	10.4	10.6	5.9	11.2	11.1	4.8	11.7
440 nm	6.2	8.1	8.2	4.5	8.7	8.6	3.6	9
430 nm	5.1	6.6	6.6	3.6	7	6.9	2.9	7.2
420 nm	3.8	4.7	4.8	2.7	5.1	5	2.1	5.1
410 nm	2.9	3.5	3.6	2.1	3.7	3.7	1.6	3.6
400 nm	2.3	2.7	2.7	1.7	2.9	2.8	1.2	2.7
390 nm	1.7	2	2	1.3	2.1	2.1	1	1.9
380 nm	1.2	1.3	1.4	0.9	1.4	1.4	0.7	1.2
370 nm	0.8	0.9	0.9	0.7	1	1	0.5	0.8
360 nm	0.5	0.6	0.6	0.4	0.6	0.6	0.3	0.5
350 nm	0.3	0.3	0.3	0.2	0.4	0.4	0.2	0.3

Normalized spectra (all values were subtracted from those obtained for pure 1M NaCl solution without indicator):

Wavelength	norm4	norm5	norm6	norm7	Norm8	norm9	norm10
900 nm	-0.1	-3.3	-3.8	-1.9	-4.8	-5	-2.6
890 nm	0	-3.6	-4.2	-2.1	-5.3	-5.5	-2.8
880 nm	0.1	-3.7	-4.3	-2.1	-5.6	-5.8	-2.7
870 nm	0.1	-3.7	-4.6	-2.2	-6.1	-6.2	-2.5
860 nm	0.3	-3.8	-4.8	-2.2	-6.4	-6.6	-2.4
850 nm	0.3	-3.7	-4.9	-2.3	-6.7	-6.7	-2.2
840 nm	0.9	-3.1	-4.5	-1.8	-6.4	-6.4	-1.6
830 nm	0.9	-3	-4.6	-1.8	-6.7	-6.7	-1.4
820 nm	1	-2.8	-4.6	-1.6	-6.7	-6.8	-1.2
810 nm	1	-2.7	-4.5	-1.6	-6.8	-6.8	-1.2
800 nm	1.1	-2.5	-4.2	-1.4	-6.6	-6.7	-1
790 nm	1.2	-2.3	-4.1	-1.3	-6.5	-6.6	-0.8
780 nm	1.2	-2.1	-3.9	-1.1	-6.4	-6.5	-0.6
770 nm	1.2	-1.9	-3.7	-1.1	-6.3	-6.4	-0.4
760 nm	1.1	-1.7	-3.6	-1	-6.3	-6.2	-0.2
750 nm	1	-1.7	-3.5	-1	-6.3	-6.2	-0.1
740 nm	1	-1.5	-3.3	-0.9	-6.4	-6.3	0.2
730 nm	1.1	-1.5	-3.4	-0.9	-6.6	-6.5	0.4
720 nm	1.2	-1.3	-3.4	-0.7	-7	-6.7	0.7
710 nm	1.8	-1	-3.9	-0.5	-7.8	-7.5	1.7
700 nm	0	-3	-4	0	-11	-10	2.5
690 nm	-0.4	-1.4	-2.4	0	-9.4	-9.4	4.2
680 nm	-1.1	-1.1	-2.1	0.6	-5.9	-6.6	4.5
670 nm	-0.2	-0.8	-1.7	0.3	-4.5	-4.6	6.3
660 nm	-0.3	-0.8	-1.7	0.6	-4.3	-4.3	9.8
650 nm	-0.4	-0.8	-1.8	1	-3.8	-4	14.2
640 nm	-0.3	-0.8	-1.6	1.5	-3.1	-3.4	18.1
630 nm	-0.3	-0.7	-1.6	1.9	-2.7	-3.1	20.3
620 nm	-0.3	-0.8	-1.6	1.9	-2.6	-2.9	20.5
610 nm	0.1	-0.6	-1.5	1.8	-2.5	-2.8	19.4
600 nm	0.9	-0.3	-1.4	1.7	-2.5	-2.8	17.5
590 nm	2.8	0.1	-1.3	1.6	-2.6	-2.9	15.3
580 nm	6	0.9	-1.1	1.8	-2.7	-2.9	13.1

570 nm	9.7	1.9	-0.9	2.1	-2.9	-2.9	11.1
560 nm	12.2	2.5	-0.7	2.2	-3.1	-3	9.4
550 nm	13.2	2.9	-0.6	2.5	-2.9	-2.9	8.1
540 nm	13.1	3	-0.4	2.7	-2.7	-2.6	7
530 nm	12.6	2.9	-0.4	3.1	-2.5	-2.4	6.3
520 nm	11.7	2.7	-0.2	3.6	-2.2	-2.1	6
510 nm	10.7	2.5	-0.1	4.3	-1.8	-1.7	6.3
500 nm	10.4	2.5	0.3	5.8	-1.4	-1.2	7.8
490 nm	9.9	2.6	0.9	7.5	-0.8	-0.6	9.5
480 nm	8.8	2.5	1.2	8.5	-0.2	0	10.4
470 nm	7.4	2.2	1.5	8.7	0.3	0.5	10.4
460 nm	5.7	1.8	1.4	7.6	0.4	0.6	9
450 nm	3.9	1.3	1.1	5.8	0.5	0.6	6.9
440 nm	2.8	0.9	0.8	4.5	0.3	0.4	5.4
430 nm	2.1	0.6	0.6	3.6	0.2	0.3	4.3
420 nm	1.3	0.4	0.3	2.4	0	0.1	3
410 nm	0.7	0.1	0	1.5	-0.1	-0.1	2
400 nm	0.4	0	0	1	-0.2	-0.1	1.5
390 nm	0.2	-0.1	-0.1	0.6	-0.2	-0.2	0.9
380 nm	0	-0.1	-0.2	0.3	-0.2	-0.2	0.5
370 nm	0	-0.1	-0.1	0.1	-0.2	-0.2	0.3
360 nm	0	-0.1	-0.1	0.1	-0.1	-0.1	0.2
350 nm	0	0	0	0.1	-0.1	-0.1	0.1

APPENDIX 9: PUBLICATIONS BY THE AUTHOR RELEVANT TO THIS WORK

The list below includes publications created during this work and also research by the author relevant to the topic of the thesis.

1. Andreev P., Bourilkov J. (1985) Low Frequency Instrumentation for Potentiodynamic Studies, *Communications of the Department of Chemistry*, Bulgarian Academy of Sciences, Vol.18, Number 1.
2. Andreev P, Bourilkov J, Tonchev D. (1990) A New General Purpose Potentiostat, *41st ISE Meeting*, Prague, Proceedings I, Tu-3.
3. Iltchev N, Banov B. and Bourilkov J, Reversible Cathode Material Obtained by Electrochemical Reduction of MnO_2 in Non- aqueous Electrolyte, *Sixth International Meeting on Lithium Batteries,* May 10 - 15, 92, Munster, Germany, III- B- 10 pp. 329 - 331.
4. Bourilkov J, Iltchev N, Banov B, Wideband Potentiostat, *Fourth European Conference on Electroanalysis,* Noordvijkerhout, Holland, May 31 - June 3, 1992, Proceedings p. 14.
5. Bourilkov J, Iltchev N, Banov B (1992) Wideband Power Operational Amplifier, *Journal of Radio, Television and Electronics*, Bulgaria, June, pp. 8-10.
6. Iltchev N, Banov B, Bourilkov J, Porosity Controlled Silver Oxide Electrode, *The Tianjin International Power Sources Symposium & Trade Show*, September 22-26, 92, Tianjin, China, Ext. Abstracts pp. 158-159.
7. Banov B, Iltchev N, Bourilkov J, Mladenov M, Cobalt Stabilized Layered Lithium-Nickel Oxides, Cathodes in Lithium Rechargeable Cells, *Seventh International Meeting on Lithium Batteries,* Boston, MA, May 15-20, 1994, II-A pp. 21- 23.
8. Bourilkov, J.T., Fneer, M., Boyle, W.J.O., Grattan, K.T.V. and Palmer, A.W. (1996) Dissolved gas sensing based on composite optical fibre and electrochemical techniques, *Proceedings of the Applied Optics Divisional Conference of The Institute of Physics*, pp. 449-454, Reading, UK.

9. Bourilkov, J.T, Boyle, W.J.O, Grattan, K.T.V, (1996) A System for In-Situ Monitoring of Greenhouse Gases Distribution in the Anoxic Zones of the Black Sea, *Proposal for Cooperation in Science and Technology with CCE/NIS (INCO-COPERNICUS-*1995/96).
10. Bourilkov J., Belz M., Boyle W.J.O., Grattan K.T.V. (1998) Electrical pH Control in Aqueous Solutions, *Conference on Process Monitoring Applications of Fiber Optic Sensors*, 4 November, Boston, *SPIE Proceedings* Vol. 3538, pp. 268 – 277.
11. Walsh Fr, Pozin M, Bourilkov J, Tikhonov K, Analysis of Modes of Failure of Lithium – Ion Packs, *9th International Meeting of Lithium Batteries,* 12 – 17 July 1998, Edinburgh, Scotland, United Kingdom, Book of Abstracts, Poster III, Fri 105.
12. Bourilkov, J, Zuraw, M, Hybrid Power Supply for Portable Devices, *Duracell GSC/GATC Annual Meeting*, Bethel, Connecticut, December 2001.
13. Klein, D.N., Bourilkov, J.T. (2002), Hybrid Energy Systems for Mobile Devices, *IMPACCT, May 2, 2002, New York City, NY.*
14. Bourilkov, J. T., Klein, D.N., Rotondo, J., Gillette CO Patent US 20030155887, WO200371651, Hybrid Power Supply, USA, February 2002.
15. Bourilkov, J. T., Klein, D.N., Rotondo, J., Gilicinski, A.G., Gillette CO, US 2004/0174072, Fuel Cell Hybrid Power Supply, USA, filed March 5, 2003, Pub. Date September 9, 2004.

APPENDIX 10: HYBRID CIRCUIT DIAGRAMS (V1&V2)

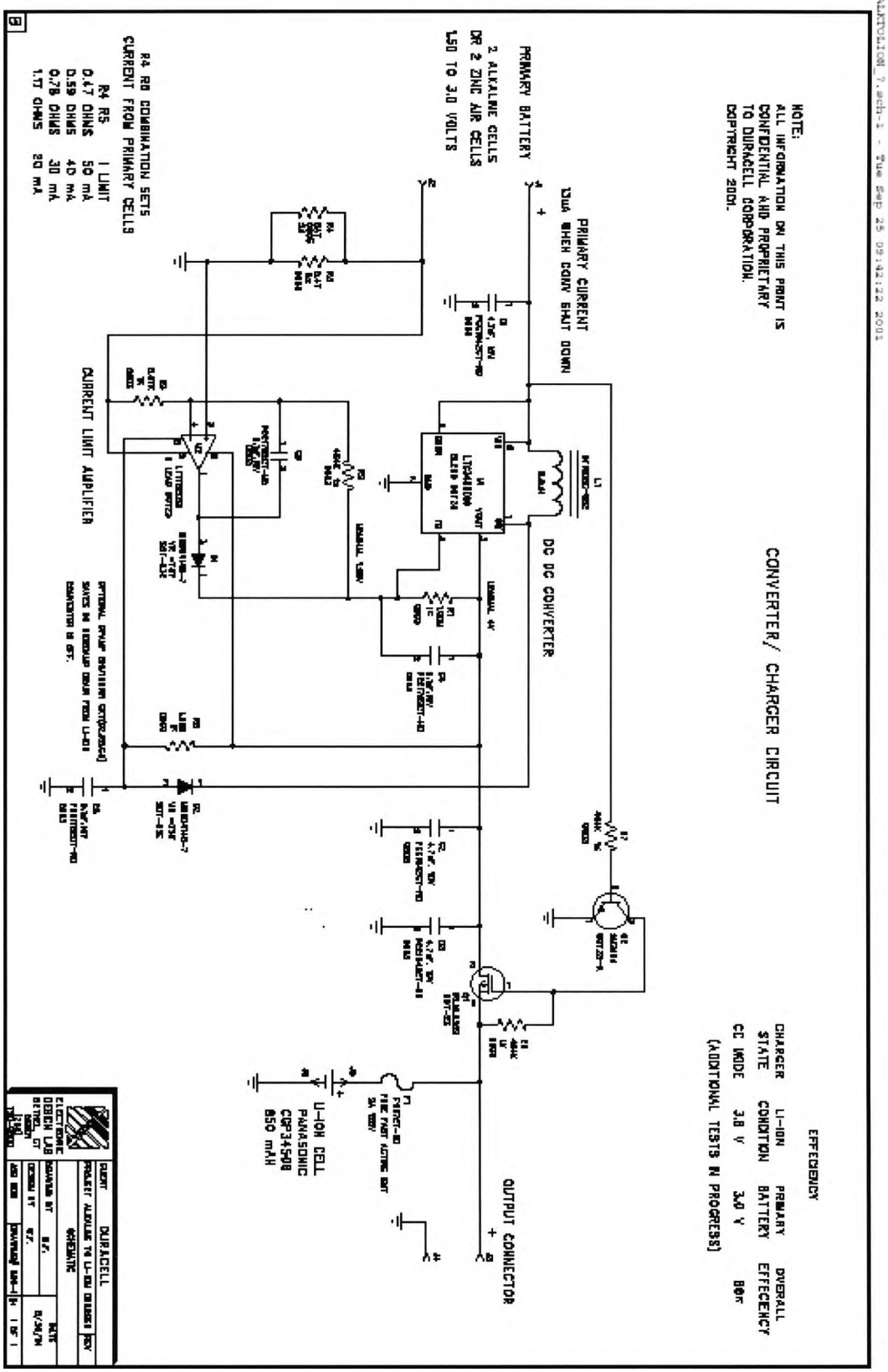

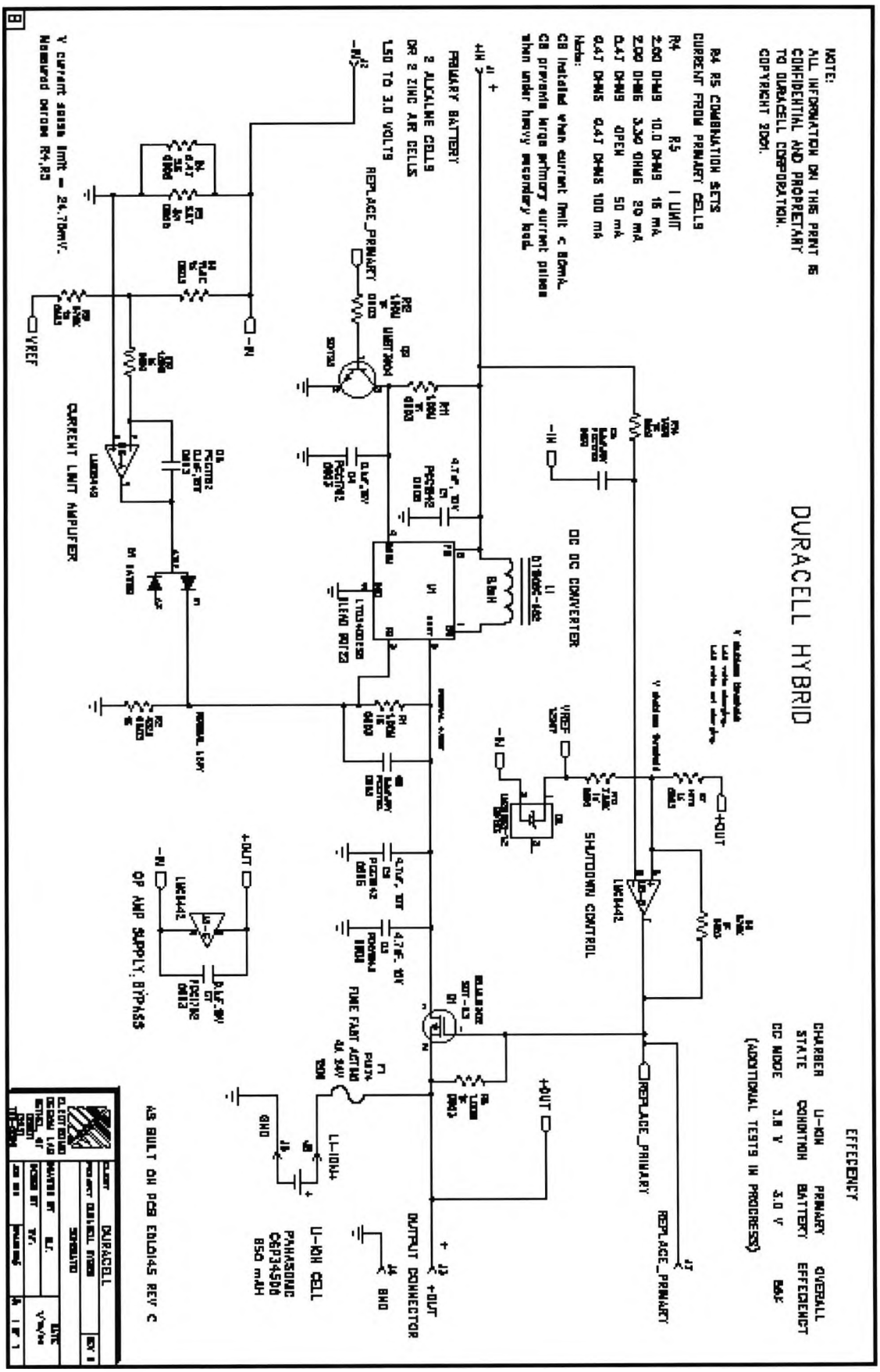
NOTE:
ALL INFORMATION ON THIS PRINT IS CONFIDENTIAL AND PROPRIETARY TO DURACELL CORPORATION.
COPYRIGHT 2001.
R4 R5 COMBINATION SETS
CURRENT FROM PRIMARY CELLS
R4 R5 I LIMIT
2.00 OHMS 10.0 OHMS 15 mA
2.00 OHMS 3.30 OHMS 29 mA
0.47 OHMS OPEN 50 mA
0.47 OHMS 0.47 OHMS 100 mA
Note:
CB installed when current limit < 80mA.
CB prevents high primary current pulses when under heavy secondary load.
PRIMARY BATTERY
2 ALKALINE CELLS
OR 2 ZINC AIR CELLS
1.50 TO 3.0 VOLTS
REPLACE_PRIMARY
CURRENT LIMIT AMPLIFIER
DC DC CONVERTER
SHUTDOWN CONTROL
OP AMP SUPPLY BYPASS
FINE FAST ACTING
Li-ION CELL
PANASONIC
CGP34500
850 mAH
OUTPUT CONNECTOR
EFFICIENCY
CHARGER STATE
DC MODE
Li-ION CONDITION
PRIMARY BATTERY
3.0 V
OVERALL EFFICIENCY
(ADDITIONAL TESTS IN PROGRESS)
AS BUILT ON PCB EDL0145 REV C
DURACELL
DURACELL HYBRID
SCHEMATIC